Documento de referencia

Volumen V

Apéndices

Ministerio de Medio Ambiente

Universidad de Cantabria UC

G.I.O.C.
Grupo de Ingeniería Oceanográfica y de Costas

DOCUMENTO DE REFERENCIA

Diciembre de 2000

ÍNDICE

VOLUMEN I. DINÁMICAS

- **SECCIÓN 1. MECÁNICA DE ONDAS**

  Introducción

  Movimiento oscilatorio, Magnitudes características de las ondas

  Definición de los parámetros adimensionales

  Regímenes y teorías de ondas

  Planteamiento general del problema de contorno

  Teoría lineal de ondas

  Teoría no lineal de ondas

  Bibliografía

- **SECCIÓN 2. ANÁLISIS DEL OLEAJE**

  Capítulo 1. Introducción

  Capítulo 2. Conceptos básicos para la descripción del oleaje

  Capítulo 3. Modelos estadísticos para el análisis del oleaje a corto plazo

  Capítulo 4. Propiedades espectrales del oleaje

  Capítulo 5. Modelos de predicción del oleaje a corto plazo

  Capítulo 6. Descripción del oleaje a largo plazo: regímenes

  Capítulo 7. Bibliografía

- **SECCIÓN 3. TRANSFORMACIÓN DEL OLEAJE EN LAS PROXIMIDADES DE LA COSTA**

  Introducción

  Conceptos previos

  Asomeramiento

  Refracción

  Difracción

  Refracción – difracción

  Reflexión

  Disipación

  Transformación del oleaje

  Bibliografía

- **SECCIÓN 4. HIDRODINÁMICA EN LA ZONA DE ROMPIENTES**

  Capítulo 1. Introducción

  Capítulo 2. Asomeramiento y rotura del oleaje

  Capítulo 3. Ecuaciones generales promediadas

  Capítulo 4. Aplicaciones de las ecuaciones generales promediadas al cálculo de las características medias del flujo en la zona de rompientes

  Capítulo 5. Flujo medio vertical transversal en la zona de rompientes

  Capítulo 6. Dinámica de la zona de ascenso-descenso

- **SECCIÓN 5. ONDAS LARGAS**

  Introducción

  La marea astronómica

  Ecuaciones fundamentales

  Propagación 1-D de las ondas largas

  Propagación con fricción

Marea meteorológica (Storm surge)
Ondas largas inducidas por el oleaje. Ondas infragravitatorias
Bibliografía

- SECCIÓN 6. TRANSPORTE DE SEDIMENTOS
  - Capítulo 1. Introducción
  - Capítulo 2. Flujo de agua y perfil de velocidades
  - Capítulo 3. Rugosidad de lecho
  - Capítulo 4. El transporte de sedimentos
  - Capítulo 5. Bibliografía

- SECCIÓN 7. DINÁMICA Y TRANSPORTE DE SEDIMENTOS EN RÍAS Y ESTUARIOS
  - Capítulo 1. Introducción general
  - Capítulo 2. Desembocaduras
  - Capítulo 3. Estuarios
  - Capítulo 4. Bibliografía

VOLUMEN II. PROCESOS LITORALES

- SECCIÓN 1. PROCESOS LITORALES
  - Capítulo 1. Introducción general
  - Capítulo 2. Morfología de playas a largo plazo: perfil de equilibrio
  - Capítulo 3. Morfología de playas a largo plazo: forma en planta de equilibrio
  - Capítulo 4. Morfodinámica de playas a largo y medio plazo
  - Capítulo 5. Procesos litorales en rías y estuarios

VOLUMEN III. OBRAS

- SECCIÓN 1. OBRAS
  - Capítulo 1. Introducción general
  - Capítulo 2. Clasificación y tipología de las obras de protección del litoral
  - Capítulo 3. Cálculo funcional de estructuras de protección del litoral
  - Capítulo 4. Estabilidad de estructuras de protección del litoral
  - Capítulo 5. Materiales
  - Capítulo 6. Análisis de riesgo
  - Capítulo 7. Bibliografía

Volumen IV. MEDIO AMBIENTE LITORAL

- SECCIÓN 1. ECOSISTEMAS LITORALES
  - Capítulo 1. El medio marino
  - Capítulo 2. Zona intermareal
  - Capítulo 3. Ecosistemas litorales
  - Capítulo 4. Comunidades intermareales

- SECCIÓN 2. IMPACTO AMBIENTAL
  - Capítulo 1. Introducción
  - Capítulo 2. Impacto ambiental
  - Capítulo 3. Evaluación del impacto ambiental
  - Capítulo 4. Los estudios de impacto
  - Capítulo 5. EsIA: Introducción

Capítulo 6. EsIA: Análisis del medio
Capítulo 7. EsIA: Análisis del proyecto
Capítulo 8. EsIA: Análisis de impacto

Volumen V. APÉNDICES:

APÉNDICE I.

- SECCIÓN 1. REFERENCIAS

Referencias bibliográficas

Libros
Revistas
Normativa
Bases de datos y direcciones de Internet interesantes
Congresos y conferencias
Centros de investigación

- SECCIÓN 2. MÉTODOS EXPERIMENTALES

Capítulo 1. Modelos físicos
Capítulo 2. Análisis dimensional
Capítulo 3. Principios de la semejanza
Capítulo 4. Modelos hidrodinámicos
Bibliografía

APÉNDICE II. AVANCES TÉCNICOS

Prólogo

El presente documento es el *Volumen V. Apéndices* del Documento de Referencia, que es uno de los textos elaborados dentro del proyecto "Modelo de Ayuda a la Gestión del Litoral".

Dicho proyecto, desarrollado por la Universidad de Cantabria para la Dirección General de Costas del Ministerio de Medio Ambiente ha tenido como objetivos fundamentales:

- Conocer con precisión la dinámica y la evolución de los sistemas costeros,
- Diseñar con fiabilidad las estrategias de actuación necesarias para evitar la regresión de la costa y la inundación de las zonas bajas litorales,
- Establecer una metodología para el diseño, ejecución y seguimiento de las actuaciones a realizar en la costa española
- Recopilar la experiencia española en el campo de la Ingeniería Litoral.

La estructura y objetivos particulares de los textos y modelos desarrollados en el seno del proyecto se presenta en el cuadro adjunto:

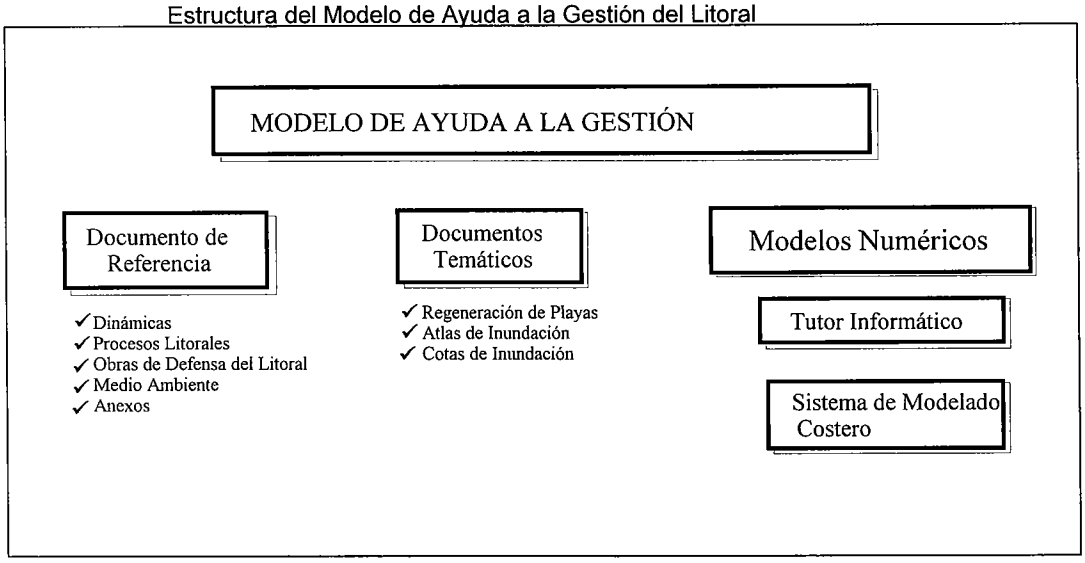

El Documento de Referencia es un compendio enciclopédico en el que se recoge el estado del arte de los conocimientos necesarios para sustentar los diferentes documentos temáticos y modelos numéricos elaborados.

La estructura general del Documento de Referencia es la siguiente:

Volumen I. Dinámicas
Volumen II. Procesos litorales
Volumen III. Obras de protección del litoral
Volumen IV. Medio ambiente litoral
Volumen V. Apéndices

Los Documentos Temáticos tienen como objetivo desarrollar la metodología de diseño de diversas actuaciones en la costa.

Entre los Documentos Temáticos desarrollados se encuentran:

Volumen 1. Regeneración de playas.
Volumen 2. Cota de Inundación
Volumen 3. Atlas de Cota de Inundación

Los Modelos Numéricos tienen un doble objetivo:

- Facilitar la aplicación de la información del Documento de Referencia en soporte informático (Tutor Informático de Costas, Tic).
- Ofrecer un paquete de programas numéricos que permitan la correcta utilización de la metodología propuesta en los Documentos Temáticos.

Cada uno de los modelos desarrollados cuenta con un manual habiéndose editado los siguientes:

Modelo de Propagación de Ondas (Oluca)
Modelo de Corrientes en Playas (Copla)
Modelo de Erosión / Sedimentación (Eros)
Modelo de Perfil Transversal (Petra)
Modelo de Sistema de Modelado Costero (SMC)

Aunque el Documento de Referencia trata de incluir todos los conocimientos teóricos necesarios, se ha optado en algunos casos específicos, como son el del Documento de Cota de Inundación o en algunos de los manuales de los modelos numéricos, por incluir en los mismos una gran parte de los fundamentos teóricos que los sustentan complementando así algunas partes del Documento de Referencia.

Santander, Diciembre de 2000

APÉNDICE I

Sección 1.

REFERENCIAS

DOCUMENTO DE REFERENCIA

ÍNDICE

REFERENCIAS

1. Referencias bibliográficas 1
1.1 Libros 1
1.2 Revistas 19
1.3 Normativa 21
1.4 Bases de datos y direcciones de Internet interesantes 22
1.5 Congresos y conferencias 24
1.6 Centros de investigación 26

REFERENCIAS

1. REFERENCIAS BIBLIOGRÁFICAS

1.1. Libros

A lo largo de las páginas siguientes se consignan una serie de obras que este Concursante utiliza en su labor docente e investigadora en el campo de la Ingeniería Oceanográfica. Los textos se han ordenado alfabéticamente por autores.

La lista bibliográfica tiene dos niveles de información o subapartados. Por un lado se ha incorporado, aquella bibliografía, más directamente relacionada con los PROGRAMAS y que va seguida de un pequeño comentario, que se refiere a su contenido y valoración; y por otro, una referencia bibliográfica y de especialización que, no son fuentes directas de los PROGRAMAS, sino que responden a necesidades de investigación o de desarrollo de Tesis Doctorales. En consecuencia, este subapartado debe considerarse como el soporte de conocimientos técnicos teóricos, que el Concursante conoce y dispone, pudiendo, o no, tener en su contenido una aplicación directa a los PROGRAMAS. Es precisamente en el capítulo destinado a la exposición de PROGRAMAS, donde se formulará una bibliografía directamente aconsejada para la preparación del tema, que en lo fundamental se introduce en el presente apartado.

Es probable que el lector encuentre en estas Fuentes muchos libros que son imprescindibles para una formulación teórica y práctica de la Ingeniería Oceanográfica, pero también es probable que a su juicio, existan ausencias significativas. En cualquier caso, esta relación puede ser una aproximación inicial.

- **Abramowitz, M. y Stegun, I.**. Handbook of Mathematical Functions Dover Publications, Inc. 1972.

Herramienta matemática muy útil y que sin duda es muy empleada no solo en la Ingeniería Oceanográfica sino en todo los campos de la Ciencia y de la Técnica. Hoy en día este texto es menos relevante gracias al libro Numerical Recipies, que ofrece en formato numérico muchas de las herramientas presentadas en este libro así como software tal como Mathematica o Mathlab.

- **Anikouchine, W.A. y Sternberg, R.W**. The World Ocean. Prentice Hall, Inc. 1981.

Un libro de introducción a los temas oceanográficos que cubre de una manera muy elemental prácticamente todos los aspectos de la oceanografía, geología, química, circulación atmosférica y oceánica, ondas, sedimentación, instrumentación y algunos aspectos de la biología marina. Un libro de lectura sencilla recomendable para los alumnos como introducción.

- **Autores Varios**. Shore Protection Manual. (2 Vol.) U.S. Army Coastal Engineering Research Center. 1984.

Es un auténtico manual de Ingeniería de Costas, que carece de todo rigor científico aunque tiene el valor de ser un buen manual, es decir, que proporciona soluciones para casi todos los problemas del ingeniero práctico. Este Manual se encuentra en la actualidad en fase de revisión y se espera una primera edición para el año 2000. Libro informativo.

- **Autores Varios**. Advances in Hydroscience. Varios Volúmenes. Academic Press Inc.

Es una colección de libros que empezaron a publicarse en 1964 (Volumen I). Cada libro recoge varios temas monográficos relacionados con las ciencias del agua y escritos por investigadores de reconocido prestigio. En la mayor parte de los volúmenes puede encontrarse algún trabajo relacionado con la Oceanografía o la Ingeniería Oceanográfica.

- **Bascom, W.** Waves and Beaches. Anchor Books. Doubleday. 1980.

Libro meramente descriptivo y con poco rigor científico pero no por ello falto de interés. El autor hace una revisión de diversos temas relacionados con la ingeniería de costas desde un punto de vista ilustrativo que tiene dos ventajas fundamentales: se concentra en la explicación de los fenómenos físicos motivando al lector a través de experiencias y fotografías, y la segunda es que se trata de un libro ameno de fácil lectura.

- **Batchelor, G.K.** An Introduction to Fluid Mechanics. Cambridge University Press. 1980.

Excelente tratado sobre mecánica de fluidos que describe los elementos fundamentales de la física de los fluidos reales haciendo énfasis en los principios generales y en la relación entre los modelos analíticos y conceptuales y la observación experimental.

- **Bendat, J.S. y Piersol, A.G.** Random Data: Analysis and Measurement Procedures. Wiley Interscience. 1986.

Revisión extendida y aumentada al libro del mismo nombre publicada por primera vez en 1966. Hace especial hincapié en los aspectos prácticos del análisis de datos aleatorios y en los procedimientos de medida. Su tratamiento de los procesos estocásticos le hace ser un libro demasiado especializado para los no iniciados en los métodos estadísticos y la teoría de la probabilidad.

- **Bruun, P.** Port Engineering. (2 Vol.) Gulf Publishing Company. 1989.

Obra cuyo contenido puede considerarse como el mayor compendio sobre ingeniería portuaria existente en la actualidad. A lo largo de sus diez capítulos incluye recomendaciones relativas a temas que varían desde la selección óptima de la localización del puerto hasta estudios económicos, pasando por diseño de las infraestructuras, atraques, dragado, transporte de sedimentos, geomorfología, etc. Incluye asimismo un capítulo dedicado exclusivamente al diseño de puertos pesqueros. Se trata de un libro fundamental para cualquier ingeniero portuario.

- **Bruun, P.**, Editor. Design and Construction of Mounds for Breakwaters and Coastal Protection. Elsevier. 1985.

En la primera parte de este libro se analiza los parámetros implicados en el diseño de diques de escollera, estudiando la hidrodinámica, interacción ola-estructura,

estabilidad, aspectos geotécnicos, etc. En la segunda parte se presenta aquellos elementos que deben utilizarse en el proceso de diseño. A continuación se describe los procesos constructivos para diques de escollera. Es importante también el hecho de que en uno de los capítulos se pasa revista a varios diques de escollera existentes en distintas partes del mundo. Es sin duda un libro de gran utilidad práctica al ser el libro más completo relativo a diques de escollera.

- **Chakrabarti,S.K.** Hydrodynamic of Offshore Structures. Computational Mechanics Publications and Springer Verlag, 1987

El autor es uno de los grandes especialistas en el tema de la Estructuras Offshore. Su libro es un excelente tratado del tema tanto desde el punto de vista conceptual como metodológico.

- **Daily, J.W.y Harleman D.R.** Fluids Dynamics. Addison--Wesley Publising Co. 1966.

Este libro puede clasificarse como un clásico. En él, los temas de hidrodinámica son tratados al tiempo con profundidad y de forma amena lo que hace del mismo un excelente libro de consulta para los alumnos.

- **Dalrymple, R.A.**, Editor. Physical Modelling in Coastal Engineering. A.A. Balkema. 1985.

Libro resultante de la reunión de expertos que tuvo lugar en la Universidad de Delaware en 1981 sobre el modelado de fenómenos físicos en la ingeniería de costas.

Esta dividido en cuatro partes en las que se presenta una introducción al modelado, la generación de ondas en el laboratorio, modelado del transporte de sedimentos y finalmente, diversas aplicaciones del modelado a casos reales. Es un libro importante para investigadores en el campo de los modelos.

- **Dean, R.G., Dalrymple, R.A.** Water Wave Mechanics for Engineers and Scientists. Prentice--Hall Inc. 1984 y World Scientific. 199

Este libro es quizás el mejor texto de carácter educativo a la hora de introducir al alumnado en la teoría de ondas. De una manera muy bien explicada y sencilla de entender, los autores analizan desde la teoría lineal de ondas aspectos de la propagación, refracción, difracción, ondas largas, teoría de ondas sobre lechos reales, fuerzas, etc. Incluyen asimismo una introducción a la teoría no lineal de ondas y presentan en otro capítulo el oleaje irregular.

Cada uno de los capítulos se completa con una serie de problemas que ayudan al alumno a entender y aplicar los conceptos desarrollados en cada lección. Constituye sin duda un de los libros de texto más importantes en la Ingeniería Oceanográfica.

- **Dingemans, M.W.** Water Wave Propagation over Uneven Bottoms, Vols I and II. World Scientific, 1997

Libro sobre teoría de ondas redactado en forma enciclopédica al tratar de presentar lo realizado hasta la fecha de su publicación sobre los Regímenes de Stokes y de Boussinesq. Es un libro para especialistas o estudiosos de la teoría de ondas de gravedad, completo, bien presentado y con una notable lista de referencias. Su consulta es una necesidad para iniciar cualquier trabajo de investigación.

- **Dronkers, J.J.** Tidal Computations in Rivers and Coastal Waters. North-Holland Publishing Company. Amsterdam. 1964.

Probablemente el libro con más información relativa a la generación de la marea y a las diferentes técnicas para su estudio y predicción.

- **Dronkers, J. and Van Leussen, W.** Eds. Physical Processes in Estuaries. Springer--Verlag. 1988.

Este libro está realizado por diferentes autores de reconocido prestigio en el tema de estuarios. El libro comprende dos secciones, una dedicada a los procesos dinámicos y de transporte de masa en los estuarios y otra referente al transporte de sedimentos cohesivos. Cada sección se inicia con un capítulo que realiza una recopilación del estado del arte del tema.

- **Dyer, K.R.** Estuaries: A Physical Introduction. John Wiley & Sons. 1973.

Texto de carácter introductorio, con una base matemática elemental, que inicia al lector en los fenómenos dinámicos que tienen lugar en un estuario. Partiendo de una clasificación de los estuarios, el autor nos introduce en los fenómenos inducidos en los estuarios por la turbulencia, la marea, gradientes de densidad, etc. Es un texto muy adecuado para iniciarse en el estudio de estuarios.

- **Fisher, B.H. List, E.J. Koh, R.C. Imberger, J. y Brooks, N.H.** Mixing in Inland and Coastal Waters. Academic Press, Inc. 1982.

En este libro se aborda el tema de la mezcla y transporte de sustancias en el medio marino. Cada concepto se aborda desde sus fundamentos y se desarrolla hasta sus

últimas aplicaciones. El volumen es muy adecuado, tanto como libro de texto, como elemento de consulta en temas de dilución en ríos o vertidos de emisarios submarinos.

- **Fredsoe, J. y Deigaard, R.** Mechanics of Coastal Sediment Transport. World Scientific Publishing Co. 1992.

En este libro se encuentra el estado del arte en el conocimiento del transporte de sedimentos debido a la rotura del oleaje hasta la fecha de su publicación. El libro se inicia con un repaso de la dinámica del oleaje y de las corrientes, así como de la capa límite interacción de ambas dinámicas. Posteriormente, desarrolla los aspectos básicos del transporte de sedimentos y concluye con la aplicación de todos estos conceptos al transporte longitudinal y transversal en playas.

- **Gill, A.E.** Atmosphere--Ocean Dynamics. Academic Press, Inc. 1982.

En este libro se incluye un estudio detallado e intenso sobre las circulaciones oceánicas y atmosféricas. Se presenta como estas circulaciones son impulsadas por la energía solar y se estudia la distribución de características físicas como la temperatura. Todo ello se hace con modelos matemáticos sencillos. Además estudia con detalle las ecuaciones de estado y dinámicas. Es un libro muy completo e importante especialmente para aquellos investigadores interesados en la Oceanografía.

- **Goda, Y.** Random Seas and Design of Maritime Structures. University of Tokyo Press, 1985.

En este libro se presenta la irregularidad del oleaje como concepto fundamental en el diseño de diques, espaldones y estructuras costeras en general. Aprovechando su experiencia obtenida en la costa japonesa, el autor dirige la primera parte del libro a aquellos ingenieros que necesitan respuestas inmediatas a sus problemas de diseño. A través de una serie de fórmulas empíricas el autor presenta una formulación para realizar el cálculo, de una manera sencilla y rápida de diques verticales y espaldones.
En la segunda parte del libro se presenta de una manera más científica los fundamentos teóricos del oleaje irregular.

En la actualidad se está preparando una nueva edición que será publicada próximamente por World Scientific.

- **Greenberg, M.D.** Advanced Engineering Mathematics. Prentice Hall. 1988.

Libro de matemáticas orientado en su totalidad a ingenieros. Presenta gran cantidad de las herramientas matemáticas necesarias para trabajar en la Ingeniería Oceanográfica. Todos los temas incluyen gran cantidad de ejemplos y al final una

selección de problemas aplicadas a la Ingeniería. Destacan especialmente los capítulos relativos a la resolución de ecuaciones diferenciales y a la variable compleja.

- **Grace, R. A.** Marine Outfall Systems--Planning, Design and Construction. Prentice Hall. 1987.

Uno de los libros más completos relativos al estudio de vertidos al mar y a emisarios submarinos. Comienza mediante una caracterización de los vertidos y su posible impacto sobre el medio marino. Incluye a continuación, una serie de capítulos en los que presenta la toma de datos necesaria para el seguimiento de vertidos y para el diseño de emisarios submarinos. El autor revisa asimismo las características técnicas de los emisarios e incluye, para finalizar una serie de capítulos relativos a aspectos constructivos. Un libro fundamental para ingenieros involucrados en vertidos al mar y emisarios submarinos.

- **Herbich, J.** Editor. Handbook of Ocean Engineering, 1990.

Edición enciclopédica a la que contribuyen varios autores de prestigio tratando diversos temas relacionados con la Ingeniería Oceanográfica. Los capítulos individuales son suficientemente extensos como para constituir una buena introducción para aquellos que se enfrenten por primera vez con el problema.

- **Hill, M. N.**. Editor. The Sea. (6 Vols.) Interscience Publishers, Inc. J. Wiley & Sons. 1962.

Amplio tratado sobre oceanografía cuyos tres volúmenes cubren los siguientes temas: oceanografía física, composición del agua de mar, oceanografía descriptiva y comparativa, y el estudio de los fondos oceánicos. Cada capítulo está escrito por un especialista y cabe destacar el capítulo de oleaje escrito por Cartwright y el de playas y procesos litorales de Bagnold e Inman. Esta obra ha ido completándose a lo largo del tiempo, de modo que en la actualidad consta de seis volúmenes.

- **Horikawa, K.** Coastal Engineering: An Introduction to Coastal Engineering. University of Tokyo Press. 1978.

Texto concebido como introducción a la Ingeniería Oceanográfica que trata esencialmente los temas relacionados con el oleaje, ondas largas, corrientes litorales, sedimento litoral e investigaciones de campo. Se utiliza como libro de texto en diversas universidades japonesas y está escrito con gran claridad. Sin embargo, algunos temas como la interacción oleaje-estructura están pobremente tratados.

- **Horikawa, K.** Editor. Nearshore Dynamics and Coastal Processes. University of Tokyo Press. 1988.

Este libro es el resultado de un programa de investigación de seis años de duración llevado a cabo en Japón con el fin de desarrollar modelos numéricos apropiados para predecir la evolución de las morfologías costeras debido a la presencia de estructuras generadas por el hombre. Para ello se efectuaron extensas campañas de campo que fueron combinadas con estudios teóricos y en laboratorio. El libro se divide en 5 partes. La primera se dedica a los fundamentos de la mecánica de fluidos y la hidrodinámica del oleaje. La segunda recoge una extensa descripción de los procesos litorales. En las partes tercera y cuarta se presentan unos interesantes modelos de evolución de playas consecuencia del proyecto de investigación. Se finaliza haciendo un compendio de técnicas e instrumentación para la medición de características del oleaje, corrientes, transporte de sedimento, etc. Algunos de los modelos y técnicas aquí expuestas han sido ampliamente superados, pero es un buen libro de introducción.

- **Hughes S.A.**. Physical Models and Laboratory Techniques in Coastal Engineering. World Scientific, 1993

Libro escrito por uno de los Investigadores del C.E.R.C. de los EEUU y que de manera sencilla y con ejemplos muestra el mundo de la experimentación de las obras marítimas. En el libro se analizan los temas de semejanza y los modelos de obras y de transporte de sedimentos. Se dedica un capítulo a presentar los métodos de generación de oleaje y otro a las técnicas de medida y análisis. Libro sencillo, sin complejidades teóricas que puede ser de gran utilidad a los alumnos y a los Ingenieros como libro de consulta.

- **Ippen, A.T.** Editor. Estuary and Coastline Hydrodynamics. McGraw Hill Company. 1966.

Se trata de un importante libro dentro de la Ingeniería Oceanográfica en el cual se aborda, con un nivel medio, la mayor parte de los temas relacionados con ella. Los capítulos están escritos por diferentes investigadores y trata de ondas, oleaje, mareas, interacción oleaje-estructuras y dinámica de estuarios.

- **Iribarren, R. y Nogales, C.** Obras Marítimas. Oleaje y Diques. Editorial Dossat. S.A. 1964.

Este libro aunque ya superado en muchos aspectos por el paso del tiempo, tiene sin duda un gran valor fundamentalmente por lo que representa en la historia de la Ingeniería Oceanográfica en España.

- **Isaacson, E. e Isaacson M.** Dimensional Methods in Engineering and Physics. Edward Arnold Publisher Ltd. 1975.

Un gran libro sobre Análisis Dimensional como método para obtener relaciones entre variables físicas. Hace un tratamiento matemático riguroso del Teorema Pi de Buckingham y a través de la independencia física establece las posibilidades de aumentar la precisión de los resultados del Análisis Dimensional con la ampliación del conjunto de referencia tradicional (Longitud, Masa, Tiempo). El libro tiene un gran interés teórico y práctico para su uso por estudiantes y profesionales por su claridad y multitud de ejemplos en varias ramas de la Física.

- **King, C.A.M.** Beaches and Coasts. Edward Arnold Publisher Ltd.. 1972.

Libro básico sobre la morfodinámica de las playas y las costas, distinguiéndolas por su escala de variación. Analiza prácticamente todos los temas relacionados con los procesos litorales. Es algo anticuado en el tratamiento de la dinámica marina, sin embargo, es un libro valioso para la docencia por la gran cantidad de ejemplos con los que ilustra los diferentes temas.

- **Kinsman, B.** Wind Waves. Prentice Hall Inc. 1965.

Este libro constituyó en su época una especie de estado del arte en lo que se refiere a las oscilaciones de corto período. En la actualidad ha quedado algo anticuado en aspectos tales como generación de oleaje, previsión o análisis espectral. Al igual que el anterior, es un libro que presenta muy buenos ejemplos que pueden ayudar en las tareas docentes.

- **Komar, P.D.** Beach Processes and Sedimentation. Prentice Hall. 1976.

Libro de gran interés para estudiantes, ya que sin entrar muy profundamente en el rigor físico-matemático de las teorías hidrodinámicas y de movimiento de sedimentos, describe de una manera muy acertada los distintos factores que intervienen en los procesos litorales y la respuesta de la playa a sus variaciones.

En 1998 ha salido una nueva versión ampliada incluyendo los procesos asociados a las ondas infragravitatorias. Esta nueva edición ha sido publicada por Prentice Hall pero se encuentra agotada. .

- **Kowalik, Z. and Murty, T.S.** Numerical Modelling of Ocean Dynamics. World Scientific. 1993.

Este libro pretende introducir al lector en la aplicación del método de las diferencias finitas en el modelado de la dinámica oceánica y revisar otras técnicas más complejas. El libro muestra varios ejemplos sobre el modelado numérico de procesos de transporte, marea, tsunamis, etc. Es un libro indispensable para aquellos que quieran introducirse en el modelado numérico de la dinámica marina.

- **Kundu, P.K.** Fluid Mechanics. Academic Press Inc.. 1990.

Libro sobre mecánica de fluidos e hidrodinámica que presenta la particularidad de ser muy claro y de fácil lectura. Presenta además la característica de tener dos capítulos muy interesantes sobre teoría de ondas y sobre mecánica de fluidos aplicada a la atmósfera y al océano.

- **Lamb, H.** Hydrodynamics. Dover Publications Inc.. 1932.

Libro clásico sobre la dinámica de líquidos y gases. Básico para todos los investigadores y estudiosos de la hidrodinámica.

- **Le Blond, P.H. y Mysak, L.A.** Waves in the Ocean. Elsevier Scientific Publishing Co. 1980.

Es un completo tratado sobre la dinámica de los movimientos oscilatorios en el océano, cubriendo todo tipo de ondas, desde las capilares hasta las ondas planetarias. Incluye los resultados más importantes de la investigación en este campo obtenidos durante la últimas décadas. Libro difícil cuyo estudio requiere mucho tiempo.

- **Le Méhauté, B.** An Introduction to Hydrodynamics and Water Waves. Springer Verlag. 1976.

Se trata de un buen libro de introducción en los temas de hidrodinámica y ondas. Trata de conjugar los aspectos físicos y los matemáticos, presentando una buena colección de problemas de aplicación.

- **Liu, L.F., Editor.** Advances in Coastal and Ocean Engineering. World Scientific. Varios volúmenes.

El Prof. Liu es el editor de esta prestigiosa colección de volúmenes que comenzó su andadura en 1996. En cada uno de sus volúmenes se recogen entre 5 y 8 artículos de los más prestigiosos investigadores en el área de la ingeniería oceanográfica. Los

artículos suelen enfocarse como revisiones generales o como un medio de difundir nuevas aportaciones a un tema concreto. Aunque inicialmente son recomendables para tareas investigadoras, son también adecuados para introducirse en un tema concreto.

- **Losada, M.A.** Estabilidad de Playas: Morfodinámica de los Procesos Litorales. Universidad de Cantabria. 1988.

Este libro constituye un repaso general al estado del conocimiento de la estabilidad de playas. En un primer capítulo se introduce al lector en el problema estudiando la evolución histórica del conocimiento y proporcionando los fundamentos necesarios para el entendimiento de los capítulos posteriores. En los capítulos 2 y 3 se presenta los fenómenos de transformación del oleaje así como los fundamentos del transporte de sedimentos y su aplicación a la estabilidad de playas. En los dos siguientes capítulos se estudia las distintas formas de equilibrio de las playas y se presenta los modelos que explican y cuantifican la variabilidad de los perfiles de playa. El libro finaliza introduciendo al lector en los métodos experimentales de laboratorio para el estudio de la variabilidad de los perfiles de playa.

- **Massel, S.R.** Hydrodynamics of Coastal Zones. Elsevier Oceanography Series, 48. Elsevier. 1989.

Este libro realiza una completa visión general del modelado del oleaje. Incluye aspectos deterministas y estadísticos explicando todos los conceptos de forma muy clara. Incluye también un capítulo muy completo relativo a corrientes.

- **Massel, S.R.** Ocean Surface Waves: their Physics and Prediction. World Scientific, 1996

Este libro nace con vocación de manual de referencia para investigadores y profesionales de la previsión del oleaje. En él se presenta las descripciones estadística y espectral del oleaje y varios métodos y técnicas de previsión de oleaje. Una contribución importante del libro es la introducción en el mundo occidental de las teorías y métodos de la escuela de Ingeniería Oceanográfica Rusa, totalmente desconocida e ignorada durante muchos años. Libro de consulta, aunque quizás algo elevado para los alumnos de carrera.

- **McDowell, D.M. y O'Connor.** Hydraulic Behaviour of Estuaries. The McMillan Press Ltd. 1977.

Los autores realizan una introducción al estudio de estuarios y sistemas mareales, concentrando especialmente el interés sobre aquellos métodos y técnicas útiles al

ingeniero. Estas técnicas se presentan en los dos últimos capítulos del libro, y se basan en medidas de campo, análisis numérico y modelos físicos. Es un libro orientado fundamentalmente a ingenieros.

- **Mei, Chiang C.** The Applied Dynamics of Ocean Surface Waves. World Scientific. 1989.

Este libro es el resultado de un curso de dos semestres realizado por el autor en 1974 en el M.I.T. para estudiantes graduados en Ingeniería Oceanográfica y Civil. El libro presenta temas teóricos seleccionados de la dinámica de ondas en el océano, incluyendo sus principios básicos y sus aplicaciones en costas y estructuras offshore. Es un gran libro para investigadores y estudiosos al que le falta el tratamiento estadístico de los temas, ya que está contemplado íntegramente desde el punto de vista determinista.

- **Meyer, R.E.**. Editor. Waves on Beaches. Academic Press. 1972.

Recoge el estado del conocimiento y últimas investigaciones en los temas más importantes de la dinámica marina sobre playas y transporte de sedimentos hasta la fecha de su publicación. Cada capítulo está escrito por un investigador destacado y constituye un libro de gran interés para los investigadores en el tema de procesos litorales.

- **Miller, A. y Anthes, R.A.** Meteorology. Charles E. Merril Publishing Co. 1980.

Un pequeño libro de introducción a los temas de meteorología cuya lectura se recomienda a los alumnos. Los autores explican de una manera muy clara y sencilla la circulación atmosférica en sus diversas escalas además de algunos aspectos climáticos y de previsión meteorológica.

- **Milne-Thompson, L.M.** Theoretical Hydrodynamics. McMillan. 1960.

Tratado básico de hidrodinámica teórica conocido por la mayor parte de las personas que han trabajado en estos temas. Recomendable para los alumnos como libro de consulta.

- **Nayfeh, A.** Perturbation Methods. Wiley--Interscience Publication. John Wiley & Sons. 1973.

Para la resolución de las ecuaciones de gobierno y condiciones de contorno de cualquier problema no lineal, es necesario recurrir a diversas formas de aproximación,

soluciones numéricas o una combinación de ambas. En este libro se presenta las técnicas de los métodos de perturbación de una forma unificada, indicando sus similitudes, diferencias y ventajas así como sus limitaciones. Todo ello planteando ejemplos correspondientes a diferentes ramas de la Física y la Ingeniería.

- **Newland, D.E.** Vibraciones Aleatorias y Análisis Espectral. Editorial AC. 1983.

Versión en español del libro publicado en inglés en 1975. Libro de gran claridad y precisión adecuado para estudiantes. Tiene dos objetivos principales: introducir las ideas fundamentales de las funciones aleatorias y tratar con cierta profundidad el análisis espectral de gran utilización en el proceso de las medidas de los fenómenos físicos.

- **Nielsen, P.** Coastal Bounday Bottom Boundary Layers and Sediment Transport. World Scientific Publ., 1992

Libro dedicado al transporte de sedimentos en playas y en la plataforma continental escrito con la visión personal del autor cuya perspectiva física e intuitiva de los procesos es una fuente continua de nuevas ideas. Libro quizás mas útil para un especialista que para los alumnos.

- **Open University**. Waves, tides and shallow-water processes. Pergamon Press. 1989.

Un libro interesante y sencillo, escrito por un conjunto de investigadores y con fines docentes. Presenta los mecanismos esenciales del oleaje, la marea y los procesos de transformación de las mismas de forma descriptiva. Aconsejable como libro introductorio.

- **Panton, R.L.** Incompressible Flow . Wiley--Interscience Publication. John Wiley & Sons. 1984.

Este libro presenta, con una base matemática importante, conceptos fundamentales relativos a las características de flujos desde pequeños hasta elevados números de Reynolds. Con el fin de ayudar al lector el autor introduce varios ejemplos específicos de flujo incompresible. Los capítulos relativos a capa límite son muy completos.

- **Pedlosky, J.** Geophysical Fluid Dynamics. Springer Verlag. 1987.

Se trata de un libro dedicado a la aplicación de la mecánica de fluidos a la dinámica de fluidos a gran escala, tanto en los océanos como en la atmósfera. El autor consigue

aunar el razonamiento físico e intuitivo y el análisis matemático; discute los problemas más importantes de la dinámica de fluidos sobre los océanos, incluyendo las ecuaciones del movimiento y sus formas aproximadas, las diversas escalas del movimiento y particularmente la aproximación geostrófica y la teoría de inestabilidad de flujos. Es un excelente libro de consulta para investigadores en el campo de la Oceanografía Física.

- **Phillips, O.M.** The Dynamics of the Upper Ocean. Cambridge University Press. 1980.

Un excelente libro, de gran altura científica, que trata los complejos problemas de la generación y descripción físico-matemática del oleaje, las ondas internas y la turbulencia oceánica. Es un libro denso, muy avanzado y de lectura difícil.

- **Pickard, G.L. y Emery, W.L.** Descriptive Physical Oceanography. An Introduction. Pergamon Press. 1982.

En este libro se realiza un introducción descriptiva a la Oceanografía. En más de 200 páginas sin una sola ecuación, los autores describen las propiedades físicas del agua de mar, las distribuciones de las mismas en los océanos, la circulación de las masas de agua y la instrumentación y técnicas para la medición de distintos parámetros. Es un libro muy interesante para fijar conceptos, pero debe ser complementado con otros libros.

- **Pond, S. y Pickard, G.L.** Introductory Dynamical Oceanography. Pergamon Press. 1983.

Este libro se complementa totalmente con el anterior. Sirve como introducción a la dinámica oceanográfica y está especialmente indicado para Ingenieros Oceanográficos que se quieren introducir en la Oceanografía. El libro recoge los objetivo y procesos básicos de la dinámica oceanográfica y hace hincapié en sus limitaciones. Introduce métodos de trabajo, como la adimensionalización de las ecuaciones que sirve para entender mucho mejor el carácter físico de los términos que componen las ecuaciones.

- **Pylarczykl, K.W.** Dikes and Revetments: Design, Maintenance and Safety Assessment. Balkema. 1998.

Libro de interés para técnicos dedicados al diseño y construcción de obras de protección del litoral. Dirigido a ingenieros especialistas en ingeniería litoral, interesados en un libro de consulta rápida que ofrezca métodos y formulaciones para el diseño de diques de defensa de costas.

- **Rahman, M.** Water Waves. Oxford University Press. 1995.

El propósito fundamental de este libro es realizar una introducción a diversos aspectos físicos y matemáticos de la teoría de ondas. El autor se centra en aquellos problemas cuya solución puede abordarse analíticamente. Aunque el libro presenta grandes similitudes con el libro de Dean y Dalrymple, es un buen complemento para el alumno de Ingeniería Oceanográfica.

- **Raudkivi, A.J.** Loose Boundary Hydraulics. Balkema. 1998.

La cuarta edición de este libro incorpora los últimos avances en el área del transporte de sedimentos. Es un libro indispensable para aquellos que deseen tener, en un único volumen, una clara y completa recopilación de formulaciones relacionadas con el transporte de sedimentos. El libro cubre transporte eólico, fluvial, marino, sedimentos cohesivos planteando los diferentes aspectos desde un punto de vista empírico-práctico.

- **Sarpkaya, T. e Isaacson M.** Mechanics of Wave Forces on Offshore Structures. Van Nostrand Reinhold Company. 1981.

Una excelente obra que debe poseer todos los ingenieros interesados en las obras marítimas offshore. Consta de nueve capítulos que cubren desde una revisión de los conceptos hidrodinámicos fundamentales hasta modelos, pasando por un excelente resumen de las teorías de ondas y del oleaje por un estudio de las fuerzas que este ejerce sobre las estructuras. Concede mucha importancia a los principios y a los conceptos físicos fundamentales y presenta una gran cantidad de resultados experimentales para contrastar las distintas teorías. Un magnifico libro de consulta.

- **Sawaragi,T.** Coastal Engineering-Waves, Beaches,Wave-Structure Interactions. Developments in Geotechnical Engineering,78. Elsevier. 1995

Libro redactado con ocasión de la jubilación del profesor Sawaragi en el que se presentan los grandes temas relacionados con la Ingeniería Oceanográfica, tal y como su título indica. Los diferentes capítulos están redactados por los alumnos del Profesor, que realizaron la tesis doctoral bajo su tutoría y hoy en día son renombrados investigadores en el área. El libro tiene dos partes claramente diferenciadas: en la primera se presentan los fundamentos relativos a la dinámica del oleaje, interacción onda-estructura y transporte de sedimentos; en la segunda parte se presentan diferentes aplicaciones. Libro importante de consulta y aprendizaje.

- **Silvester, R.** Coastal Engineering. (2 Vol.) Elsevier Scientific Publishing Co.. 1974.

Es un libro que trata casi todos los temas de la Ingeniería Marítima (generación, propagación y acción del oleaje sobre obras y estructuras, sedimentación, estuarios, mareas, efluentes y modelos). Es un libro poco científico, en el que el autor no trata los principios básicos ni los planteamientos de las teorías. Tiene una importante laguna en el tratamiento estadístico del oleaje. En la parte de obras es prácticamente un manual.

- **Silvester, R. Y Hsu, J.R.C.** Coastal Stabilization. World Scientific. 1997.

Este libro se dedica primordialmente a la discusión de las diferentes posibles actuaciones para la defensa de la costa. Las formas en planta de equilibrio como elemento de protección de costas u otras actuaciones convencionales como diques, espigones, regeneraciones de playa, etc. son presentadas con detalle mediante la presentación de casos prácticos.

- **Sleath, J.F.A.** Sea Bed Mechanics. John Wiley & Sons. 1984.

Este libro estudia los diversos aspectos implicados en el flujo de un fluido cerca del lecho marino, corrientes, disipación de energía, formación de ripples y dunas y el transporte de sedimentos. Es un compendio de información, resultante de la visión homogénea de numerosos artículos publicados en este campo. Es sin duda uno de los libros más completos en este tema. Muy recomendable para alumnos.

- **Stoker, J.J.** Water Waves. Interscience Publishers Inc.. John Wiley & Sons. 1957.

Presenta la teoría matemática del movimiento oscilatorio en líquidos con superficie libre y aplicaciones a una amplia variedad de problemas físicos. La mayor parte de los problemas aquí presentados aparecen en muchos de los otros libros sobre teoría de ondas publicados posteriormente. Aun así, es interesante especialmente las soluciones que se presentan haciendo uso de la variable compleja.

- **Sumer, M. y Fredose, J.** Hydrodynamics around cylindrical structures. World Scientific. 1997.

Este libro se dedica al estudio de la interacción ola-corriente con cilindros, enfocándose sobre el flujo alrededor del cilindro, las fuerzas sobre el cilindro y las

vibraciones inducidas en estructuras esbeltas. El libro es una buena introducción al tema en cuestión para alumnos de Master y de Doctorado.

- **Svendsen, I. A. y Jonsson, I.G.** Hydrodynamics of Coastal Regions. Technical University of Denmark. 1980.

Un libro muy claro y recomendable para estudiantes, que trata los problemas básicos de la teoría de ondas de pequeña amplitud y de amplitud finita, el efecto del fondo en la propagación y la reflexión. Añade además una serie de interesantes ejercicios educativos. Un texto, en suma, que combina de manera casi perfecta la sencillez y claridad en la exposición con el rigor físico-matemático de las teorías.

- **Tennekes, H. y Lumley, J.L.** A First Course in Turbulence. The MIT Press. 1990.

Este texto ha sido escrito para estudiantes, ingenieros y científicos con muy diferentes bases educacionales. En el se introduce al lector en el fenómeno de la turbulencia sin realizar difíciles desarrollos matemáticos, favoreciendo el entendimiento físico de una manera intuitiva. Constituye probablemente el texto introductorio al problema, aun sin resolver por completo, de la turbulencia.

- **Tomczack, M. and Godfrey, J.S.** Regional Oceanography: An Introduction. Pergamon Press. 1994.

Un libro interesante en el que se presenta la oceanografía física desde el punto de vista regional. Los autores muestran los principales procesos asociados a la ocenografía física describiendo los mismo en cada uno de los océanos y mares más importantes del planeta.

- **van Rijn, L.C.**. Sediment Transport under Waves and Currents. Acqua Publ., 1995.

Libro escrito a partir de las notas de clase que el autor imparte en la Universidad de Utrecht en Holanda, con estilo de Manual. No proporciona mucha información teórica, sin embargo es claro a la hora de establecer los métodos de cálculo.

- **Whitehouse, R.** Scour at Marine Structures. Thomas Telford. 1998.

En este libro se hace un compendio del conocimiento existente sobre la erosión inducida por el oleaje y las corrientes en estructuras marítimas. El autor analiza los resultados reales y de laboratorio existentes así como las aproximaciones analíticas y

numéricas al problema, para finalmente dar una metodología útil para determinar tanto la erosión potencial como la extensión de la misma para una estructura dada.

- **Wiegel, R.L.** Oceanographical Engineering. Prentice Hall Inc.. 1964.

Libro clásico de la Ingeniería Oceanográfica, donde el autor aborda muchos de los temas que a ella le competen. El tratamiento de algunos temas es, lógicamente, anticuado. Sin embargo, los ejemplos presentados son muy ilustrativos y útiles para la docencia.

- **Wood, I.R., Bell, R.G. and Wilkinson, D.L.** Ocean Disposal of Wastewater. World Scientific. 1993.

Este libro ofrece una visión global de la problemática que se establece al realizar vertidos al mar. Se centra especialmente en el diseño del emisario y sus difusores después de revisar la normativa anglosajona. Proporciona métodos para calcular la dilución inicial así como para realizar un seguimiento posterior del vertido. Interesante para introducirse en este tema de la ingeniería litoral.

1.2. Revistas

Bajo este epígrafe se incluyen las publicaciones nacionales e internacionales de carácter periódico en las que los temas de la Ingeniería Oceanográfica son prioritarios o aparecen dentro del marco general de la Mecánica de Fluidos o de la Oceanografía Física. Obviamente no se incluyen todas las publicaciones, sino solo aquellas que juzgamos de interés y creemos necesario su conocimiento tanto desde el punto de vista ingenieríl como investigador.

Primeramente se citan aquellas revistas que directamente se dirigen al área de la Ingeniería litoral, gestión del litoral, etc.

- Applied Ocean Research, ELSEVIER
- Coastal Engineering, ELSEVIER
- Journal of Coastal Engineering, World Scientific (anteriormente Coastal Engineering in Japan)
- Journal of Coastal Research, Coastal Research Foundation
- Journal of Waterway, Port, Coastal and Ocean Engineering, American Society of Civil Engineers (ASCE).
- Ocean Engineering, Pergammon Press
- PIANC Bulletin
- Shore & Beach, American Shore & Beach Preservation Association
- Shoreline and Coastal Management
- Terra et Aquae

A continuación se enumeran revistas que cubren cualquier campo de la oceanografía y más orientadas hacia las ciencias marinas.

- Continental Shelf Research
- Estuarine, Coastal and Shelf Science
- Journal of Experimental Marine Biology and Ecology
- Journal of Geophysical Research, American Geophysical Union
- Journal of Marine Research.
- Journal of Physical Oceanography.
- Marine Geology, ELSEVIER

La siguiente lista corresponde a revistas que no siendo específicas del área de la Ingeniería Oceanográfica, recogen en muchas ocasiones secciones o artículos de importancia para algunas de las áreas que cubre nuestra especialidad.

- Experiments in Fluids
- Fluids and Structures
- Hydromechanics and Hydraulic Engineering Abstracts. Delft Hydraulics Laboratory.
- Ingeniería del Agua
- International Journal for Numerical Methods in Fluids
- Journal of Engineering Mechanics, American Society of Civil Engineers, ASCE.
- Journal of Fluid Mechanics. Cambridge University Press.
- Journal of Hydraulic Engineering. American Society of Civil Engineers, AS CE.
- Journal of Hydraulic Research, IAHR.
- Proceedings of the Royal Society. The Royal Society of London.
- Physics of Fluids
- Revista de Obras Públicas
- Wave Motion. Elsevier Science Publishers. Amsterdam (Holanda). Publicación mensual.

Es importante destacar que muchas de estas revistas pueden encontrarse en su formato electrónico en Internet.

Además, también es necesario hacer un comentario sobre la ingente proliferación de revistas científicas que se está produciendo en los últimos años. Esto, sin duda, esta produciendo una dispersión importante del conocimiento dado que es prácticamente imposible pretender tener suscripciones a todas las revistas que pueden considerarse interesantes. Por otro lado, el aumento del número de revistas trae consigo una altísima especialización así como, seguramente, una reducción en la calidad de las mismas.

1.3. Normativa

En la docencia de el área de la Ingeniería Oceanográfica se explicará la normativa española relativa a Puertos y Costas, que puede encontrarse en las diversas publicaciones de los Ministerios de Fomento y de Medio Ambiente. Sin embargo, merecen una mención especial, por su importancia, las publicaciones resultado del Programa de Recomendaciones para Obras Marítimas (ROM).

Recomendaciones para Obras Marítimas (ROM)

El Ministerio de Obras Públicas y Transportes (MOPT), a través de la Dirección General de Puertos, y hoy en día el Ente Público PUERTOS del ESTADO, está llevando a cabo desde 1987 un programa de desarrollo tecnológico en el ámbito de las Obras Marítimas y Portuarias, con el objetivo de redactar y difundir un conjunto de Recomendaciones o "Códigos de Buena Práctica" para el proyecto y ejecución de dichas obras, que constituyan un embrión de la Normativa española en este campo de la ingeniería. Estas Recomendaciones para Obras Marítimas (ROM), pretenden definir un conjunto ordenado de criterios técnicos que, sin tener por el momento carácter vinculante o normativo, orienten a proyectistas, directores y constructores de obras portuarias hacia la obtención de niveles de calidad y garantía exigibles en dichas obras.

El programa ROM tiene redactado o en fase avanzada de elaboración, hasta la fecha, los siguientes códigos:

Recomendaciones Generales

ROM 0.1-89: Redacción de Proyectos.
ROM 0.2-90: Acciones en el Proyecto de Obras Marítimas y Portuarias.
ROM 0.3-91: Acciones Medioambientales I: Oleaje
ROM 0.4-91: Acciones Medioambientales II: Viento

Recomendaciones Específicas

ROM 0.5-94: Recomendaciones Geotécnicas para el Proyecto de Obras Marítimas y Portuarias.
ROM 0.6-94: Recomendaciones para Pavimentos en Areas Portuarias
ROM 0. ~98: Recomendaciones para Obras de Abrigo frente a la Acción del Oleaje.
ROM 0. ~98: Recomendaciones para Escolleras en Obras Marítimas

Como ya se ha dicho anteriormente estas publicaciones, aunque aún solo tienen el carácter de recomendaciones, son empleadas en la práctica en cualquier proyecto

del área de la Ingeniería Oceanográfica. Por ello, se considera que, aunque solo sea de algunas de sus partes, el conocimiento de las mismas por parte del alumno es absolutamente necesario.

1.4. Bases de datos y direcciones de Internet interesantes

Hoy en día Internet posibilita el acceso a una gran cantidad de información relativa a cualquier área del saber o técnica. Como es obvio el área de la Ingeniería Oceanográfica no se ha mantenido al margen de esta fuente de información haciendo posible encontrar una gran cantidad de datos interesantes en la red.

La mayor parte de estas bases de datos, ya sean datos oceanográficos o referencias bibliográficas, son accesibles a través de Internet. Incluso las bases de datos generadas en proyectos específicos europeos suelen estar disponibles para los participantes en el proyecto a través de Internet.

De entre las direcciones en Internet de mayor interés cabe destacar:

- http://www.geocities.com/CapeCanaveral/Launchpad/9631/hydro.html

Contiene información sobre el software disponible en el área de la ingeniería oceanográfica

- http://puertos.es/home.html

Esta es la dirección del servidor del Programa de Clima Marítimo con información general sobre este Programa tan importante.

- http://puertos.es/redes.html

Corresponde a las redes del Programa de Clima Marítimo que como se sabe mantiene la red de boyas, mareógrafos y radares de nuestro litoral. A través de esta dirección se puede obtener información relativa a oleaje, mareas, etc.

- http://diu.cms.udel.edu/woce/oceanic.html

Esta es la página central del gran proyecto WOCE cuyo objetivo fundamental es la investigación del océano. En ella se pueden encontrar gran cantidad de datos relativos a corriente oceánicas.

- http://www.ncep.noaa.gov/

Dirección principal de la NOAA que es la agencia estadounidense responsable todos la mayor parte de los estudios y proyectos de investigación que se hacen en el medio marino. Tiene gran cantidad de información general, publicaciones, datos oceanográficos, etc.

- http://www.mpc.ncep.noaa.gov/

En esta dirección se pueden obtener datos de corrientes, oleaje, vientos, etc. en todo el mundo. Estos datos son facilitados por NOAA.

- http://www.nodc.noaa.gov/

Página central de la NODC (National Oceanographic Data Center) donde también se pueden encontrar gran cantidad de datos oceanográficos.

- http://128.160.23.42/dbdbv/dbdbv.html

La Armada de los Estados Unidos cuenta también con un gran cantidad de información disponible relativa al medio marino. En esta dirección puede encontrarse información relativa a batimetrías, datos oceanográficos, etc.

- http://hlnet.wes.army.mil/software/aces/

El Coastal Engineering Research Center (CERC) de los Estados Unidos, tiene en esta página toda la información relativa al software que ha ido desarrollando como herramienta para la realización de estudios y proyectos en el área de la ingeniería de costas. El CERC cuenta también con una importante colección de publicaciones e informes técnicos en los que han ido recogiendo los resultados de sus trabajos.

- http://www.aos.princeton.edu/WWWPUBLIC/htdocs.pom/

Esta página recoge toda la información relativa al modelo tridimensional para el estudio de la dinámica marina de mayor difusión en todo el mundo, el Princeton Oceanic Model desarrollado por Blumberg y Mellor.

- http://www.dhi.dk/general/dhisoft.htm

En esta dirección se puede obtener toda la información relativa a los modelos desarrollados por el Danish Hydraulic Institute.

Por otro lado, con los diferentes buscadores que hay disponibles en Internet se puede realizar cualquier tipo de búsqueda con el fin de averiguar que información hay disponible.

1.5. Congresos y conferencias

Los congresos y conferencias son eventos importantes por tres razones fundamentales:

1. Permiten conocer el estado del arte de la investigación en un campo concreto.

2. Suelen tener como resultado unos "Proceedings" con artículos sumamente útiles en la labor investigadora, dependiendo de la conferencia.

3. Son un foro para intercambiar ideas y fomentar posibles actividades conjuntas entre investigadores de diferentes centros y países.

El congreso más importante del mundo sobre ingeniería litoral es, sin duda alguna, por número de congresistas, difusión y repercusión de sus Proceedings es el "International Conference on Coastal Engineering (ICCE)" organizado cada dos años por la American Society of Civil Engineers (ASCE). La primera edición de esta conferencia tuvo lugar en 1954, estando programada la vigesimoséptima edición en Sydney en Julio del 2000.

La American Society of Civil Engineers (ASCE) organiza también conferencias sectoriales, las más importantes en su temática, con mayor o menor regularidad. Entre ellas se encuentran:

- Coastal Structures

Conferencia específica sobre obras marítimas celebrada en su última edición en Santander y, por primera vez, fuera de los Estados Unidos.

- Coastal Sediments

Esta conferencia aborda todos los temas relacionados con el transporte de sedimentos.

- Coastal Dynamics

Coastal Dynamics está destinada a reunir a aquellos investigadores que investigan las diferentes dinámicas que aparecen en el litoral. Se prima especialmente aquellos artículos que tengan información relativa a investigación realizada en el campo.

- Coastal Zone

Los contenidos de esta conferencia van en general dirigidos a la gestión integral de la costas.

- Ports

Cualquier tema portuario, obras marítimas, explotación de puertos, etc. tiene cabida en esta conferencia.

Otros congresos de gran interés organizados por otras instituciones son, por ejemplo,

- Offshore Technology Conference
- Port and Ocean Engineering under Artic Conditions (POAC)
- IAHR Congress
- Coastal and Port Engineering in Developing Countries (COPEDEC)
- Jornadas Españolas de Puertos y Costas
- American Geophysical Union Fall and Spring Meetings
- Hydroinformatics
- Coastal Engineering, Wessex
- Marina, Wessex

Además de estos, que son congresos bien establecidos en cuanto a su organización, cada año se celebran gran cantidad de simposiums, seminarios y reuniones en todo el mundo.

1.6. Centros de investigación

A continuación se presenta una lista, por países, de aquellos centros relevantes que se dedican a la investigación y desarrollo en el área de la Ingeniería Oceanográfica. La mayor parte de ellos cuenta con publicaciones en las que presentan los resultados de sus trabajos, generalmente en forma de informes técnicos.

Alemania

- Universidad de Hamburgo
- Universidad Braunschweig

Canada

- National Research Council. Hydraulics Laboratory.
- Universidad de British Columbia

Dinamarca

- Institute of Hydrodynamics and Hydraulic Engineering (ISVA). Technical University of Denmark.
- Danish Hydraulic Institute (DHI)
- Universidad de Aalborg

España

- Canal de Experiencias Hidrodinámicas
- Centro de Estudios de Puertos y Costas (CEPYC), CEDEX
- Centro de Salvamento Marítimo Jovellanos, Marina Mercante
- Consejo Superior de Investigaciones Científicas, CSIC
- Instituto Español de Oceanografía
- Puertos del Estado
- Universidad de Cádiz
- Universidad de Cantabria
- Universidad de Granada
- Universidad de La Coruña
- Universidad Politécnica de Cataluña
- Universidad Politécnica de Madrid
- Universidad Politécnica de Valencia
- Universidad de Las Palmas

Holanda

- Delft Hydraulics
- Delft University of Technology

Japón

- Port and Harbour Research Institute
- Universidad de Yokohama
- Universidad de Osaka

Noruega

- Norwegian Institute of Technology (SINTEF)
- Universidad de Trondheim

Reino Unido

- Proudman Oceanographic Lab
- HR Wallingford
- Universidad de Bristol
- Universidad de Plymouth
- Universidad de Edimburgo

U.S.A.

- Coastal Engineering Research Center (CERC)
- Center for Applied Coastal Research (Universidad de Delaware)
- Scripps Institution of Oceanography
- Oregon State University
- University of Florida
- Texas A&M
- Massachussetts Institute of Technology (MIT)
- Woods Hole Oceanographic Institution

Sección 2.

MÉTODOS EXPERIMENTALES

DOCUMENTO DE REFERENCIA

ÍNDICE

MÉTODOS EXPERIMENTALES

Capítulo 1. Modelos físicos 1

1.1 Introducción 1

1.2 Ventajas y desventajas de los modelos físicos 1

1.3 Tipos de modelo 2

1.4 Otras definiciones 3

Capítulo 2. Análisis dimensional 4

2.1 Principio del análisis dimensional 4

2.2 Monomios adimensionales para fluidos 5

Capítulo 3. Principios de la semejanza 7

3.1 Introducción 7

3.2 Requisitos para la semejanza 7

3.3 Factor de escala 8

3.4 Semejanza geométrica 8

3.5 Semejanza cinemática 9

3.6 Semejanza dinámica 11

3.7 Semejanza hidráulica 14

3.8 Criterios específicos 14

3.9 Importancia de la semejanza del número de Froude 20

3.10 Distorsión de los modelos 24

Capítulo 4. Modelos hidrodinámicos 27
4.1 Introducción a los modelos hidrodinámicos 27
4.2 Modelos de ondas de corto período 28

Bibliografía 46

Capítulo 1. MODELOS FÍSICOS

1.1. INTRODUCCIÓN

Se denomina modelo físico a la reproducción (generalmente a escala reducida) de un sistema físico de tal modo que las fuerzas dominantes actuantes sobre el sistema queden representadas en el modelo en las proporciones correctas.

Los objetivos para la realización de un modelo físico son fundamentalmente:

a) Aumentar el conocimiento cualitativo de un fenómeno aún no descrito o entendido.

b) Obtener mediciones para contrastar un resultado teórico.

c) Obtener mediciones de algunos fenómenos sumamente complicados e inabordables teóricamente.

1.2. VENTAJAS Y DESVENTAJAS DE LOS MODELOS FÍSICOS

Ventajas de los modelos físicos:

1) Estudio del sistema físico sin hipótesis simplificativas necesarias para los modelos analíticos o numéricos.

2) El tamaño reducido de los modelos físicos permite la obtención de una gran cantidad de datos a bajo coste. Las medidas en el campo requieren un mayor coste y son más complejas.

Desventajas de los modelos físicos:

1) *Efectos de escala.*
Se produce en modelos más pequeños que el prototipo, cuando no se ha podido realizar correctamente la analogía de todas las variables o su interrelación. Los efectos de escala son al modelo físico como las hipótesis simplificativas a los modelos teóricos. Un típico efecto de escala en los modelos de ingeniería de costas es el hecho de que las fuerzas viscosas son relativamente mayores en el modelo que en el prototipo.

2) *Efectos de laboratorio.*
Dan lugar a diferencias entre el modelo y el prototipo y son debidas a las limitaciones del laboratorio como son las técnicas de generación de ondas, los contornos del canal o tanque, etc.

1.3. TIPOS DE MODELO

Modelos de lecho fijo son aquellos cuyos contornos no pueden ser modificados por la hidrodinámica del proceso estudiado. Se utilizan para el estudio de ondas, corrientes o fenómenos hidrodinámicos similares. También para el estudio de la interacción de ondas con obstáculos, principalmente para la evaluación de fuerzas. Los efectos de escala asociados a este tipo de modelos son bastante bien conocidos.

Los **modelos de lecho móvil** son aquellos que incluyen un lecho que puede variar de acuerdo con las fuerzas hidrodinámicas presentes. Los efectos de escala que se producen no son tan bien conocidos, como para los modelos de lecho fijo. Por ello, los resultados deben ser utilizados con cierta cautela. Este tipo de modelos abarca el estudio de evolución de perfiles de playa, erosión de dunas, desarrollo de formas de lecho, estudios de erosión, etc. Otro tipo de clasificación podría realizarse respecto al alcance temporal dividiendo los modelos en:

1) a corto plazo
2) a largo plazo.

Los primeros se dedican a estudiar la evolución del sistema físico en un período de horas o, a lo sumo días. Sin embargo, los modelos a largo plazo pretenden simular el comportamiento en un período de días a años.

1.4. OTRAS DEFINICIONES

- Se llama **prototipo** a la situación que desea ser modelada.

- Se define **escala** como una proporción constante entre características cuantificables de modelo y prototipo, las cuales son cocientes entre los valores de un parámetro dado correspondientes al prototipo y al modelo.

- **Criterio de escalamiento** son condiciones matemáticas formales que se imponen a las escalas.

- La **semejanza** es una condición que se produce cuando un modelo da una respuesta similar a la del prototipo.

- El **modelo matemático** es una representación matemática de la física de un proceso. Estos modelos pueden ser resueltos analíticamente en casos simples mientras que para casos más complejos precisan soluciones numéricas.

- Un caso particular del modelo matemático es el **modelo numérico** en el cual las ecuaciones que gobiernan el proceso físico son discretizadas y resueltas mediante algoritmos numéricos utilizando un ordenador. La discretización puede ser realizada en el espacio y en el tiempo.

- Un **modelo híbrido** es aquel en el que, debido a la complejidad del flujo, es necesario combinar los resultados de modelos físicos y matemáticos para representar el proceso sometido a estudio.

Capítulo 2. ANÁLISIS DIMENSIONAL

2.1. PRINCIPIOS DE ANÁLISIS DIMENSIONAL

El primer paso a la hora de analizar un fenómeno físico es determinar qué variables físicas se encuentran involucradas en el mismo. El siguiente paso consistirá en realizar estudios teóricos o experimentales para determinar las relaciones funcionales entre estas variables. Evidentemente, a mayor número de variables, mayor será el número de experimentos necesarios para conocer las relaciones. Sin embargo, el esfuerzo se verá notablemente reducido si varias variables pueden ser combinadas para formar una nueva variable adimensional. El Análisis Dimensional es un procedimiento racional para combinar varias variables físicas para formar un producto adimensional (monomio) reduciendo, por tanto, el número de variables que precisa ser considerado para estudiar un proceso físico.

Para realizar un análisis dimensional es necesario seguir los siguientes pasos:

1) Identificar las variables independientes del proceso.

2) Decidir qué variables pueden ser consideradas como dependientes.

3) Determinar cuantos productos adimensionales pueden obtenerse.

4) Reducir el conjunto total de variables al número indicado de productos adimensionales.

2.2. MONOMIOS ADIMENSIONALES PARA FLUIDOS

Una vez determinadas las variables del problema será necesario formar una serie de monomios adimensionales a partir del análisis dimensional y del conocimiento del problema. Esto es importante debido a las siguientes razones:

1) El uso de monomios adimensionales reduce el número de variables que debe ser estudiado ya sea experimental, numéricamente o mediante campañas de campo.

2) Mediante gráficos adimensionales se puede cubrir un rango de parámetros más amplio.

3) Los gráficos adimensionales pueden obtenerse a partir de modelos físicos siempre y cuando se haya preservado la escala de los monomios adimensionales entre prototipo y modelo.

4) Los monomios adimensionales pueden ser utilizados como base para escalar modelos contribuyendo tanto a su diseño como a la interpretación de los resultados.

5) El uso de monomios adimensionales posibilita una planificación de ensayos y presentación de resultados de forma condensada y sistemática.

La formación de monomios adimensionales puede ser algo arbitraria. A veces, a partir de la observación y del conocimiento del problema pueden definirse monomios tales como: el parámetro de caída del grano ($H/\omega T$), el índice de rotura (H_b/h). En otras ocasiones dichos monomios surgen de las derivaciones matemáticas, para teoría lineal (H/L), el parámetro de Ursell, (L^2H/h^3), de la teoría de Stokes, etc.

Estos parámetros son propios de la ingeniería de costas, sin embargo, existe una serie de monomios adimensionales característicos de la mecánica de fluidos en general que son de gran importancia. Dichos monomios se recogen en la Tabla número 1.

TABLA N.° 1

Número de Reynolds	$Re = \frac{\rho V L}{\mu} = \frac{V L}{\nu}$
Número de Froude	$Fr = \frac{v}{\sqrt{g L}}$
Número de Euler (coef. de presión)	$Eu = \frac{F}{\rho V^2 L^2} = \frac{p}{\rho V^2}$
Número de Weber	$We = \frac{\rho V^2 L}{\sigma}$
Número de Cauchy	$Ca = \frac{\rho V^2}{E}$
Número de Mach	$Ma = \frac{V}{c}$
Número de Strouhal	$St = \frac{\omega L}{V}$

ρ = densidad
V = velocidad
L = longitud
μ = coeficiente de viscosidad dinámica
ν = coeficiente de viscosidad cinemática
g = aceleración de la gravedad
F = fuerza
p = presión
σ = tensión superficial
E = módulo de elasticidad
c = velocidad del sonido
ω = frecuencia angular

Estos números fueron establecidos mediante argumentos físicos antes de la aparición del análisis dimensional.

Capítulo 3. PRINCIPIOS DE LA SEMEJANZA

3.1. INTRODUCCIÓN

Idealmente, un modelo bien diseñado debería mostrar el mismo comportamiento (a escala reducida) que el prototipo. Para un modelo de un proceso hidrodinámico este comportamiento semejante debiera incluir velocidad, aceleración, transporte de masa y las fuerzas resultantes sobre el objeto sometido a estudio o sobre los contornos. La semejanza es alcanzada cuando todos los factores importantes del fenómeno se encuentran escalados entre el prototipo y el modelo mientras que aquellos que no lo están deben ser de carácter despreciable en la naturaleza del fenómeno.

3.2. REQUISITOS PARA LA SEMEJANZA

Los modelos físicos pueden suministrar tanto información cualitativa como cuantitativa. Los requisitos para la semejanza dependen del problema que pretende ser estudiado así como del grado de exactitud que se desee obtener en la reproducción del comportamiento del prototipo. Se llama modelo completamente semejantes a aquel en el que todos los valores de monomios adimensionales relevantes para el problema se conservan iguales a los del prototipo. La semejanza geométrica es un requisito

indispensable para la semejanza completa. Otro tipo de semejanzas son la cinemática y la dinámica.

3.3. FACTOR DE ESCALA

Se denomina escala a la relación entre un parámetro del prototipo y el valor del mismo parámetro en el modelo.

$$N_x = \frac{X_p}{X_m} = \frac{\text{Valor de X en el prototipo}}{\text{Valor de X en el modelo}}$$

Muchas de las escalas no pueden ser obtenidas independientemente sino utilizando otras previamente definidas, así, por ejemplo para la velocidad:

$$N_V = \frac{V_p}{V_m} = \frac{\left(\frac{L}{t}\right)_p}{\left(\frac{L}{t}\right)_m} = \left(\frac{L_p}{L_m}\right)\left(\frac{t_m}{t_p}\right) = \frac{N_L}{N_t}$$

3.4. SEMEJANZA GEOMÉTRICA

La semejanza geométrica entre dos objetos o sistemas existe si el cociente entre las correspondientes dimensiones lineales es igual. Esta semejanza es independiente del movimiento y concierne exclusivamente a la forma. Los modelos que poseen semejanza geométrica se llaman modelos sin distorsionar y tanto las escalas verticales como horizontales son las mismas. Estos modelos son verdaderas miniaturas del prototipo que incluyen detalles del prototipo incluso tales como la rugosidad superficial.

Ejemplo:

La ecuación del perfil de equilibrio es:

$$h = A\, x^{\frac{2}{3}}$$

Se desea reproducir este perfil en un canal de oleaje con la escala $N_L = 25$. Determina la escala del parámetro A.

$$\frac{h_p}{h_m} = \frac{A_p x_p^{2/3}}{A_m x_m^{2/3}}$$

$$\frac{h_p}{h_m} = \left(\frac{A_p}{A_m}\right)\left(\frac{x_p}{x_m}\right)^{\frac{2}{3}} \quad - \quad N_A = \frac{N_h}{N_x^{2/3}}$$

Si el modelo es sin distorsionar $N_h = N_x = N_L$

$$N_A = N_L^{1/3} = (25)^{\frac{1}{3}} = 2.92$$

Por tanto, deberá emplearse la siguiente relación:

$$\frac{A_p}{A_m} = 2.92$$

3.5. SEMEJANZA CINEMÁTICA

La semejanza cinemática concierne exclusivamente al movimiento de las partículas y se produce cuando el cociente entre todas las componentes del campo de velocidades del prototipo y el modelo es el mismo para todas las partículas y en todo instante. Si existe semejanza cinemática en un modelo con semejanza geométrica las trayectorias de las partículas son semejantes a las del prototipo.

Ejemplo:

¿Cuál es el escalamiento necesario para tener semejanza cinemática para ondas (teoría lineal) cuya longitud viene dada por la siguiente ecuación?

$$L = \frac{gT^2}{2\pi} \tanh\left(\frac{2\pi h}{L}\right)$$

L = longitud de la onda
g = aceleración de la gravedad
T = período de la onda
h = profundidad

Obsérvese que $\left(\frac{2\pi h}{L}\right)$ es adimensional, por tanto, en un modelo sin distorsionar deberá conservarse esta relación, es decir:

$$\frac{\left(\frac{2\pi h}{L}\right)_p}{\left(\frac{2\pi h}{L}\right)_m} = \left(\frac{h_p}{h_m}\right)\left(\frac{L_m}{L_p}\right) = \frac{N_h}{N_{LON}}$$

Es evidente, que esta relación también es válida cuando se trata de la tanh de dichos parámetros.

La relación entre las escalas de la longitud de onda y del período puede encontrarse de:

$$\frac{\left[L = \frac{gT^2}{2\pi} \tanh\left(\frac{2\pi h}{L}\right)\right]_p}{\left[L = \frac{gT^2}{2\pi} \tanh\left(\frac{2\pi h}{L}\right)\right]_m}$$

que puede ponerse como:

$$\frac{L_p}{L_m} = \left(\frac{g_p}{g_m}\right)\left(\frac{T_p}{T_m}\right)^2$$

$$N_{LON} = N_g \bullet N_T^2$$

Es claro que $N_g = 1$ y que cuando el modelo no es distorsionado $\frac{N_h}{N_{LON}} = 1$. Además, dado que $N_{LON} = N_L$, se llega a que para tener semejanza cinemática deberá cumplirse,

$$N_T = \sqrt{N_L}$$

3.6. SEMEJANZA DINÁMICA

Hemos visto que la semejanza cinemática es independiente de las propiedades del fluido y por ello ésta seguirá cumpliéndose incluso con diferentes densidades del fluido para modelo y prototipo. Sin embargo, las fuerzas que las ondas ejercen sobre una estructura o los contornos no serán semejantes en el modelo a no ser que se satisfagan una serie de condiciones adicionales relativas a las propiedades del fluido. Estas condiciones conducen a la semejanza dinámica.

La semejanza dinámica entre dos sistemas que poseen semejanzas geométricas y cinemáticas precisa que el cociente de todas las fuerzas vectoriales del sistema sea el mismo.

La semejanza dinámica proviene de la 2ª Ley de Newton:

$$m\frac{dV}{dt} = \sum_n F_n$$

Para problemas de la mecánica de fluidos la 2ª Ley de Newton puede escribirse como:

$$\vec{F}_i = \vec{F}_g + \vec{F}_\mu + \vec{F}_\sigma + \vec{F}_e + \vec{F}_{pr}$$

donde:

$\vec{F}_i$ = fuerzas de inercia (masa x aceleración)
$\vec{F}_g$ = fuerzas gravitatorias
$\vec{F}_\mu$ = fuerzas viscosas
$\vec{F}_\sigma$ = fuerzas debidas a la tensión superficial
$\vec{F}_e$ = fuerzas de compresión
$\vec{F}_{pr}$ = fuerzas de presión

La semejanza dinámica global implica,

$$\frac{(\vec{F}_i)_p}{(\vec{F}_i)_m} = \frac{(\vec{F}_g + \vec{F}_\mu + \vec{F}_\sigma + \vec{F}_e + \vec{F}_{pr})_p}{(\vec{F}_g + \vec{F}_\mu + \vec{F}_\sigma + \vec{F}_e + \vec{F}_{pr})_m}$$

Además, la semejanza perfecta requiere que individualmente todas las fuerzas satisfagan:

$$\frac{(\vec{F}_i)_p}{(\vec{F}_i)_m} = \frac{(\vec{F}_g)_p}{(\vec{F}_g)_m} = \frac{(\vec{F}_\mu)_p}{(\vec{F}_\mu)_m} = \frac{(\vec{F}_\sigma)_p}{(\vec{F}_\sigma)_m} = \frac{(\vec{F}_e)_p}{(\vec{F}_e)_m} = \frac{(\vec{F}_{pr})_p}{(\vec{F}_{pr})_m}$$

que en función de las escalas puede ponerse como:

$$N_{\vec{F}_i} = N_{\vec{F}_g} = N_{\vec{F}_\mu} = N_{\vec{F}_\sigma} = N_{\vec{F}_e} = N_{\vec{F}_{pr}}$$

Esta condición garantiza que la influencia relativa de cada fuerza actuante sobre el sistema mantenga las proporciones entre el modelo y el prototipo.

Ejemplo:

Semejanza dinámica en la estabilidad de un dique de escollera.

El modelo de un dique de escollera ha sido construido con piedras con un peso medio de 5 Newton (~500 g). El modelo muestra que para oleaje irregular el dique falla para olas con altura de ola significante H_S = 0.3 m. ¿Qué peso será necesario para resistir en el prototipo olas de H_S = 10 m?. Asume que el modelo presenta semejanza geométrica y que la piedra del prototipo tiene el mismo peso específico que la correspondiente al modelo. Para este caso se asumirá que no existe diferencia alguna al emplear agua dulce en el modelo.

La escala longitudinal viene determinada por:

$$N_L = \frac{(H_S)_p}{(H_S)_m} = \frac{10\,\text{m}}{0.3\,\text{m}} = 33.3$$

El peso de las piezas es $W_S = \gamma_S \bullet V_S$, donde V_S es el volumen de la piedra y γ_S su peso específico. En función de las escalas,

$$N_{W_S} = \frac{(W_S)_p}{(W_S)_m} = \frac{(\gamma_S)_p}{(\gamma_S)_m} \bullet \frac{(V_S)_p}{(V_S)_m} = N_{\gamma_S} N_{V_S}$$

Dado que el material es el mismo en el prototipo y en el modelo $N_{\gamma_S} = 1$. Asimismo, en un modelo con semejanza geométrica la escala volumétrica es simplemente, $N_{V_S} = N_L^3$. Substituyendo,

$$N_{W_S} = \frac{(W_S)_p}{(W_S)_m} = N_L^3 = (33.3)^3 = 37037$$

Por tanto, el modelo indica que el peso necesario para resistir olas de H_S = 10 m en el prototipo es:

$$(W_S)_p = 37037\,(W_S)_m = 37037 \bullet 5\,N = 185.2\,KN \approx 19\,T$$

3.7. SEMEJANZA HIDRÁULICA

La obtención de una semejanza completa en la que todas las relaciones entre fuerzas sean constantes e iguales es imposible salvo en el caso de que utilicemos la escala del prototipo. En la mayor parte de los casos, la experiencia y el sentido común servirán para determinar aquellas relaciones para las cuales es imprescindible mantener la semejanza y aquellas para las que puede admitirse ciertas desviaciones, intentando introducir ciertas correcciones teóricas que corrijan dichas desviaciones.

En cualquier caso, la exactitud del modelo viene condicionada por los objetivos que se pretende alcanzar en el estudio.

3.8. CRITERIOS ESPECÍFICOS

La experiencia ha indicado que la mayor parte de los problemas en hidráulica puede ser simplificado hasta la interacción entre dos fuerzas fundamentalmente. Ello permite desarrollar criterios de semejanza de forma teórica.

Las fuerzas de inercia se encuentran siempre presentes en los problemas de mecánica de fluidos. Por tanto, esta fuerza debe ser equilibrada por alguna de las otras fuerzas mencionadas anteriormente. El primer paso consistirá en la expresión de las fuerzas en función de sus unidades físicas.

Por tanto,

$\vec{F}_i$ = masa x aceleración = $(\rho L^3)\left(\frac{V^2}{L}\right) = \rho L^2 V^2$

donde la aceleración ha sido tomada como convectiva (por ejemplo $u\frac{\partial u}{\partial x}$)

$\vec{F}_g$ = masa x aceleración de la gravedad = $\rho L^3 g$

$\vec{F}_\mu$ = viscosidad x $\frac{\text{velocidad}}{\text{distancia}}$ x área = $\mu\left(\frac{V}{L}\right)L^2 = \mu V L$

$\vec{F}_\sigma$ = unidad de tensión superficial x longitud = σL

$\vec{F}_e$ = módulo de elasticidad x área = $E L^2$

$\vec{F}_{pr}$ = unidad de presión x área = $p L^2$

donde:

ρ = densidad del fluido
L = longitud
V = velocidad
t = tiempo
g = aceleración de la gravedad
μ = viscosidad dinámica
σ = tensión superficial
E = módulo de elasticidad
p = presión

El cociente entre la fuerza de inercia y cualquiera de las otras fuerzas dará la influencia de estas fuerzas para cada tipo de flujo.

Obligando a que este cociente entre fuerzas sea el mismo en el modelo y en el prototipo llegamos a un criterio de semejanza para cada una de las relaciones entre las mismas. Estos criterios de semejanza se exponen a continuación.

3.8.1. Criterio de Froude

El parámetro que expresa la influencia relativa de las fuerzas de inercia y gravitatorias en un flujo hidrodinámico viene dado por la raíz cuadrada del cociente entre las fuerzas de inercia y de gravedad, es decir:

$$\sqrt{\frac{\text{fuerzas de inercia}}{\text{fuerzas de gravedad}}} = \sqrt{\frac{\rho L^2 V^2}{\rho L^3 g}} = \frac{V}{\sqrt{gL}} = F_r$$

Este es el número de Froude. También puede interpretarse como el número que da la importancia relativa entre las fuerzas de inercia actuantes sobre la partícula de fluido y el peso de la partícula. En algunas ocasiones también se presenta como el cuadrado de la definición anterior, $\left(\frac{V^2}{gL}\right)$.

Obligando a que el número de Froude sea igual en el modelo y el prototipo se llega a,

$$\left(\frac{V}{\sqrt{gL}}\right)_p = \left(\frac{V}{\sqrt{gL}}\right)_m$$

$$\frac{V_p}{V_m} = \sqrt{\left(\frac{g_p}{g_m}\right)\left(\frac{L_p}{L_m}\right)}$$

que en función de las escalas y operando es,

$$\frac{N_V}{\sqrt{N_g N_L}} = 1 \qquad N_{F_r} = 1$$

Esta ecuación representa el criterio de Froude que debe cumplirse para flujos en los que las fuerzas de inercia son equilibradas por las fuerzas de gravedad principalmente (por ejemplo ondas de gravedad). Este es el caso de casi todos los flujos con superficie libre. Los modelos de ingeniería de costas deben satisfacer, por tanto, este criterio de Froude.

3.8.2. Criterio de Reynolds

Cuando son las fuerzas viscosas las que dominan el flujo el parámetro más importante es el que relaciona las fuerzas de inercia con las viscosas, por tanto:

$$\frac{\text{fuerzas de inercia}}{\text{fuerzas viscosas}} = \frac{\rho L^2 V^2}{\mu V L} = \frac{\rho L V}{\mu} = \frac{L V}{\nu} = \_e$$

que se conoce como número de Reynolds. La interpretación física del número de Reynolds es que éste da la importancia relativa entre las fuerzas de inercia y las fuerzas viscosas sobre una partícula de fluido. En principio Reynolds utilizó este número para diferenciar entre flujo laminar y flujo turbulento.

La semejanza es alcanzada cuando el número de Reynolds es el mismo en el modelo y el prototipo.

$$\left(\frac{\rho LV}{\mu}\right)_p = \left(\frac{\rho LV}{\mu}\right)_m$$

$$\left(\frac{V_p}{V_m}\right)\left(\frac{L_p}{L_m}\right)\left(\frac{\rho_p}{\rho_m}\right) = \frac{\mu_p}{\mu_m}$$

En función de las escalas:

$$\frac{N_V N_L N_\rho}{N_\mu} = 1 \qquad N_{\_e} = 1$$

El criterio de Reynolds es de aplicación para modelar flujos en los que las fuerzas viscosas sean predominantes, como, por ejemplo, problemas de capa límite y de fuerzas sobre cilindros con pequeños números de Reynolds.

3.8.3. Criterio de Weber

El número de Weber establece la relación entre las fuerzas de inercia y las fuerzas debidas a la tensión superficial,

$$\frac{\text{fuerzas de inercia}}{\text{fuerzas de tensi n sup}} = \frac{\rho L^2 V^2}{\sigma L} = \frac{\rho V^2 L}{\sigma}$$

La tensión superficial puede ser importante en la interfase entre dos fluidos. Si estas fuerzas deben ser tenidas en cuenta será de aplicación el criterio de Weber igualando dicho número en el modelo y prototipo.

$$\left(\frac{\rho_p}{\rho_m}\right)\left(\frac{V_p}{V_m}\right)^2\left(\frac{L_p}{L_m}\right)=\left(\frac{\sigma_p}{\sigma_m}\right)$$

que en función de las escalas es:

$$\frac{N_p (N_V)^2 N_L}{N_\sigma}=1 \qquad N_{We}=1$$

En general, en los problemas de ingeniería de costas los efectos de la tensión superficial no son importantes aunque pueden hacer acto de presencia en los modelos como consecuencia de la reducción de las dimensiones.

3.8.4. Criterio de Euler

Aunque la presión suele tomarse como magnitud dependiente, determinada a partir de las demás, pueden presentarse situaciones en las que las fuerzas de presión sean las fuerzas predominantes actuando sobre el fluido. Para esos casos, el número de Euler nos da una indicación de la importancia relativa entre las fuerzas de presión y las de inercia

$$\frac{\text{fuerzas de presi n}}{\text{fuerzas de inercia}}=\frac{pL^2}{\rho L^2 V^2}=\frac{p}{\rho V^2}$$

El criterio de Euler se deriva a partir de asumir que:

$$\left(\frac{p}{\rho V^2}\right)_p=\left(\frac{p}{\rho V^2}\right)_m$$

$$\frac{p_p}{p_m}=\left(\frac{\rho_p}{\rho_m}\right)\left(\frac{V_p}{V_m}\right)^2$$

que en términos de las escalas es:

$$\frac{N_p}{N_\rho N_V^2}=1 \qquad N_{Eu}=1$$

3.8.5. Número de Strouhal

Las fuerzas de inercia pueden ser debidas a dos tipos de aceleración. Las aceleraciones convectivas son debidas a la variación del campo de velocidades entre dos puntos diferentes del fluido y vienen matemáticamente representadas por $u\left(\frac{\partial u}{\partial x}\right)$, $v\left(\frac{\partial v}{\partial y}\right)$, etc. La aceleración local es debida a las variaciones temporales en el campo de velocidades del fluido que tienen lugar en un punto. Representan el carácter oscilatorio del flujo y vienen representadas por términos como $\frac{\partial u}{\partial t}$ $\frac{\partial v}{\partial t}$. En función de sus unidades físicas las fuerzas de inercia debidas a las aceleraciones pueden expresarse como,

$$\text{fuerza de inercia temporal} = (\rho L^3)\left(\frac{V}{t}\right)$$

$$\text{fuerza de inercia convectiva} = (\rho L^3)\left(\frac{V^2}{L}\right)$$

La importancia relativa de cada una de ellas se obtiene a partir del siguiente cociente,

$$\frac{\text{fuerzas de inercia temporales}}{\text{fuerzas de inercia convectivas}}=\frac{(\rho L^3)\left(\frac{V}{t}\right)}{(\rho L^3)\left(\frac{V^2}{L}\right)}=\frac{L}{Vt}$$

que se conoce como número de Strouhal. Este parámetro adimensional es importante para flujo oscilatorio donde el período de oscilación viene dado por la variable t. El número de Strouhal se pone, algunas veces, en función de la frecuencia angular, $\frac{\omega L}{V}$.

Si se desea aplicar un criterio de semejanza basado en el número de Strouhal, se tiene:

$$\left(\frac{L}{Vt}\right)_p = \left(\frac{L}{Vt}\right)_m$$

$$\left(\frac{L_p}{L_m}\right) = \left(\frac{V_p}{V_m}\right)\left(\frac{t_p}{t_m}\right)$$

que en función de las escalas se pone como:

$$\frac{N_L}{N_V N_t} = 1 \qquad N_{S_t} = 1$$

Esta escala es la misma que se obtiene para la velocidad a partir de las dimensiones fundamentales de la misma. Por tanto, para flujo oscilatorio es importante conseguir la semejanza del número de Strouhal.

3.9. IMPORTANCIA DE LA SEMEJANZA DEL NÚMERO DE FROUDE

Para los problemas que se afrontan en la ingeniería de costas las fuerzas asociadas con la tensión superficial o la compresión elástica son relativamente pequeñas y por tanto pueden ser despreciadas. Por ello, la selección de un adecuado escalamiento del problema debe basarse en la evaluación de si las fuerzas de gravedad o de inercia son las predominantes en el problema. Por tanto, los números de Reynolds y Froude son importantes en la ingeniería de costas puesto que la semejanza de uno de estos números, junto con la semejanza geométrica, ofrecen las condiciones necesarias para garantizar la semejanza hidrodinámica en la inmensa mayoría de los problemas abordados. Es, sin embargo, necesario resaltar que las fuerzas gravitatorias predominan en la mayoría de los flujos con superficie libre, con lo cual, la mayor parte de los modelos deben ser diseñados con el criterio de Froude.

En cualquier caso, es necesario reducir los efectos viscosos en el modelo, dado que estos pueden llegar a constituir un efecto de escala. Por ejemplo, la fricción en el fondo por efecto de la viscosidad en un modelo reducido de un puerto puede llegar a ser

mucho mayor que en el prototipo. Por ello, las ondas que en el modelo tengan que propagarse una gran distancia sufrirán una disminución de la altura de ola mucho mayor que en el prototipo. La corrección de este problema puede realizarse mediante la reducción de las distancias de propagación o la inclusión de forma teórica, de unos factores de corrección de las pérdidas por efecto de la fricción comenzando con mayores alturas de ola relativas en el modelo.

Ejemplo:

Obtención de la escala temporal para los criterios de Froude y Reynolds.

El criterio de Froude implica:

$$N_V = \sqrt{N_g N_L}$$

Dado que la velocidad es dimensionalmente longitud/tiempo (así como por la conservación del número de Strouhal), la escala de la velocidad es dimensionalmente equivalente a $\frac{N_L}{N_t}$. Substituyendo en el criterio de Froude y operando:

$$N_t = \sqrt{\frac{N_L}{N_g}}$$

que es la escala temporal para el criterio de Froude. Dado que $N_g = 1$,

$$N_t = \sqrt{N_L}$$

La escala temporal de Froude puede expresarse también en función de los parámetros del fluido asociados al modelo y al prototipo, teniendo en cuenta que para el peso específico:

$$N_\gamma = N_\rho N_g$$

despejando N_g y substituyendo en la ecuación de la escala temporal,

$$N_t = \sqrt{\frac{N_\rho N_L}{N_\gamma}}$$

Para el criterio de Reynolds la escala temporal se encuentra de forma sencilla substituyendo $N_V = \frac{N_L}{N_t}$ en dicho criterio

$$\frac{N_V N_L N_\rho}{N_\mu} = 1$$

y operando:

$$N_t = \frac{(N_L)^2 N_\rho}{N_\mu}$$

que es la escala temporal de Reynolds.

La tabla adjunta incluye las escalas de parámetros físicos del flujo para los criterios de Reynolds y Froude.

Si fuera posible satisfacer simultáneamente los criterios de Froude y de Reynolds la mayor parte de los fenómenos físicos de la ingeniería de costas podrían ser modelados con considerable precisión. Este criterio conjunto resulta de igualar ambos criterios, por tanto:

$$\frac{N_V}{\sqrt{N_g N_L}} = \frac{N_V N_L N_p}{N_\mu}$$

que puede reducirse a:

$$N_\mu = N_g^{1/2} N_L^{3/2} N_\rho$$

Teniendo en cuenta que la escala de la viscosidad cinemática es $N_\nu = \frac{N_\mu}{N_\rho}$ y dado que $N_g = 1$, se llega a que:

$$N_\nu = N_L^{3/2}$$

El problema radica en encontrar un fluido para el modelo que tenga la viscosidad cinemática apropiada. Por ejemplo, para $N_L = 10$, el fluido del modelo debería tender una viscosidad cinemática 30 veces menor que la del prototipo. Asumiendo que el fluido del modelo es agua, no existe fluido que pueda satisfacer dicha condición.

Ejemplo:

Fuerza de arrastre sobre un cuerpo sumergido.

En problemas de ingeniería de costas la hidrodinámica se escala de acuerdo con el criterio de Froude. ¿Qué requisito adicional debe cumplirse en el escalamiento para que las fuerzas de arrastre sobre un cuerpo sumergido sean modeladas adecuadamente?.

La fuerza de arrastre de un fluido se determina como,

$$F_D = C_D \rho A V^2$$

donde:

F_D = fuerza de arrastre
C_D = coeficiente de arrastre, función de los números de Reynolds y Froude
ρ = densidad del fluido
A = área frontal del cuerpo
V = velocidad del fluido

El criterio para escalar F_D es:

$$N_{F_D} = N_{C_D} N_\rho N_A N_V^2$$

De la tabla (2) para el criterio de Froude podemos sustituir las correspondientes escalas para fuerza, área y velocidad llegando a:

$$N_L^3 N_\gamma = N_{C_D} N_\rho \left(N_L^2\right)\left(\frac{N_L N_\gamma}{N_\rho}\right)$$

que se reduce a:

$$N_{C_D} = 1$$

Por tanto, con un modelo tipo Froude la fuerza estará bien modelada siempre y cuando el valor del coeficiente de arrastre sea el mismo para el modelo y el prototipo. Esto obliga a que el número de Reynolds del modelo sea suficientemente elevado para que el coeficiente de arrastre sea independiente de dicho número, en general $\Re e = 10.000$

3.10. DISTORSIÓN DE LOS MODELOS

Siempre que uno de los criterios de semejanza antes mencionados no sea satisfecho por el modelo, se dice que el modelo está distorsionado. Sin embargo, esta definición es demasiado estricta dado que casi nunca se cumple y por ello nos referimos a modelos distorsionados como aquellos en los que no se cumple la semejanza geométrica. En estos modelos las escalas horizontal y vertical son distintas. En general, en ingeniería de costas se utiliza modelos con una escala horizontal mucho mayor que la vertical reduciendo la superficie necesaria para su construcción pero incrementando las pendientes.

Los modelos distorsionados tienen las siguientes

ventajas:

- reducción del espacio necesario para su construcción
- reducción de costes

- incremento de los gradientes de la superficie y por tanto mayor facilidad para medirlas

y desventajas:

- las velocidades pueden ser reproducidas de forma incorrecta en magnitud y dirección
- algunos detalles del flujo no cumplen la semejanza
- refracción y difracción pueden ser reproducidas de forma incorrecta
- aparición potencial de efectos de escala no conocidos
- dificultad en la determinación del grado apropiado de distorsión.

Characteristic	Dimension	Froude	Reynolds
Geometric			
Length	$[L]$	N_L	N_L
Area	$[L^2]$	${N_L}^2$	${N_L}^2$
Volume	$[L^3]$	${N_L}^3$	N_L^3
Kinematic			
Time	$[T]$	$N_L^{1/2}N_\rho^{1/2}N_\gamma^{-1/2}$	$N_L^2 N_\rho N_\mu^{-1}$
Velocity	$[LT^{-1}]$	$N_L^{1/2}N_\rho^{-1/2}N_\gamma^{1/2}$	$N_L^{-1}N_\rho^{-1}N_\mu$
Acceleration	$[LT^{-2}]$	$N_\gamma N_\rho^{-1}$	$N_L^{-3}N_\rho^{-2}N_\mu^2$
Discharge	$[L^3T^{-1}]$	$N_L^{5/2}N_\rho^{-1/2}N_\gamma^{1/2}$	$N_L N_\rho^{-1} N_\mu$
Kinematic Viscosity	$[L^2T^{-1}]$	$N_L^{3/2}N_\rho^{-1/2}N_\gamma^{1/2}$	$N_\rho^{-1}N_\mu$
Dynamic			
Mass	$[M]$	$N_L^3 N_\rho$	$N_L^3 N_\rho$
Force	$[MLT^{-2}]$	$N_L^3 N_\gamma$	$N_\rho^{-1}N_\mu^2$
Mass Density	$[ML^{-3}]$	N_ρ	N_ρ
Specific Weight	$[ML^{-2}T^{-2}]$	N_γ	$N_L^{-3}N_\rho^{-1}N_\mu^2$
Dynamic Viscosity	$[ML^{-1}T^{-1}]$	$N_L^{3/2}N_\rho^{1/2}N_\gamma^{1/2}$	N_μ
Surface Tension	$[MT^{-2}]$	$N_L^2 N_\gamma$	$N_L^{-1}N_\rho^{-1}N_\mu^2$
Volume Elasticity	$[ML^{-1}T^{-2}]$	$N_L N_\gamma$	$N_L^{-2}N_\rho^{-1}N_\mu^2$
Pressure and Stress	$[ML^{-1}T^{-2}]$	$N_L N_\gamma$	$N_L^{-2}N_\rho^{-1}N_\mu^2$
Momentum, Impulse	$[MLT^{-1}]$	$N_L^{7/2}N_\rho^{1/2}N_\gamma^{1/2}$	$N_L^2 N_\mu$
Energy, Work	$[ML^2T^{-2}]$	$N_L^4 N_\gamma$	$N_L N_\rho^{-1} N_\mu^2$
Power	$[ML^2T^{-3}]$	$N_L^{7/2}N_\rho^{-1/2}N_\gamma^{3/2}$	$N_L^{-1}N_\rho^{-2}N_\mu^3$

Tabla n.º 2. (De Hughes, S.A. (1993))

Capítulo 4. MODELOS HIDRODINÁMICOS

En los capítulos anteriores hemos repasado las bases fundamentales para la realización de modelos físicos en ingeniería de costas. A continuación pasaremos a describir algunos aspectos prácticos importantes para el diseño y elaboración de estos modelos.

4.1. INTRODUCCIÓN A LOS MODELOS HIDRODINÁMICOS

En la ingeniería de costas se usan dos tipos de modelos fundamentalmente: *modelos de lecho fijo y modelos de lecho móvil*. Los primeros son útiles en el estudio de los fenómenos hidrodinámicos en la costa mientras que los segundos son clave para el entendimiento del transporte de sedimentos. Aunque, en realidad, en los modelos de lecho móvil la hidrodinámica juega un papel primordial, incluiremos bajo el concepto de modelo hidrodinámico únicamente los de lecho fijo. Este capítulo se dedicará al estudio de éstos exclusivamente, dejando los de lecho móvil para más adelante.

La hidrodinámica en la costa incluye procesos tales como el oleaje o las corrientes. Es práctica común realizar una separación del oleaje con base en su período distinguiendo entre ondas de corto período; 1 - 20 seg. y ondas de largo período con variaciones entre minutos o días.

Esta división facilita ostensiblemente el modelado tanto físico como numérico dado que, en cada caso, algunos términos de las ecuaciones de gobierno predominan sobre

otros. Esto simplifica el modelo dado que la semejanza dinámica suele alcanzarse mediante el balance entre solo dos fuerzas.

Los modelos de onda corta se utilizan para el estudio de los efectos inducidos por ondas de viento o swell sobre estructuras costeras, playas o sobre la navegación. Los modelos de onda larga son propios para el estudio de mareas, tsunamis u otras ondas de largo período y la interacción en puertos, estuarios o desembocaduras. Existen algunos problemas en ingeniería de costas que precisan el estudio de ambos fenómenos. Sin embargo, en general, no es posible estudiar simultáneamente en un modelo único ambos tipos de ondas.

4.2. MODELOS DE ONDAS DE CORTO PERÍODO

El alcance de los estudios con onda corta es muy amplio pudiéndose realizar modelos en un canal de oleaje, asumiendo que el problema es bidimensional (2-D), o en un tanque de oleaje que permita el estudio de problemas de carácter tridimensional (3-D).

Los modelos pueden ser empleados ya sea para estudiar un problema real o para estudiar casos idealizados que permitan un mejor conocimiento de un problema dado y posibiliten la formulación de especificaciones ingenieriles válidas para el diseño. Las ondas utilizadas en el proceso del modelado pueden ser regulares, aproximándose así, al modelo teórico, o irregulares para garantizar un reflejo más fiel de lo que sucede en la naturaleza. En cualquier caso los resultados del modelo dependen completamente de la adecuada simulación del oleaje.

Se define como ondas de corto período aquellas ondas de gravedad que satisfacen que:

$$kh > \frac{\pi}{10} \qquad \frac{h}{L} > \frac{1}{20}$$

donde k es el número de onda, h la profundidad y L la longitud de onda.

Los modelos físicos de ondas de corto período se consideran no disipativos o totalmente turbulentos. Es decir, en este tipo de modelo se considera que no se producen pérdidas de energía por fricción antes de la rotura y que una vez que ésta tiene lugar la pérdida de energía es total y viene asociada a los procesos de disipación turbulenta ligados a los mecanismos de rotura. A continuación se incluye una relación con algunos de los diferentes problemas que pueden ser estudiados mediante un modelo

de ondas de corto período en lecho fijo, tanto para oleaje monocromático como irregular:

- asomeramiento (2-D y 3-D)
- cinemática de las ondas (2-D y 3-D)
- refracción (3-D)
- difracción (3-D)
- teoría no lineal de ondas (2-D y 3-D)
- rotura (2-D y 3-D)
- fuerzas sobre objetos (2-D y 3-D)
- reflexión y transmisión de ondas (2-D y 3-D)
- interacción ola-corriente (2-D y 3-D)
- runup y rebase (2-D y 3-D)
- grupos de ondas (2-D y 3-D)
- estudio de trazadores para el seguimiento cualitativo de trayectorias de sedimentos (3-D)
- desembocaduras (3-D)

4.2.1. Adimensionalización para modelos de ondas de corto período

Ecuaciones de Gobierno

Las ecuaciones de gobierno para un fluido incompresible con superficie libre son continuidad:

$$\frac{\partial u}{\partial x}+\frac{\partial v}{\partial y}+\frac{\partial w}{\partial z}=0$$

y las ecuaciones de Navier-Stokes

x:

$$\frac{\partial u}{\partial t}+u\frac{\partial u}{\partial x}+v\frac{\partial u}{\partial y}+w\frac{\partial u}{\partial z}=-\frac{1}{\rho}\frac{\partial p}{\partial z}+\nu\left(\frac{\partial^2 u}{\partial x^2}+\frac{\partial^2 u}{\partial y^2}+\frac{\partial^2 u}{\partial z^2}\right)-$$

$$-\left[\frac{\partial}{\partial x}\overline{(u'^2)}+\frac{\partial}{\partial y}\overline{(u'v')}+\frac{\partial}{\partial z}\overline{(u'w')}\right]$$

y:

$$\frac{\partial v}{\partial t} + u\frac{\partial v}{\partial x} + v\frac{\partial v}{\partial y} + w\frac{\partial v}{\partial z} = -\frac{1}{\rho}\frac{\partial p}{\partial y} + \nu\left(\frac{\partial^2 v}{\partial x^2} + \frac{\partial^2 v}{\partial y^2} + \frac{\partial^2 v}{\partial z^2}\right) -$$

$$-\left[\frac{\partial}{\partial x}\overline{(u'v')} + \frac{\partial}{\partial y}\overline{(v'^2)} + \frac{\partial}{\partial z}\overline{(v'w')}\right]$$

z:

$$\frac{\partial w}{\partial t} + u\frac{\partial w}{\partial x} + v\frac{\partial w}{\partial y} + w\frac{\partial w}{\partial z} =$$

$$= -\frac{1}{\rho}\frac{\partial p}{\partial z} - g + \nu\left(\frac{\partial^2 w}{\partial x^2} + \frac{\partial^2 w}{\partial y^2} + \frac{\partial^2 w}{\partial z^2}\right) -$$

$$-\left[\frac{\partial}{\partial x}\overline{(u'w')} + \frac{\partial}{\partial y}\overline{(v'w')}\frac{\partial}{\partial z}\overline{(w'^2)}\right]$$

donde:

u, v, w: componentes del campo de velocidades en las direcciones x, y, z de los ejes cartesianos.

u', v', w': componentes de las fluctuaciones turbulentas del campo de velocidades en la dirección de los ejes cartesianos.

g: aceleración de la gravedad

p: presión

ρ: densidad del fluido

ν: viscosidad cinemática del fluido

Los términos a la izquierda de las ecuaciones de Navier-Stokes corresponden a las aceleraciones temporales y convectivas del fluido mientras que a la derecha se encuentran las tensiones tangenciales viscosas, las tensiones de Reynolds y las fuerzas externas actuantes sobre el fluido, en este caso la gravedad. Estas ecuaciones son de aplicación para los fenómenos de ondas de corto período.

Los criterios para un adecuado escalamiento pueden derivarse de la adimensionalización de las ecuaciones utilizando las siguientes definiciones y substituyendo:

$$\hat{u} = \frac{u}{V}; \quad \hat{v} = \frac{v}{V}; \quad \hat{w} = \frac{w}{W}$$

$$\hat{x} = \frac{x}{X}; \quad \hat{y} = \frac{y}{X}; \quad \hat{z} = \frac{z}{Z}$$

$$\hat{t} = \frac{t}{T}; \quad \hat{p} = \frac{p}{P}$$

donde:

V = velocidad horizontal característica
W = velocidad vertical característica
X = longitud horizontal característica
Z = longitud vertical característica
T = tiempo característico
P = presión característica

Las longitudes y velocidades características se han tomado diferentes en vertical y horizontal con el fin de dejar abierta la posibilidad de un modelo distorsionado geométricamente.

Sin embargo, con el fin de facilitar el problema, se toma las mismas velocidades características para adimensionalizar las tensiones de Reynolds y el flujo no turbulento. Se hubiera llegado al mismo resultado partiendo de velocidades características diferentes.

Substituyendo en las ecuaciones y multiplicando por X/V se llega a la ecuación de continuidad adimensional:

$$\frac{\partial \hat{u}}{\partial \hat{x}} + \frac{\partial \hat{v}}{\partial \hat{y}} + \left(\frac{XW}{ZV}\right)\frac{\partial \hat{w}}{\partial \hat{z}} = 0$$

Análogamente substituyendo en las ecuaciones de movimiento y multiplicando las dos primeras ecuaciones por (X/V^2) y la tercera por (Z/W^2) se llega a:

x:

$$\left(\frac{X}{VT}\right)\frac{\partial \hat{u}}{\partial \hat{t}} + \hat{u}\frac{\partial \hat{u}}{\partial \hat{x}} + \hat{v}\frac{\partial \hat{u}}{\partial \hat{y}} + \left(\frac{XW}{ZV}\right)\hat{w}\frac{\partial \hat{u}}{\partial \hat{z}} = -\left(\frac{P}{\rho V^2}\right)\frac{\partial \hat{p}}{\partial \hat{x}} +$$

$$+\left[\left(\frac{\nu}{XV}\right)\frac{\partial^2 \hat{u}}{\partial \hat{x}^2} + \left(\frac{\nu}{XV}\right)\frac{\partial^2 \hat{u}}{\partial \hat{y}^2} + \left(\frac{\nu X}{Z^2 V}\right)\frac{\partial^2 \hat{u}}{\partial \hat{z}^2}\right] -$$

$$-\left[\frac{\partial}{\partial \hat{x}}\overline{(\hat{u}'^2)} + \frac{\partial}{\partial \hat{y}}\overline{(\hat{u}'\,\hat{v}')} + \left(\frac{XW}{ZV}\right)\frac{\partial}{\partial \hat{z}}\overline{(\hat{u}'\,\hat{w}')}\right]$$

y:

$$\left(\frac{X}{VT}\right)\frac{\partial \hat{v}}{\partial \hat{t}} + \hat{u}\frac{\partial \hat{v}}{\partial \hat{x}} + \hat{v}\frac{\partial \hat{v}}{\partial \hat{y}} + \left(\frac{XW}{ZV}\right)\hat{w}\frac{\partial \hat{v}}{\partial \hat{z}} = -\left(\frac{P}{\rho V^2}\right)\frac{\partial \hat{p}}{\partial \hat{y}} +$$

$$+\left[\left(\frac{\nu}{XV}\right)\frac{\partial^2 \hat{v}}{\partial \hat{x}^2} + \left(\frac{\nu}{XV}\right)\frac{\partial^2 \hat{v}}{\partial \hat{y}^2} + \left(\frac{\nu X}{Z^2 V}\right)\frac{\partial^2 \hat{v}}{\partial \hat{z}^2}\right] -$$

$$-\left[\frac{\partial}{\partial \hat{x}}\overline{(\hat{u}'\,\hat{v}')}+\frac{\partial}{\partial \hat{y}}\overline{(\hat{v}'^{2})}+\left(\frac{XW}{ZV}\right)\frac{\partial}{\partial \hat{z}}\overline{(\hat{v}'\,\hat{w}')}\right]$$

z:

$$\left(\frac{Z}{WT}\right)\frac{\partial \hat{w}}{\partial \hat{t}}+\left(\frac{ZV}{XW}\right)\left[\hat{u}\frac{\partial \hat{w}}{\partial \hat{x}}+\hat{v}\frac{\partial \hat{w}}{\partial \hat{y}}\right]+\hat{w}\frac{\partial \hat{w}}{\partial \hat{z}}=-\left(\frac{P}{\rho W^{2}}\right)\frac{\partial \hat{p}}{\partial \hat{z}}-$$

$$-\left(\frac{gZ}{W^{2}}\right)+\left[\left(\frac{\nu Z}{X^{2}V}\right)\frac{\partial^{2}\hat{w}}{\partial \hat{x}^{2}}+\left(\frac{\nu Z}{X^{2}W}\right)\frac{\partial^{2}\hat{w}}{\partial \hat{y}^{2}}+\left(\frac{\nu}{ZW}\right)\frac{\partial^{2}\hat{w}}{\partial \hat{z}^{2}}\right]-$$

$$-\left[\left(\frac{ZV}{XW}\right)\left(\frac{\partial}{\partial \hat{x}}\overline{(\hat{u}'\,\hat{w}')}+\frac{\partial}{\partial \hat{y}}\overline{(\hat{v}'\,\hat{w}')}\right)+\frac{\partial}{\partial \hat{z}}\overline{(\hat{w}'^{2})}\right]$$

Si dos sistemas deben ser regidos por estas ecuaciones adimensionales, la solución, en función de los parámetros adimensionales será la misma para cada sistema siempre que los coeficientes adimensionales permanezcan invariados. Quiere esto decir, que la semejanza completa será alcanzada para cualquier fenómeno de superficie libre regido por dichas ecuaciones de Navier-Stokes si el valor de los coeficientes adimensionales en dichas ecuaciones es el mismo para el prototipo y el modelo. En primer lugar, es importante determinar si es posible la realización de modelos distorsionados geométricamente. Esto puede resolverse analizando los valores de los coeficientes del término de presión:

$$\frac{\dfrac{P_p}{\rho_p V_p}}{\dfrac{P_m}{\rho_m V_m}}=\frac{N_p}{N_\rho N_V^{2}}=1 \quad y \quad \frac{N_p}{N_\rho N_W^{2}}=1$$

Dado que ambos cocientes son igual a la unidad pueden ser igualados entre si, resultando:

$$N_V = N_W$$

Analicemos ahora el criterio que resulta de mantener el cociente entre los coeficientes de la componente vertical de la aceleración convectiva en las ecuaciones horizontales:

$$\frac{N_X N_W}{N_Z N_V} = 1$$

Dado que se obtuvo que $N_V = N_W$ este cociente se reduce a:

$$N_X = N_Z$$

Lo que implica que las escalas vertical y horizontal deben ser iguales. Por tanto, el primer criterio para poder alcanzar la semejanza dinámica en un modelo hidrodinámico es que los modelos de ondas de corto período no pueden ser distorsionados geométricamente. La semejanza geométrica es un requisito imprescindible en los modelos de ondas de corto período para alcanzar la semejanza dinámica. En función de las ecuaciones adimensionales, la semejanza geométrica implica que tanto las condiciones iniciales como de contorno deben ser las mismas en el modelo y en el prototipo.

Una vez aceptado el hecho de que este tipo de modelos no puede ser distorsionado, puede reemplazarse N_X y N_Z por una escala de longitudes sin distorsionar N_L y asimismo considerarse que el campo de velocidades, horizontal y vertical tiene una escala N_V. Esto conduce a la siguiente simplificación de las ecuaciones:

$$\frac{\partial \hat{u}}{\partial \hat{x}} + \frac{\partial \hat{v}}{\partial \hat{y}} + \frac{\partial \hat{w}}{\partial \hat{z}} = 0$$

x:

$$\left(\frac{L}{VT}\right)\frac{\partial \hat{u}}{\partial \hat{t}}+\hat{u}\frac{\partial \hat{u}}{\partial \hat{x}}+\hat{v}\frac{\partial \hat{u}}{\partial \hat{y}}+\hat{w}\frac{\partial \hat{u}}{\partial \hat{z}}=-\left(\frac{P}{\rho V^2}\right)\frac{\partial \hat{p}}{\partial \hat{x}}+$$

$$+\left(\frac{\nu}{LV}\right)\left[\frac{\partial^2 \hat{u}}{\partial \hat{x}^2}+\frac{\partial^2 \hat{u}}{\partial \hat{y}^2}+\frac{\partial^2 \hat{u}}{\partial \hat{z}^2}\right]-$$

$$-\left[\frac{\partial}{\partial \hat{x}}\overline{(\hat{u}'^2)}+\frac{\partial}{\partial \hat{y}}\overline{(\hat{u}'\,\hat{v}')}+\frac{\partial}{\partial \hat{z}}\overline{(\hat{u}'\,\hat{w}')}\right]$$

y:

$$\left(\frac{L}{VT}\right)\frac{\partial \hat{v}}{\partial \hat{t}}+\hat{u}\frac{\partial \hat{v}}{\partial \hat{x}}+\hat{v}\frac{\partial \hat{v}}{\partial \hat{y}}+\hat{w}\frac{\partial \hat{v}}{\partial \hat{z}}=-\left(\frac{P}{\rho V^2}\right)\frac{\partial \hat{p}}{\partial \hat{y}}+$$

$$+\left(\frac{\nu}{LV}\right)\left[\frac{\partial^2 \hat{v}}{\partial \hat{x}^2}+\frac{\partial^2 \hat{v}}{\partial \hat{y}^2}+\frac{\partial^2 \hat{v}}{\partial \hat{z}^2}\right]-$$

$$-\left[\frac{\partial}{\partial \hat{x}}\overline{(\hat{u}'\,\hat{v}')}+\frac{\partial}{\partial \hat{y}}\overline{(\hat{v}'^2)}+\frac{\partial}{\partial \hat{z}}\overline{(\hat{v}'\,\hat{w}')}\right]$$

z:

$$\left(\frac{L}{VT}\right)\frac{\partial \hat{w}}{\partial \hat{t}}+\hat{u}\frac{\partial \hat{w}}{\partial \hat{x}}+\hat{v}\frac{\partial \hat{w}}{\partial \hat{y}}+\hat{w}\frac{\partial \hat{w}}{\partial \hat{z}}=-\left(\frac{P}{\rho V^2}\right)\frac{\partial \hat{p}}{\partial \hat{z}}-$$

$$-\left(\frac{gL}{V^2}\right)+\left(\frac{\nu}{LV}\right)\left[\frac{\partial^2 \hat{w}}{\partial \hat{x}^2}+\frac{\partial^2 \hat{w}}{\partial \hat{y}^2}+\frac{\partial^2 \hat{w}}{\partial \hat{z}^2}\right]-$$

$$-\left[\frac{\partial}{\partial \hat{x}}\overline{(\hat{u}'\hat{w}')}+\frac{\partial}{\partial \hat{y}}\overline{(\hat{v}'\hat{w}')}+\frac{\partial}{\partial \hat{z}}\overline{(\hat{w}'^2)}\right]$$

Condiciones de semejanza para modelos de ondas de corto período

El número de monomios adimensionales independientes en las ecuaciones de gobierno se ha reducido a cuatro imponiendo al modelo la condición de mantener las mismas proporciones geométricas que el prototipo. Obsérvese que los monomios obtenidos fueron ya previamente derivados a partir del análisis dimensional. El coeficiente correspondiente a las aceleraciones temporales (L/VT) fue denominado número de Strouhal. El coeficiente del término de presiones ($P/\rho V^2$) es el número de Euler y el correspondiente al término gravitatorio (gL/V^2) es el inverso del número de Froude. Además el coeficiente de los términos viscosos corresponde al inverso del número de Reynolds (ν/LV). Por ello, se puede observar que estos números aparecen en la descripción matemática del fenómeno físico.

Como se dijo anteriormente, la semejanza completa solo puede alcanzarse si estos coeficientes toman los mismos valores en el modelo y en el prototipo. Igualando los coeficientes del prototipo con los del modelo y realizando los cocientes de cada variable del prototipo y del modelo contenidas en los coeficientes se llega a las siguientes condiciones para la semejanza completa.

· **Condición 1**

A partir del término gravitatorio:

$$\frac{N_\nu}{\sqrt{N_g N_L}}=1$$

lo que implica que el número de Froude debe ser el mismo en el modelo y en el prototipo.

· **Condición 2**

Del término de las aceleraciones convectivas:

$$\frac{N_L}{N_V N_T} = 1$$

que implica que el número de Strouhal debe conservarse en el modelo. Esto se consigue para los modelos de ondas tomando como escala para el tiempo el cociente entre los períodos de prototipo y modelo. Las condiciones 1 y 2 pueden ser combinadas para obtener la escala de tiempos de Froude:

$$N_T = \sqrt{\frac{N_L}{N_g}}$$

· **Condición 3**

A partir del término de las tensiones viscosas:

$$\frac{N_L N_V}{N_V} = 1$$

lo que implica que el número de Reynolds debe ser el mismo en el prototipo y el modelo.

· **Condición 4**

Finalmente, a partir del término de presiones:

$$\frac{N_p}{N_\rho N_V^2} = 1$$

lo que obliga a la conservación del número de Euler.

Estas cuatro condiciones constituyen los criterios de semejanza para modelar los flujos con superficie libre regidos por las ecuaciones de continuidad y de Navier - Stokes.

El modelo debe permanecer geométricamente sin distorsionar y se asume que la tensión superficial y compresibilidad son despreciables al no haber sido tenidos en cuenta en las ecuaciones.

Las condiciones 1 y 2 representan la base para escalar los fenómenos hidrodinámicos de ondas de corto período en modelos sin distorsionar.

Estas condiciones, en esencia, implican que la escala de Froude debe ser utilizada siendo la escala del período de la onda la misma que la escala temporal de Froude. Si se cumple el criterio de Froude todos los términos de la ecuación, con excepción de los correspondientes a las tensiones tangenciales, son semejantes. Esto incluye los términos de las tensiones de Reynolds por tanto se concluye que:

Los modelos de ondas de corto período mantienen la semejanza de los procesos turbulentos disipativos:

De la Condición 3 se concluye que, los efectos viscosos solo pueden ser modelados en modelos de ondas de corto período si se cumplen tanto el criterio de semejanza de Froude como el de Reynolds. Sin embargo, ya comentamos anteriormente la dificultad para garantizar la semejanza de los números de Reynolds y Froude en un mismo modelo y en general los modelos en ingeniería de costas no satisfacen la semejanza del número de Reynolds.

La Condición 4 queda automáticamente satisfecha puesto que la escala de la presión N_p se considera como el cociente independiente para obtener la semejanza dinámica (ver apartado 3), y se determina una vez fijados todos los demás cocientes entre fuerzas. Si asumimos que se cumple el criterio de Froude, la escala de la presión se obtiene de las condiciones 1 y 4 llegando a que:

$$N_p = N_\rho N_g N_L \qquad N_p = N_g N_L$$

A partir de las condiciones de semejanza impuestas de las ecuaciones se puede concluir que los modelos hidrodinámicos de ondas de corto período están dominados fundamentalmente por los efectos de la gravedad e inercia y que el modelo no puede ser distorsionado. Las tensiones tangenciales viscosas solo pueden ser correctamente escaladas en un modelo reducido con criterio de Froude si se cumple el criterio de

Reynolds. Sin embargo, las tensiones tangenciales turbulentas si satisfacen el criterio de Froude.

Por ello los modelos de ondas de corto período pueden ser no disipativos, siendo los efectos viscosos y capilares despreciables, como ocurre antes de la rotura o ser altamente disipativos en una distancia relativamente corta como ocurre en los procesos turbulentos que se desencadenan en la rotura. En realidad siempre se producirán algunas pérdidas por los efectos de la viscosidad y de la tensión tangencial pero estos efectos de escala pueden minimizarse hasta ser despreciables.

Refracción y Difracción en modelos de ondas de corto período

Como ya se dijo anteriormente este tipo de modelos no puede ser distorsionado dado que ello conllevaría la alteración de las condiciones de flujo en el modelo. Esta cuestión queda clara al analizar el problema de la refracción. La refracción puede ser estudiada mediante la ley de Snell que establece que:

$$\frac{\sin\theta_1}{C_1} = \frac{\sin\theta_2}{C_2}$$

donde θ *en el* ángulo entre la cresta y la batimétrica local y C la celeridad de la onda. Los subíndices indican diferentes localizaciones.

Operando en dicha ecuación y estableciendo las escalas se obtiene el criterio para escalar la refracción:

$$N\left(\frac{\sin\theta_1}{\sin\theta_1}\right) = N\left(\frac{C_2}{C_1}\right)$$

Para modelar de forma correcta la refracción es necesario que $N\left(\frac{\sin\theta_2}{\sin\theta_1}\right)=1$ y esto es solo posible si $N\left(\frac{C_2}{C_1}\right)=1$

Utilizando la ecuación de la dispersión en teoría lineal se obtiene que:

$$\frac{C_2}{C_1} = \frac{\tanh\left(\frac{2\Pi h_2}{L_2}\right)}{\tanh\left(\frac{2\Pi h_1}{L_1}\right)}$$

Imponiendo la igualdad de este cociente en modelo y prototipo se obtiene:

$$\left[\frac{\tanh\left(\frac{2\Pi h_2}{L_2}\right)}{\tanh\left(\frac{2\Pi h_1}{L_1}\right)}\right]_p = \left[\frac{\tanh\left(\frac{2\Pi h_2}{L_2}\right)}{\tanh\left(\frac{2\Pi h_1}{L_1}\right)}\right]_m$$

Finalmente, introduciendo la escala para la longitud de onda ($N_{LON} = L_p/L_m$) y la correspondiente a la profundidad ($N_h = h_p/h_m$) en la ecuación anterior se llega a:

$$\frac{\tanh\left[\frac{N_h}{N_{LON}}\left(\frac{2\Pi h_2}{L_2}\right)\right]}{\tanh\left[\frac{N_h}{N_{LON}}\left(\frac{2\Pi h_1}{L_1}\right)\right]} = \frac{\tanh\left(\frac{2\Pi h_2}{L_2}\right)}{\tanh\left(\frac{2\Pi h_1}{L_1}\right)}$$

que a la postre es la condición necesaria para un modelado correcto de la refracción. Para satisfacer esta ecuación es necesario que $N_{LON} = N_h$. Esto puede cumplirse de dos maneras:

1.- $N_{LON} = N_h = N_L$ donde N_L es una escala sin distorsionar para un modelo sin distorsionar.

2.- $N_{LON} = N_h$ con $N_{LON} \neq N_h$, es decir N_{LON} es diferente a la escala horizontal.

Para el segundo caso el problema se presenta al no obtenerse un adecuado modelado de la difracción. La difracción depende notablemente del monomio adimensional X/L, donde X es una distancia horizontal, según ha sido observado por diferentes autores.

Por tanto, para encarar adecuadamente la difracción es necesario que $_{(X/L)} = 1$ lo que significa que la escala de la longitud de onda debe ser la misma que la correspondiente a la longitud horizontal, es decir $N_{LON} = N_X$.

Por tanto, se puede concluir que la reproducción correcta de los procesos de refracción y difracción en un modelo reducido según Froude para ondas de corto período precisa que el modelo sea geométricamente no distorsionado.

4.2.2. Efectos propios del laboratorio y de escala en modelos de ondas de corto período

Los efectos de laboratorio y de escala son dos factores importantes que afectan a los resultados del modelo y por ello es fundamental conocer su alcance.

Efectos propios del laboratorio

Para modelos de onda corta los efectos de laboratorio están asociados a:

1.- Limitaciones del flujo por efecto de los contornos.

2.- Efectos no lineales no deseados introducidos en el proceso de la generación del oleaje o de la corriente.

3.- Simplificación de las solicitaciones a las que está sometido el prototipo (por ejemplo considerar oleaje unidireccional).

En un tanque siempre existe la posibilidad de generación de ondas transversales, así como de la aparición de efectos no lineales tales como la generación de armónicos de orden superior o de ondas largas espúrias producto de la generación de las ondas mediante la utilización de una función de transferencia obtenida a partir de la teoría lineal para realizar el movimiento de la pala.

Los contornos de los tanques condicionan la bidimensionalidad del flujo hidrodinámico. Sin embargo, esta limitación es tan obvia que siempre es considerada a priori.

Otro efecto de los contornos es la re-reflexión inducida por la pala. Para resolver este problema se toman diferentes precauciones:

- Colocación de playas disipadoras de energía o de placas verticales porosas que minimizan la reflexión al final del tanque hasta valores inferiores al 5% de la onda incidente.

- Los experimentos se realizan con series de ondas calculadas de tal forma que se garantice que la medición ha finalizado antes de que la re-reflejada llegue a la pala.

- Instalación en la pala de elementos o mecanismos capaces de detectar y absorber la energía reflejada.

En tanques el efecto de las paredes es importante sobre la hidrodinámica. Las ondas con incidencia oblicua pueden generar corrientes longitudinales que den lugar a corrientes de retorno en los laterales del tanque. Esto reduce la zona en la que se pueden tomar medidas.

Efectos de escala

Los efectos de escala en modelos de onda corta se deben fundamentalmente a la hipótesis de que la gravedad es la fuerza dominante que equilibra las fuerzas de inercia. Realizar el escalamiento basándose en esta hipótesis da lugar a un modelado incorrecto de las otras fuerzas tales como viscosidad, elasticidad, tensión superficial, etc.

Aunque algunos autores han presentado métodos para disminuir estos efectos el procedimiento habitual es cuantificarlos y examinar los resultados del modelo de forma crítica y utilizar la experiencia para interpretar los mismos. En los modelos de ondas de corto período realizados según el criterio de Froude la falta de semejanza en las fuerzas viscosas y tensión superficial puede dar lugar a efectos de escala en la reflexión, transmisión y la disipación por efectos de la fricción y de la rotura.

. Reflexión:

La reflexión de playas o estructuras con taludes muy rígidos podrá ser mayor o menor que la que tiene lugar en el prototipo, según los casos. La reflexión inducida por paredes lisas suele ser menor en el modelo que en el prototipo debido al aumento de fricción que tiene lugar en el modelo (la superficie es relativamente más rugosa que en el prototipo). Sin embargo, los coeficientes de reflexión para superficies porosas son mayores en el modelo que en el prototipo dado que el flujo a través del medio poroso se ve afectado por los efectos viscosos en el modelo y por tanto la estructura se comporta como si fuera menos porosa que en la realidad. Este problema se corrige en el modelo aumentando el tamaño de la escollera respecto al obtenido por consideraciones geométricas. Si el papel de la reflexión en el proceso sometido a estudio es importante, el procedimiento usual es obtener la reflexión real utilizando una escala mayor (1:10 - 1:20) con el tamaño de la escollera reducido según criterios geométricos. Esta escala mayor garantiza que el flujo sea turbulento

al igual que sucede en el prototipo. Posteriormente se realiza el modelo a la escala necesaria para su montaje en el tanque y se colocan estructuras absorbentes adicionales para reducir la reflexión al valor deseado.

. Transmisión:

Si un dique de escollera o un absorbedor es modelado con tamaños de la escollera reducidos del prototipo por criterios geométricos únicamente, la transmisión será relativamente menor en el modelo. Las pérdidas por efecto de la fricción son mayores en el modelo a medida que la onda se propaga y esto es sobre todo aparente en las escalas típicas utilizadas para modelos portuarios. Este efecto de escala se contrarresta aumentando el tamaño de la escollera frente al correspondiente a criterios geométricos de tal modo que:

$$\frac{L_p}{L_m} = K \frac{D_p}{D_m} \qquad N_L = K\, N_D$$

donde, L, corresponde a una longitud característica del modelo sin distorsionar, D, es una dimensión lineal representativa del tamaño de la escollera y, K, es un factor mayor que la unidad. La Méhauté (1965) utilizó consideraciones analíticas y datos para realizar un gráfico para la obtención de K.

Asumió que los efectos de escala son despreciables en el manto exterior y que el prototipo y modelo tienen la misma distribución granulométrica en el núcleo. Su método sirve, por tanto, para corregir los efectos de escala debidos al flujo a través del núcleo de la estructura.

En la gráfica que se adjunta las líneas continuas representan valores constantes de K. Las ordenadas son la escala geométrica $N_L = L_p / L_m$ y la abscisa un factor dimensional que combina varios parámetros para la estructura porosa.

Este factor es:

$$\frac{H_i}{\Delta L} D_p^3 P_p^5$$

donde:

H_i = altura de la onda incidente
ΔL = anchura media del núcleo
$\frac{\Delta H_i}{\Delta L}$ = gradiente de pérdida de carga producida en el núcleo
D_p = diámetro efectivo de la escollera (en centímetros) del núcleo del prototipo
P = porosidad del material del núcleo ($0 < P < 1$)

Es importante destacar que D_p debe corresponder al diámetro del material del prototipo. Los parámetros H_i y ΔL pueden corresponder ambos al prototipo o al modelo.

Keulegan (1973) realizó una serie de experimentos utilizando piedras de casi el mismo diámetro y con una porosidad de 0.46. A partir de estos experimentos desarrolló un conjunto de ecuaciones empíricas basadas en este valor de la porosidad. Sin embargo, los valores típicos de la porosidad del material del núcleo ronda 0,35 - 0,4.

Hudson (1979) modificó las ecuaciones de Keulegan introduciendo la porosidad como una variable. En concreto dio 2 ecuaciones, una para la transmisión para números de Reynolds de la estructura, R_n, mayores que 2000 en cuyo caso las pérdidas de energía se deben a disipación turbulenta y una segunda ecuación para $20 < R_n < 2000$, en la que la disipación en la estructura se debe a efectos viscosos. Las ecuaciones son las siguientes:

$R_n > 2000$

$$\left(\frac{H_i}{H_t}\right)_p = 1 + \gamma_p \left(\frac{H_i}{2h}\right)_p \left(\frac{\Delta L}{L}\right)_p$$

y,

$$\gamma_p = \frac{P_p^{-4}}{10,6}\left(\frac{L}{D}\right)_p \left(gh\frac{T^2}{L^2}\right)_p^{\frac{4}{3}}$$

$20 < R_n < 2000$

$20 < R_n < 2000$

$$\left(\frac{H_i}{H_t}\right)_m^{\frac{2}{3}} = 1 + \gamma_m \left(\frac{H_i}{2h}\right)_m^{\frac{2}{3}} \left(\frac{\Delta L}{L}\right)_m$$

y,

$$\gamma_m = \frac{P_m^{-4}}{1{,}52} \left(\frac{\nu T}{DL}\right)_m^{\frac{1}{3}} \left(\frac{L}{D}\right)_m \left(gh\frac{T^2}{L^2}\right)_m^{\frac{4}{3}}$$

En estas ecuaciones, el número de Reynolds se calcula como:

$$R_n = \frac{P\,H_i\,LD}{2\nu\,hT}$$

y las variables se definen como:

H_i = altura de ola incidente

H_t = altura de ola transmitida

L = longitud de onda incidente

h = profundidad

T = período de la onda

ν = viscosidad cinemática

D = dimensión característica del material en el núcleo (10% menor que el tomado de la curva granulométrica)

ΔL = anchura media del núcleo

g = aceleración de la gravedad

P = porosidad del núcleo

La semejanza en la transmisión precisa que:

$$\left(\frac{H_i}{H_t}\right)_p = \left(\frac{H_i}{H_t}\right)_m$$

A partir de aquí y con las fórmulas anteriores puede obtenerse el valor de K. El procedimiento usual es obtener K según Le Méhauté y Keulegan y utilizar el valor medio de ambos.

Bibliografía

Hugher, S.A. (1993). *Physical models and laboratory techniques in coastal engineering.* Advanced Series on Ocean Engineering, Vol. 7. World Scientific. Singapore.

Yalin, M.S. (1971). *Theory of hydraulic models.* McMillan Press, London, England.

APÉNDICE II

AVANCES TÉCNICOS

En este anejo al Documento de Referencia se incluyen los últimos avances técnicos desarrollados durante la elaboración del proyecto. Al ser tan novedosos, no han sido incluidos directamente en el Documento de Referencia aunque su aplicación sí se ha incorporado a las metodologías y modelos elaborados.

Por tratarse de nuevos desarrollos su difusión se ha realizado inicialmente en revistas internacionales o en conferencias por lo que se incluyen aquí en la forma en la que se han enviado o han sido ya publicados en las mismas.

1. González, M. and Medina, R. (2001) "On the application of static equilibrium bay formulations to natural and man-made beaches." Coastal Engineering, ELSEVIER, en prensa
2. Medina, R., Bernabeu, A.M., Vidal, C. and Gonzalez, M. (2001). "Relationship between beach morphodynamics and equilibrium profiles. Proceedings International Conference on Coastal Engineering, Sydney, ASCE, en prensa.
3. Gonzalez, M., Medina, R. and Losada, M.A. (1999). "Equilibrium beach profile model for perched beaches." Coastal Engineering, ELSEVIER, Vol. 36, 343-357.
4. Gonzalez, M., Medina, R., Muñoz-Perez, J.J. (2000). "Influence of coastal structures on equilibrium beach." In: Proceedings Coastal Structures'99. Balkema, Rotterdam, 747-755.
5. Ozkan-Haller, H.T., Vidal, C., Losada, I.J., Medina, R. and Losada, M.A. (2001). "Standing edge waves in pocket beaches", Journal of Geophysical Research, AGU, en prensa.

Publicado en el Coastal Engineering, ELSEVIER

ON THE APPLICATION OF STATIC EQUILIBRIUM BAY FORMULATIONS TO NATURAL AND MAN-MADE BEACHES

Mauricio Gonzalez and Raul Medina

Ocean & Coastal Research Group, Universidad de Cantabria,

E.T.S. Ingenieros de Caminos, C. y P., Dpto. Ciencias y Tecnicas del Agua y del Medio Ambiente,

Avd. de los Castros, s/n. 39005 Santander, Spain

mao@puer.unican.es medina@puer.unican.es

ABSTRACT

Crenulated-shaped bays are common features found all around the world. The most widely used formulation for representing this kind of bay is the parabolic approach proposed by Hsu and Evans (1989), who suggested a methodology to test and predict the stability of static equilibrium shapes in natural and man-made bays. Based on an analytical model of null drift current and using an empirical approach, a modified methodology is proposed. The new procedure is able to locate the downcoast starting point of the static equilibrium beach from which the parabolic plan form of Hsu and Evans is valid. This methodology is applied with good results to different natural and man-made beaches along the Atlantic and Mediterranean coasts of Spain, including tombolo-shaped beaches.

Las playas encajadas constituyen una morfología común en todo el mundo. La formulación más utilizada usualmente para modelar este tipo de playas es el modelo parabólico propuesto por Hsu y Evans (1989) que propusieron una metodología para comprobar y predecir la estabilidad de las formas de equilibrio estático en playas naturales y artificiales. En este trabajo se propone una metodología que surge a partir de una aproximación empírica como una modificación al modelo analítico de corriente nula. El nuevo procedimiento propuesto es capaz de fijar el punto aguas debajo de la forma en planta de equilibrio estático a partir de la cual es válida la forma en planta parabólica de Hsu y Evans. Esta metodología se aplica con éxito a diferentes playas naturales y artificiales a lo largo de las costas atlántica y mediterránea españolas, incluyendo playas en forma de tómbolo.

ON THE APPLICATION OF STATIC EQUILIBRIUM BAY FORMULATIONS TO NATURAL AND MAN-MADE BEACHES

Mauricio Gonzalez and Raul Medina

Ocean & Coastal Research Group, Universidad de Cantabria,
E.T.S. Ingenieros de Caminos, C. y P., Dpto. Ciencias y Tecnicas del Agua y del Medio Ambiente,
Avd. de los Castros, s/n. 39005 Santander, Spain
mao@puer.unican.es medina@puer.unican.es

ABSTRACT

Crenulate-shaped bays are common features found all around the world. The most widely used formulation for representing this kind of bay is the parabolic approach proposed by Hsu and Evans (1989), who suggested a methodology to test and predict the stability of static equilibrium shapes in natural and man-made bays. Based on an analytical model of null drift current and using an empirical approach, a modified methodology is proposed. The new procedure is able to locate the downcoast starting point of the static equilibrium beach from which the parabolic plan form of Hsu and Evans is valid. This methodology is applied with good results to different natural and man-made beaches along the Atlantic and Mediterranean coasts of Spain, including tombolo-shaped beaches.

Keywords: Equilibrium plan form formulations; Headland-bay beaches; Tombolo, Salient; Shoreline response;

1. INTRODUCTION

The formation of crenulate-shaped bays between two headlands is a common feature of beaches that experience incident waves from a predominant direction. The plan form of an equilibrium bay-shaped beach is dictated by the amount of sediment passing through it from upcoast or from a river within the bay. In this situation a constant littoral drift with continuous sediment supply to the bay is said to be in "dynamic equilibrium". Whether due to natural or man-made causes, when this sediment supply ceases in a reasonable length of time, the indentation increases and the waterline erodes back to a limiting shape which is termed "static equilibrium" (Hsu et al. 1989b). As a result no further littoral drifts are present and the net sediment transport rate in the bay decreases and eventually ceases. Today many coasts are suffering erosion due to alterations in longshore drift from causes such as diminishing supply from rivers, man-made structures built along the coast (e.g. offshore breakwaters, groins, seawalls), and the dredging of deep channels, upon which these static equilibrium conditions should be taken into account in order to design new long-term crenulate beaches.

A great number of static equilibrium-shaped models and formulations have been proposed, such as the spiral logarithm by Yasso (1965), Vichetpan (1969), Silvester (1970 a, b) and others. Hsu et al. (1987) and Hsu and Evans (1989) have shown that the logarithmic spiral does not follow the complete periphery of the equilibrium bay, proposing a parabolic relationship. This parabolic relationship is, nowadays, the most widely-used formulation for checking crenulate-shaped bays stability.

Hsu and Evans (1989) found that the shape of a static equilibrium shoreline is dependent on the obliquity of the incident wave, β, and the control line, R_0. A parabolic relationship was proposed to define the plan form of the bay

$$\frac{R}{R_0} = C_0 + C_1\left(\frac{\beta}{\theta}\right) + C_2\left(\frac{\beta}{\theta}\right)^2 \qquad (1)$$

where C_0, C_1 and C_2 are coefficients that depend on β (Hsu and Evans, 1989). R is the radii from the control point (diffraction point) to the beach line at angles $\theta (\theta > \beta)$ as is shown in the definition sketch (figure 1). R_0 is the control line from the upcoast diffraction point to the downcoast limit of the bay, where the tangent to the beach is parallel to the incident wave crests.

Hsu et al. (1989 a, b) proposed a methodology to test the stability of a given bay using the empirical parabolic model. To apply the methodology the bay must be fully-developed (meaning that the tangent to the beach at the downcoast tip is normal to the orthogonal of the persistent swell or predominant waves in the area, (see figure 1). Applying this methodology Hsu et al.'s (1989c) showed several applications of headland control in order to retain beaches in locations with erosion.

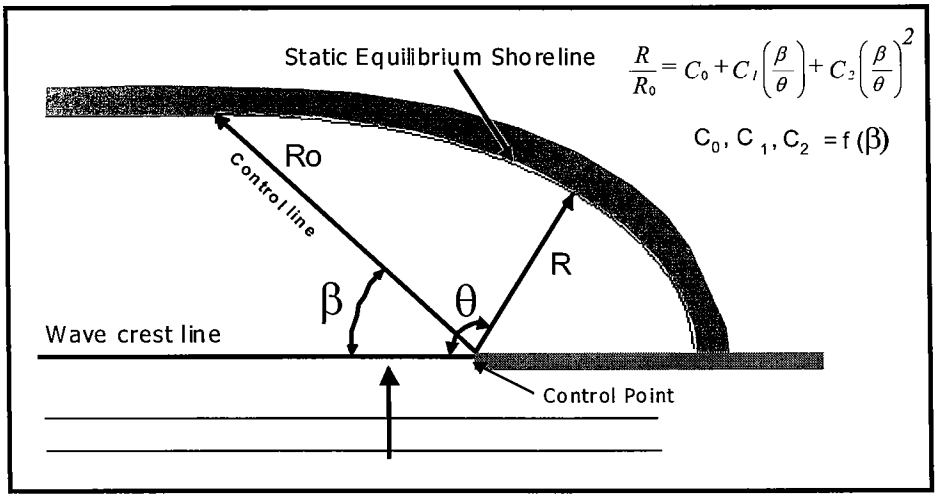

Figure 1. Definition sketch of bay in static equilibrium.

Gonzalez (1995) applied this methodology to several static equilibrium bays along the Spanish coast and concluded that it is not uniformly applicable. In this paper Gonzalez's (1995) work is reviewed and a new methodology for the design of static equilibrium beaches is presented.

The paper is organized as follows: first, a brief review of Gonzalez's (1995) work is presented, underlining the cases where Hsu et al.'s (1989 a,b) methodology cannot be applied. According to these results, analytical and empirical approaches are carried out in order to develop a modified methodology for testing or designing static equilibrium bays. Finally, the methodology is applied to some natural and man-made (headland-bay and tombolo) beaches. Some important conclusions are given at the end of the paper.

2. PREVIOUS WORK

Gonzalez (1995) applied the methodology proposed by Hsu et al. (1989 a, b) to twenty static equilibrium bays along the Spanish coast in order to test their stability. Fifteen of the beaches were fully-developed bays and five were undeveloped beaches. The main conclusions of this study were:

1. The parabolic model represents fairly well the static equilibrium plan form of the fully-developed crenulate-shaped beaches. Even though, in general there are some difficulties in defining the downcoast limit, as was also stated by Silvester (1980). Figure 2 shows an example of this situation at Motril Beach (Mediterranean coast), where it is not clear whether the initial point downcoast should be A, B or a middle point.

2. The parabolic model is applicable in tidal seas, and it can represent the high- and low-tide coastlines.

3. However, as expected, the parabolic model is unable to represent the equilibrium plan form in the beach area close to the mouth of an estuary due to the tidal dynamics.

4. Neither can it predict the effect of obstacles such as islands or islets 0(10 m) which locally influence the beach.

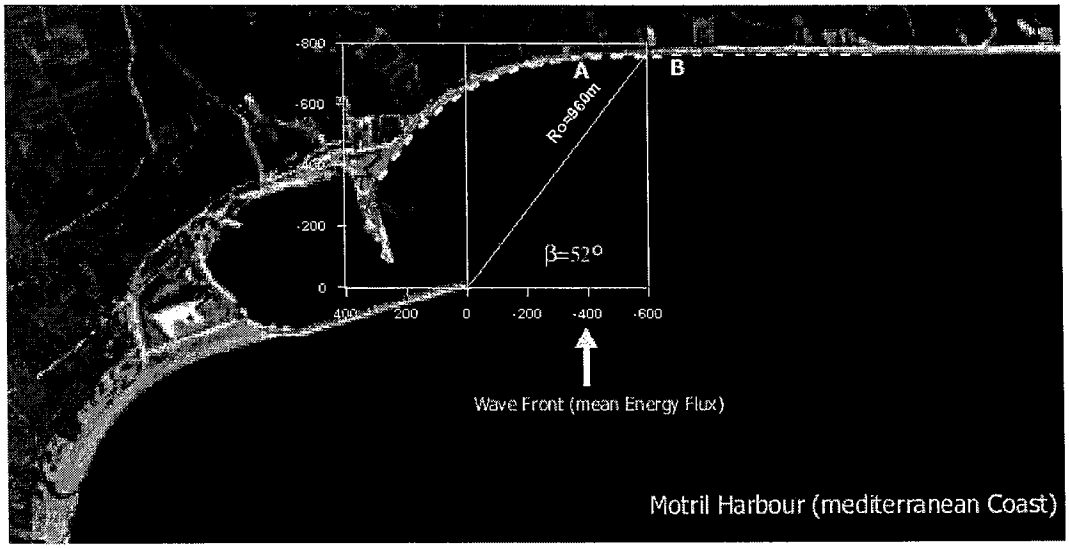

Figure 2. Aerial photograph showing the actual shoreline downcoast of Motril harbour (Spain) and the predicted static equilibrium plan form obtained following the Hsu et al. (1989 a, b) methodology. Note that the origin of the headland-shaped beach downcoast tip is unclear and can be located any point between A and B.

An example of conclusions 2, 3 and 4 is presented in figure 3, where the parabolic model is applied to high- and low-tide shorelines (5.0 m tide range) of El Puntal Beach, located in Santander (Atlantic coast). It is remarkable that the front used at the control point (The Magdalena Peninsula) corresponds with the persistent swell or predominant waves at the control point area. A good fit is found along the shoreline, except in the central area (island effect) and the area close to the tidal channel (conclusions 4 and 3)

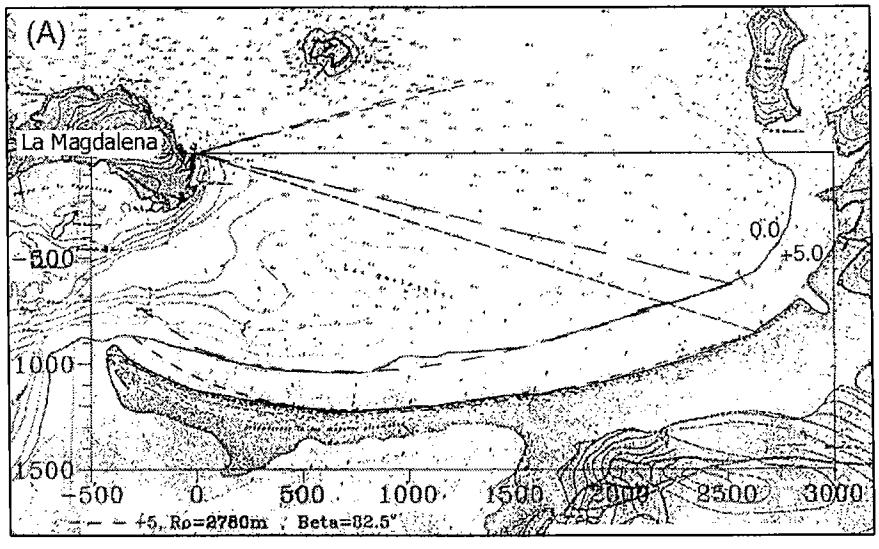

Figure 3. Comparison of the actual shoreline at El Puntal beach and the predicted equilibrium plan form. Note that both the high and low tide shorelines are adequately represented. However, the equilibrium plan form is unable to represent the area close to the mouth of the estuary , nor the influence of the offshore island at the center of the beach.

5. The methodology proposed by Hsu and Evans (1989 a, b) is adequate for testing the equilibrium plan form of existing undeveloped beaches. In order to do so, it is necessary to carry the tangent to the beach at the downcoast tip of the bay to the diffraction or control point and to use this tangent as the wave front. In figure 4 an example of said conclusion is presented. In this figure the Sardinero Beach, a static equilibrium beach located next to El Puntal Beach, is shown. It is important to note that the carried tangent is not related to the predominant waves at the control point area, in contrast with El Puntal Beach, where the front orientation used for the static equilibrium shape corresponds with the predominant wave orientation.

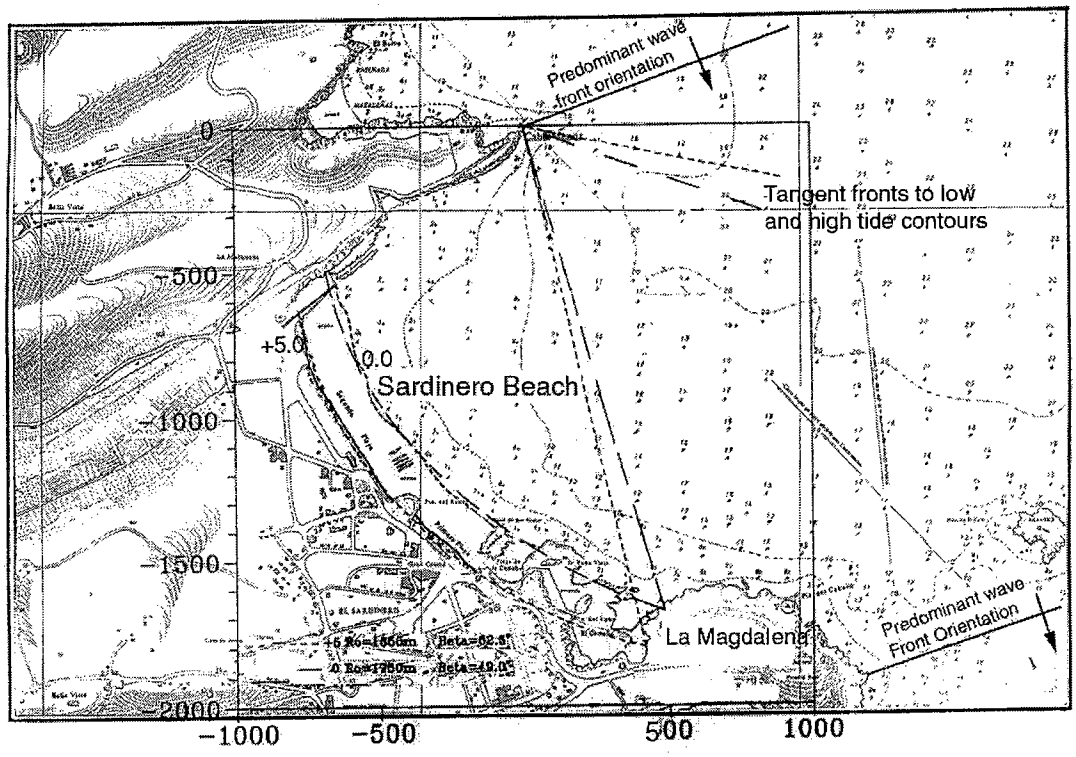

Figure 4. Comparison of the actual and the predicted static equilibrium shorelines at Sardinero beach, Spain. Following the methodology of Hsu et al. (1989 a, b), the tangent to the shoreline at the downcoast tip is used to determine the front orientation at the diffraction point. Note, however, that this orientation is not related to the predominant wave front direction.

6. It was also demonstrated that: (1) carrying the tangent at "any point" in an equilibrium shoreline to the diffraction or control point, and (2) using this as the wave front to define the Hsu et al. (1989) parabolic model, (3) it is possible to represent the static equilibrium shoreline in the upcoast direction from said point. An example of the aforementioned conclusion is shown in figure 5 for the Sardinero Beach. This feature will be used later in this work.

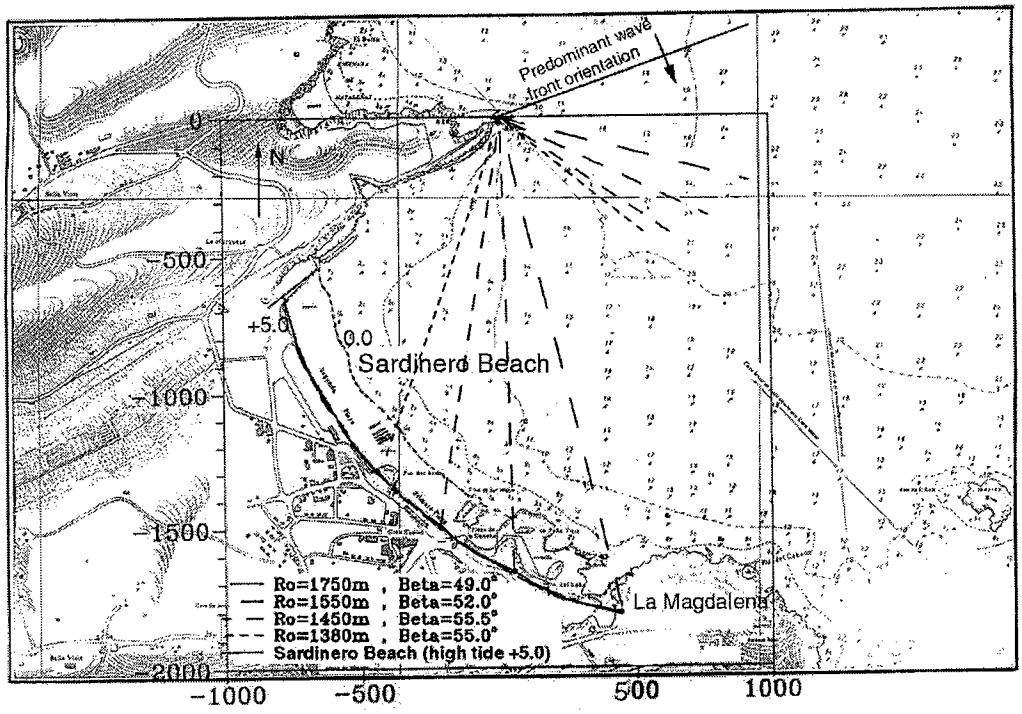

Figure 5. Predicted shorelines at Sardinero beach. Note that given a coastline point, the upcoast shoreline from that point can be represented using the tangent to the shoreline at that particular point as the orientation of the front at the diffraction point. In other words, any point can be used as the downcoast tip.

After applying the methodology proposed by Hsu et al. (1989 a, b) to several beaches along the Spanish coast, some deficiencies were noted, giving rise to the following questions:

- How can one define the downcoast tip of the fully-developed bays when the tip is unclear? In other words, is the downcoast tip of the fully-developed bay unique?

- Why must one apply different orientation fronts to two beaches in the same area with the same wave climate conditions in order to fit the static equilibrium shoreline? In other words, is the wave front unique?

- What is the criteria to be applied to define the front orientation at the control point, in order to predict the static equilibrium shoreline for undeveloped beaches (beaches without the straight alignment downcoast) or for the design of new (non-existing) beaches?

In order to answer these questions, the following semi-empirical model is proposed.

3. EQUILIBRIUM PLAN FORM CONCEPTUAL MODEL

The plan form of a beach is governed mainly by the wave-induced currents, the existing sediment (quantity, size) and the boundaries which confine the beach. Longshore currents are very important in the disposition of equilibrium beaches and, more precisely, in its plan form, given its importance on the potential transport of sand. Following Komar's (1970, 1975), Ozasa and Brampton's (1980) and using the longshore depth-integrated and time-averaged momentum equation in shallow water, Gonzalez (1995) derived a relationship for the mean time-averaged longshore current velocity $\overline{V}$ in the surf zone. This relationship can be expressed as:

$$\overline{V} = \frac{\pi}{c_f}\sqrt{gHb}\left[K_1 sin\theta_b \cos\theta_b - K_2 \frac{\partial Hb}{\partial y}\right] \tag{2}$$

where

$$K_1 = \frac{5}{32}\gamma^{1/2} tan\beta$$

$$K_2 = \frac{2K_3}{\gamma^{1/2}}\left[\frac{\gamma^2}{8}\left(\frac{3}{5}sin^2\theta_b + \frac{1}{3}\right) + \frac{1}{3}\right] \tag{3}$$

$$K_3 = \frac{5}{2\left(3\gamma^2 + 8\right)}$$

c_f is the bottom friction coefficient as expressed by Longuet-Higgins (1970), H_b is the wave height in the breaking condition, θ_b is the angle of the breaking waves to the local shoreline, γ is the breaker index (ratio of wave height to water depth at breaking, H_b/h_b), $\tan\beta$ is the average bottom slope from the shoreline to the water depth at breaking, y is the alongshore coordinate and g is the gravitational acceleration.

3.1 Static equilibrium shoreline $\left(\overline{V} = 0\right)$

According to Ho (1971) from laboratory tests, and Yamashita et al. (1992) using numerical simulations, a beach reaches a "static equilibrium shape" when the mean time-averaged longshore current velocity is negligible and the breaker wave front is almost parallel to the shoreline.

Using $\overline{V} = 0$ in eq. (2) we obtain the following relationship:

$$\frac{\partial H_b}{\partial y} = \frac{K_1}{2K_2} sin2\theta_b \tag{4}$$

assuming $\theta_b <<$, eq. (4) can be written as:

$$\theta_b = K_4 \frac{\partial H_b}{\partial y} \cong K_4 \frac{\delta H_b}{\delta y} \tag{5}$$

$$\theta_b \delta y \cong K_4 \delta H_b \cong \delta r \tag{6}$$

$$K_4 = \frac{4\gamma^2 + 32}{3\gamma \, tan\beta(3\gamma^2 + 8)} \tag{7}$$

where $\delta r, \delta y, \delta H_b, y, \theta_b$ are defined in figure 6. In this graph it is shown that δr is the deviation from the wave front to obtain the corresponding static equilibrium shoreline position. Note in eq. (6), that if we do not have the wave height longitudinal gradient, then $(\delta r = 0)$.

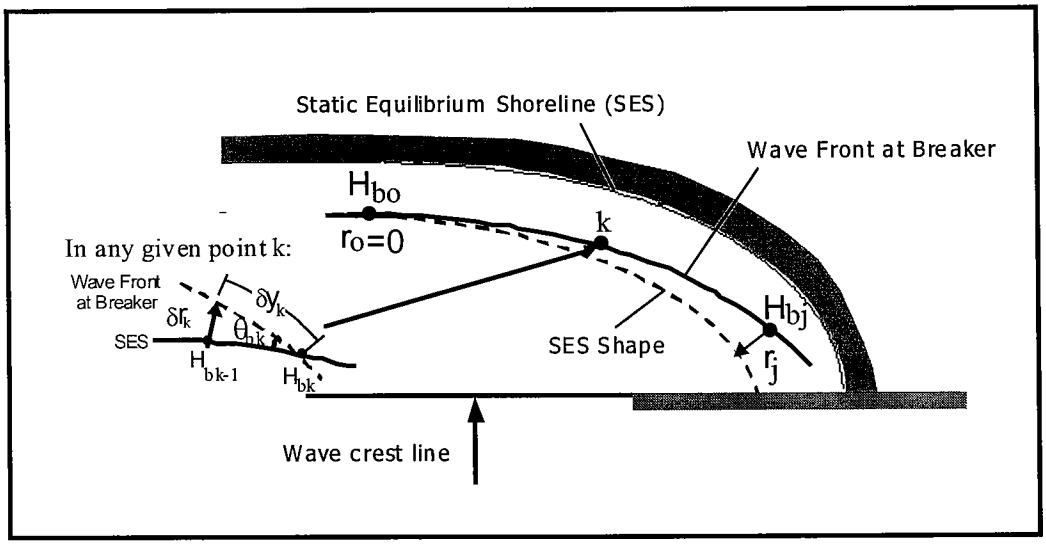

Figure 6. Definition sketch of the equilibrium plan form conceptual model.

3.2 Dynamic equilibrium shoreline $(\overline{V} = V_0)$

It is also possible to find an equilibrium shape in a beach with a continued littoral drift and with a constant sediment-transport rate (Hsu et al., 1993; Silvester et al. 1997). This "dynamic equilibrium shape" can be obtained assuming a constant mean time-averaged longshore current velocity $\overline{V} = V_0$ in eq. (2):

$$\frac{\partial H_b}{\partial y} = \frac{K_1}{2K_2} sin2\theta_b - K_5 V_0 \tag{8}$$

with

$$K_5 = \frac{c_f}{\pi\sqrt{gH_b}K_2}$$

assuming again θ_b <<, eq. (8) can be written as:

$$\theta_b \delta y \cong K_4\left[\delta H_b + K_5 V_0 \delta y\right] \cong \delta r \qquad (9)$$

It is noted that eq. (9) leads to eq. (6) when $V_0 = 0$ (static equilibrium). It is also remarked that even in the case where there are no wave height gradients (δH_b), the deviation of the coastline from the wave front, δr, is not equal to zero ($\delta r \neq 0$), which means that the wave front in the breaker line will not be parallel to the shoreline. This feature, associated with the constant current V_0, makes the dynamic equilibrium shoreline different from the static equilibrium shoreline, as previously suggested by Hsu et al. (1993) and Silvester et al. (1997).

For both static or dynamic equilibrium shapes, the following relationship can be established:

$$ES_j = WFB_j + \int_{r_0}^{r_j} dr \qquad (10)$$

where j represents any point along the wave front in the breaker line, ES_j is the static or dynamic equilibrium shoreline position in j, WFB_j is the wave front in the breaking line in j.

Using eq. (6) for static equilibrium and eq. (9) for dynamic equilibrium, eq. (10) can be written as:

$$SES_j = WFB_j - \int_{H_0}^{H_j} K_4 dH \qquad \text{for static equilibrium} \quad (11)$$

$$DES_j = WFB_j - \left[\int_{H_0}^{H_j} K_4 dH + \int_{y_0}^{y_j} K_4 K_5 V_0 dy\right] \qquad \text{for dynamic equilibrium} \quad (12)$$

assuming K_4 as a constant in the static equilibrium eq. (11), we obtain:

$$SES_j \cong WFB_j - K_4 \Delta H_j \qquad (13)$$

This means that the static equilibrium shoreline *(SES)* can be obtained from the position of the wave front at the breakerline *(WFB)*, minus a term that is proportional to the longitudinal wave height gradient. It is noteworthy that the *SES* depends on the wave height gradient and not on the incident wave height.

4. STATIC EQUILIBRIUM SHAPE BEHIND A HEADLAND

When a wave impinges a breakwater refraction and diffraction effects are present behind the barrier and three possible regions are generated (figure 7): Region (1) where the breakwater has no effect on the wave, the wave height gradients are practically zero and the wave fronts remain invariable; Region (2) where wave height gradients are present and the waves suffer only the effect of refraction; and Region (3) where wave height gradients and the turning of the fronts due to wave refraction-diffraction exist.

In figure 7 point (P_0) corresponds to the "downcoast" limit of the affected beach, where no longitudinal gradients of wave height exist due to the breakwater and, in accordance with the conceptual model eq. (13), the static equilibrium shoreline is equal to the wave front ($SES \simeq WFB = WFP$).

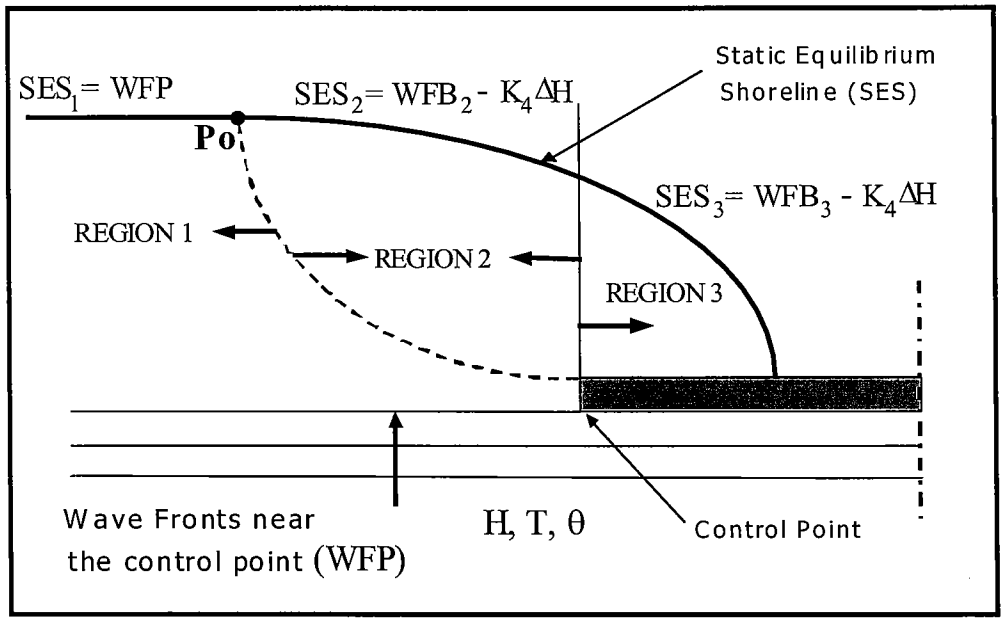

Figure 7. Definition sketch of the regions generated by an offshore barrier or breakwater. In region (1) the breakwater has no effect on the wave field, the wave height gradients are negligible and the wave fronts remain invariable; In region (2) wave height gradients are present and wave refraction is relevant; In region (3) wave height gradients and the turning of the fronts due to wave refraction-diffraction are important.

According to Gonzalez's (1995) conclusions, the parabolic formulation proposed by Hsu and Evans (1989) represents quite well the static equilibrium shoreline in bays. Therefore, this empirical formulation can be used as a solution that satisfies eq. (11). Furthermore, when using Hsu and Evans' (1989) parabolic formulation, the local tangent at "any point" along the static equilibrium shoreline *(SES)* can be used as the wave front at the control point in order to represent the SES upcoast from that particular point (see figure 5). This means that we can choose point *(P0)* as the starting point and, consequently, the orientation of the front at the control point is the predominant wave direction at the control point area.

It is noted that in order to define point *P0* for any beach, it is necessary to determine the angle, *αmin*, and the distance, *Y*, from the control point to the straight alignment downcoast as shown in figure 8.

A first approximation for *αmin* can be obtained using the analytical solution of wave diffraction for a flat bottom given by Penney and Price (1944). Gonzalez (1995) proposed an analytical expression for *αmin*, for the case of diffraction with weak refraction. The value of *αmin* was found to be a function of the dimensionless distance of the beach to the wave length, *Y/L*.

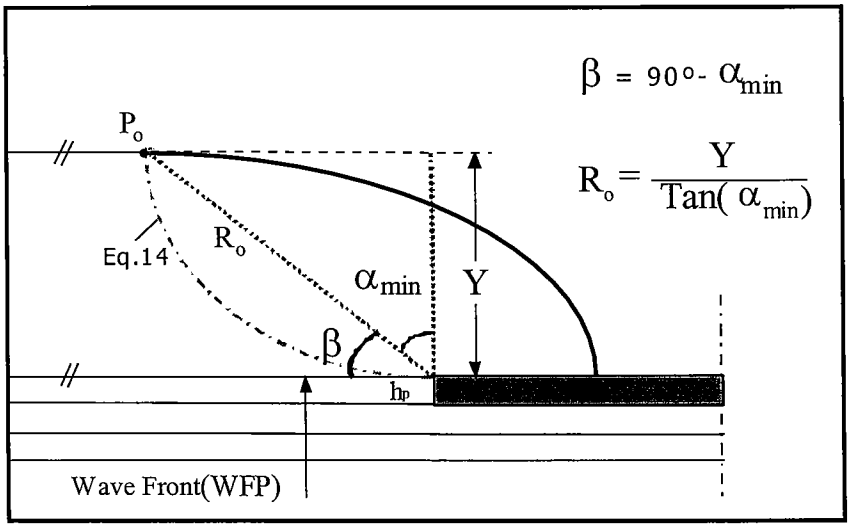

Figure 8. Definition sketch showing the relationship between the variables β and R_0, which are used in Hsu and Evans's (1989) equilibrium shape formulation (see also figure 1) and the variables α_{min} and Y used in the proposed methodology. Y is the distance from the control point to the prolongation of the straight alignment downcoast. α_{min} is related to β through $\beta=90° - \alpha_{min}$.

In natural beaches, where diffraction-refraction effects are important, the problem of finding an analytical solution is far more complex. In order to obtain an expression to define *αmin* for real beaches, an empirical approach has been carried out using data from 26 beaches along the Atlantic and Mediterranean coasts of Spain. The selected

beaches are fully-developed beaches with a straight alignment downcoast. Furthermore, in order to relate the wave length to be used in *Y/L* and the downcoast alignment to the waves in the area, wave height and wave period data series were determined in deep water for each beach. Then, these waves were propagated numerically to the beach.

Regarding the coast's orientation, it was observed that the downcoast straight alignment was parallel to the resultant wave front associated with the mean energy flux at the control point for all of the beaches. The determination of *"the wave length"*, however, was not a straightforward task since wave periods affecting a particular beach vary a lot and, for a given wave period, the wave length along the propagation area changes due to the beach profile water depth variation. A *"scaling wave length, L_S,"* was then selected for the estimation of the dimensionless distance from the control point to the beach, *Y/L*. This scaling wave length, L_S, was calculated using the mean water depth along the wave front close to the control point, h_p, and the mean wave period associated with the wave height exceeded 12 hours per year, H_{S12}, hereafter called, $T_{H_{S12}}$. According to the recorded wave data, this $T_{H_{S12}}$ had a mean probability of exceedance of 0.03 ($P[T \leq T_{H_{S12}}] = 0.97$). It is noted that the selection of that particular wave period is arbitrary. Any other characteristic period (e.g. mean, significant...) could be used to scale the distance from the control point to the beach.

Figure 9 shows the measured αmin versus Y/L_S for the selected beaches. The theoretical weak refraction solution (dashed line) and the data best-fit curve (solid line) are also plotted in figure 9.

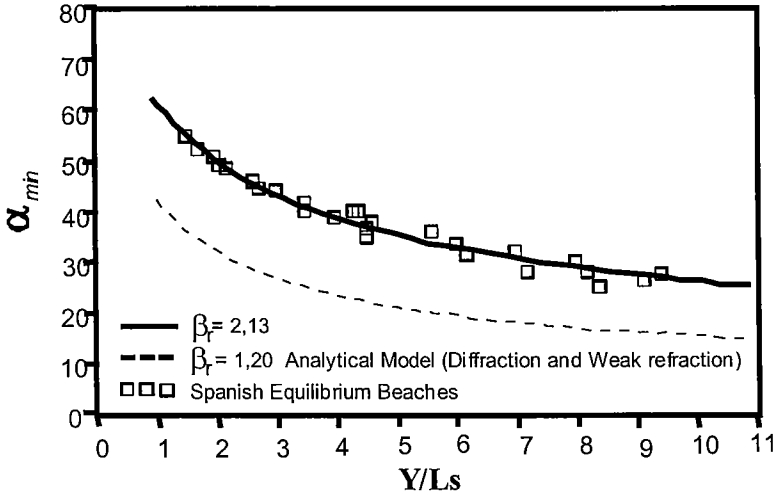

Figure 9. Value of the angle α_{min} for different dimensionless distances from the control point to the prolongation of the straight alignment downcoast (Y/L). These values have been obtained using data from 26 beaches along the Atlantic and Mediterranean coasts of Spain. The analytical expression for *αmin*, for the case of diffraction with weak refraction derived by Gonzalez (1995) is also graphed with a dashed line.

The equation of the solid curve shown can be represented by:

$$\alpha_{\min} = \arctan\left[\frac{\left(\frac{\beta_r^4}{16} + \frac{\beta_r^2}{2}\frac{Y}{L_S}\right)^{\frac{1}{2}}}{\frac{Y}{L_S}}\right] \qquad (14)$$

with $\beta r = 2.13$.

The level of confidence of 100% α_{min} is:

$$\alpha_{\min} = \alpha_{\min}\left[\beta_r = 2.13, \frac{Y}{L_S}\right] \pm 5^o \qquad (15)$$

5. PROPOSED MODEL

Using the aforementioned findings, a simple model for static equilibrium shoreline in bays can be proposed. The model is based on three fundamental aspects:

- The orientation of the wave front at the diffraction point that must be used when applying Hsu and Evans' (1989) formulation corresponds with the front of the mean energy flux of the waves at the control point area.
- The downcoast limit, point P_0, can be fixed using the proposed relationship for $\alpha min = f(Y/L_S)$, figure 9.
- The static equilibrium shoreline in bays can be obtained using the parabolic model of Hsu and Evans (1989), starting in P_0. The β and R_0 parameters are defined as:

$$\beta = 90^o - \alpha_{min} \qquad \text{and} \qquad R_0 = \frac{Y}{\cos\alpha_{min}} \qquad (16)$$

By defining these three aspects, the static equilibrium plan form of any crenulate-shaped beach can be obtained, keeping in mind that the following basic hypotheses must be fulfilled:

- Longitudinal gradients of wave height on the beach are governed only by the diffraction of the control point (diffraction point) and the refraction over the sandy beach. Local diffraction by islands, shallows, etc., cannot be represented.
- Only longshore currents associated with the wave-induced currents are important.
- Only one point of diffraction exists. If there would be any more, they should not

interact mutually along the beach.

6. HEADLAND-BAY BEACHES

The proposed model can be applied to solve a wide range of coastal engineering problems involving both fully-developed and undeveloped equilibrium bay beaches. Two different situations or applications can be distinguished: a) to test the stability of a given bay beach and, b) to design a new bay beach.

In the first case, the bay beach exists and the objective is to determine if it is in static equilibrium and, if not, what the final static equilibrium plan form will be. In the second one, there is a bay with no beach and the objective is to determine the plan form of a beach in equilibrium with the existing wave climate.

It is noted that for the simple case of testing the stability of a given bay, in the form of an aerial photograph, a hydrographic chart or a map to sufficient scale, the procedure described by Hsu et al (1989a) can be used. In this procedure it is assumed that the tangent to the beach at the downcoast tip of the bay is normal to the orthogonal of the local wave and no further data regarding the wave climate is needed. However, the following procedure must be followed if the wave climate affecting the beach is to be changed due to offshore constructions or if there is not a previous beach providing an estimation of the tangent to the beach to be carried to the control point,.

6.1 Procedure

Fully-developed beaches: To test the stability of a given fully-developed beach *(FDB)* or to design a new fully-developed bay beach, first determine the downcoast limit (point P_0) using the angle $\alpha min = f(Y/L_S)$ and obtain β and R_0 from eq. (16), see figure 8. Then use Hsu and Evans' (1989) parabolic formulation for calculating the equilibrium shape

Undeveloped beaches: To test the stability of an existing undeveloped bay beach or to predict the static equilibrium shape for newly designed undeveloped bay *(UDB),* assume that the *UDB* is part of a hypothetical *FDB,* and:

1. Determine the orientation of the wave front at the control point. This wave front corresponds with the front of the mean energy flux of the waves in the area.

2. Define one point at the shoreline P_C ($\theta_C > \beta$, R_C) as shown in figure 10:

a. To test stability: Select any point along the static equilibrium shoreline, taking into account that this point must not be affected by any other local diffraction.

b. To design a new bay beach: In this case there is no shoreline, consequently, an estimation of the location of the future shoreline is needed. Since for the static equilibrium not only the shoreline but also the complete beach profile must be placed within fixed boundaries, define the limiting offshore point, P_L, so that the lateral and bottom boundaries are able to contain the cross-shore profile. Starting at P_L and using an equilibrium beach profile formulation (e.g. Gonzalez and Medina, 1997 or Medina et al. 2000) determine point P_C (θ_C, R_C). It is remarked that any point landward P_C, see figure 10, can also be a solution of the problem yielding a different equilibrium beach with a different equilibrium shape (not parallel) and with a minor sand volume required.

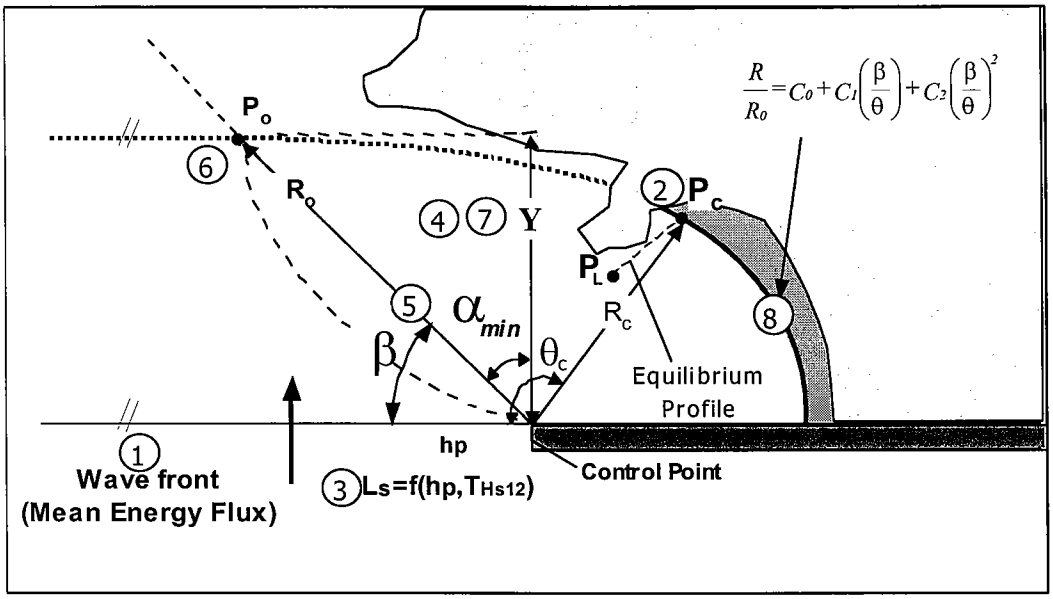

Figure 10. Definition sketch of the procedure method to test stability or to predict the static equilibrium shoreline in undeveloped bays. The numbers in the figure correspond to the different steps of the procedure.

3. Define the scaling wave length near the control point, $L_S = f(h_p, T_{H_{S12}})$, keeping in mind that h_p should be a mean water depth along the wave front close to the diffraction point and $T_{H_{S12}}$ refers to the mean wave period associated with the wave height exceeded 12 hours per year, H_{S12}.

4. Define Y for the hypothetical *FDB*, even though the straight alignment downcoast does not exist. An iterative process can be necessary. As a first approach, use the

Y value for the area through which the coastline runs in the downcoast limit (P_0).

5. Evaluate angle β using $\alpha min = f(Y/L_S)$, eq. (14) or figure 9.

$$\beta = 90° - \alpha_{min} \tag{17}$$

6. Define point P_0. This point can be defined evaluating R_0 from the parabolic model of Hsu and Evans (1989) as:

$$R_0 = \frac{R_c}{C_0 + C_1\left(\frac{\beta}{\theta_c}\right) + C_2\left(\frac{\beta}{\theta_c}\right)^2} \tag{18}$$

with C_0, C_1 and $C_2 = f(\beta)$ and R_c, θc previously defined by P_c.

7. Recalculate Y using:

$$Y' = R_0 \cos\alpha_{min} \tag{19}$$

if Y' is far from the initially supposed Y value, go back to step (4).

8. Using Hsu and Evans' (1989) parabolic formulation, radii, R, can be obtained for different angles θ, yielding the equilibrium shape.

6.2 Application of the procedure

The above stated methodology has been applied to several beaches along the Atlantic and Mediterranean coasts for both high- and low-tides with very good results. As an example, it will be applied to the : Sardinero Beach.

The Sardinero Beach, as previously described, is an undeveloped beach. The high-tide shoreline obtained following the proposed procedure is represented in figure 11. In this figure the wave front orientation at the control point associated with the wave mean energy flux, the final shoreline distance Y, the αmin and β angles, and the calculated R_0 are also shown.

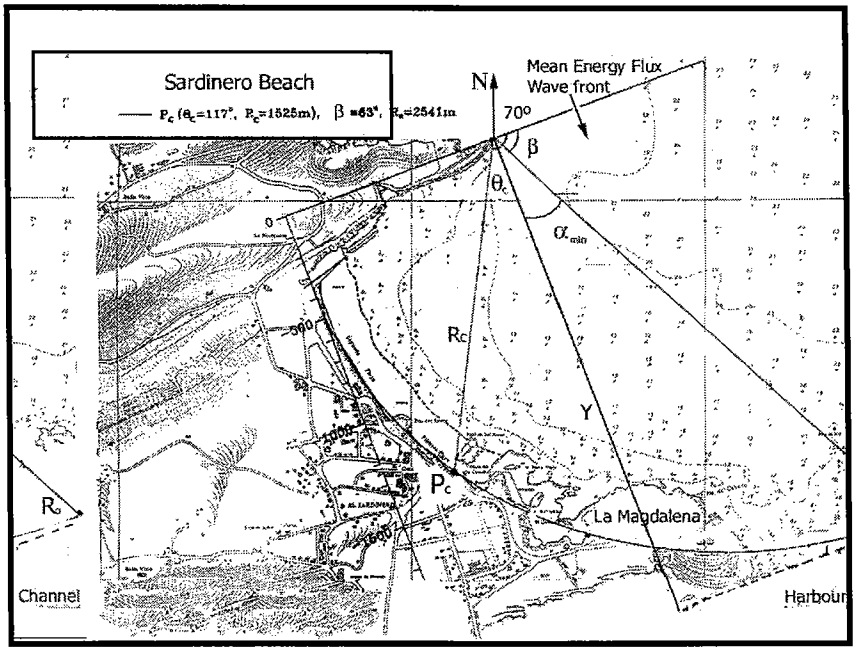

Figure 11. Application of the proposed methodology for predicting the static equilibrium shoreline in undeveloped bays to Sardinero beach. The input data needed to obtain the predicted shoreline are the direction of the mean wave energy flux at the area and point , P_c, which one wants the shoreline to pass through.

7. TOMBOLO AND SALIENT DESIGN

Using the value of αmin as the limit of the coastline affected by a breakwater, Gonzalez and Medina (1999) analyzed the main characteristic of the shoreline response to an offshore breakwater. In their work three different responses were described: (1) tombolo, (2) salient and (3) double salient. In the next section, the formulation and procedure described in this paper and new laboratory and field data are used to determine and validate the morphological characteristics of a tombolo and a salient (figures 12 and 13), which are the shoreline responses of major interest in engineering applications.

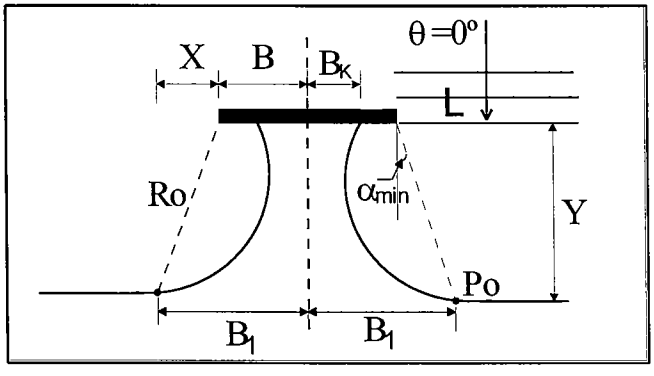

Figure 12. Definition sketch of a tombolo. The typical unknown variables, when designing a tombolo are the shoreline length affected by the breakwater, $2B_1$, and the attachment width at the breakwater, B_k. These variables are given in figure 14.

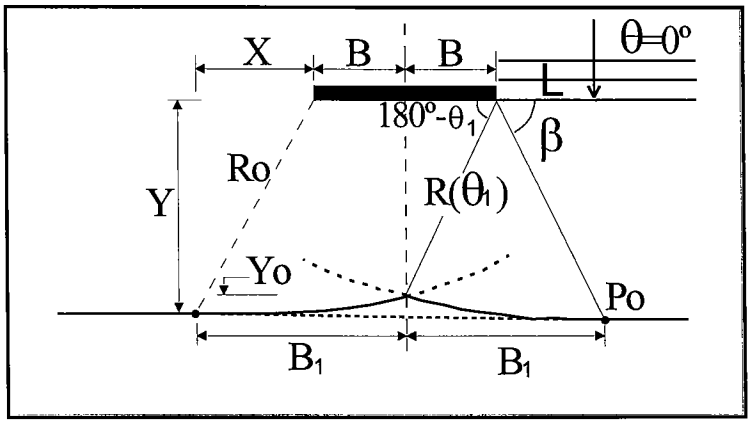

Figure 13. Definition sketch of a theoretical salient. The typical unknown variables, when designing a salient are the salient apex, Y_0, and the shoreline length affected by the breakwater, $2B_1$. These variables are given in figure 14.

7.1 Tombolo case

If the distance from the breakwater to the shoreline is close enough, and the breakwater is long with respect to the length of the incident waves, sand will accumulate behind the breakwater until a tombolo forms; that is, the shoreline continues to build seaward until it connects with the breakwater. The variables governing the equilibrium shape are (figure 12): the length of the breakwater, $2B$, the distance from the breakwater to the shoreline, Y, and the wavelength, L, which defines αmin. The unknown variables, namely, the shoreline length affected by the breakwater, $2B_1$, and the attachment width at the breakwater, B_k, can easily be obtained from Hsu and Evans' (1989) parabolic-shaped formulation and the αmin expression (eq. 14). The solutions for these variables are presented in figure 14.

7.2 Salient case

When the breakwater is far from the shoreline and its length is short with respect to the length of the incident waves, the shoreline will build a salient seaward.

The governing variables involved in the equilibrium shape of the salient are the same as in the case of the tombolo, namely: the length of the breakwater, $2B$, the distance from the breakwater to the shoreline, Y, and the wavelength, L, which defines αmin. The unknown variable is the salient apex, Y_0 (see figure 13). As in the tombolo case, the unknown variable can easily be obtained from Hsu and Evans' (1989) parabolic-shaped formulation and the αmin expression (eq. 14). The solution for this variable is also presented in figure 14.

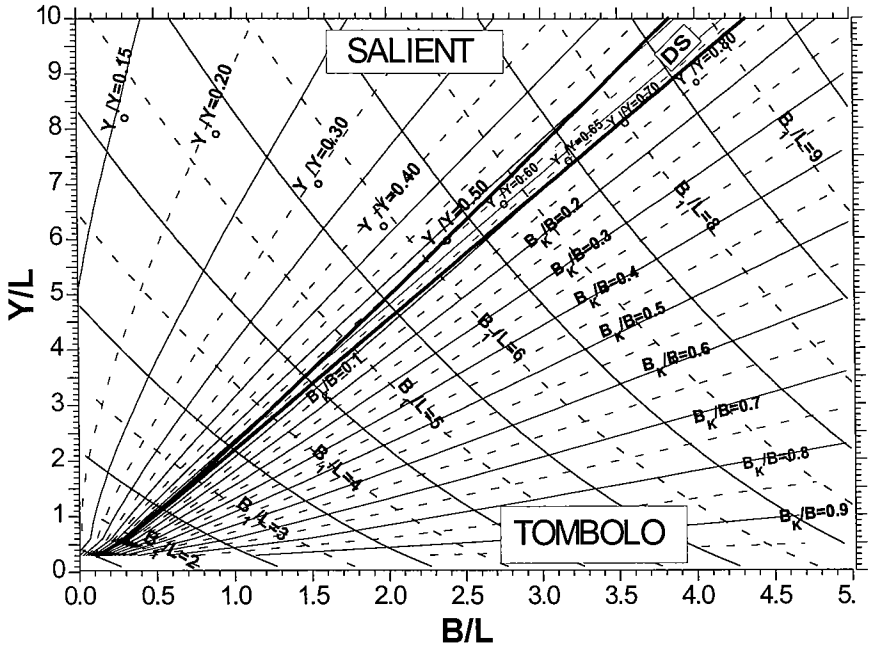

Figure 14. Variation of the non-dimensional equilibrium plan form parameters: for Tombolo: (Bk/B, B1/L) and Salient (Y0/Y, B1/L) for different values of the length of the breakwater, *2B*, the distance from the breakwater to the shoreline, *Y*, and the wavelength, *L* (see figures 12 and13 for a definition sketch of the different variables).

7.3 Validation of the proposed formulation

7.3.1 Tombolo

The present tombolo formulation has been compared to field and experimental data reported by Toyoshima (1974), Nir (1976), Rosen and Vajda (1982), Dally and Pope (1986), Gonzalez (1995) and Ming and Chiew (2000). The measured values of the different variables involved in the tombolo geometry (T_S, h_0, *L*, *B/L*, *Y/L*, B_k/B, B_1/L, *2B/Y*) and the estimated values of the unknown variables (B_k/B, B_1/L), obtained from present formulation, are given in table 1. All dimensions in table 1 are given in meters and in seconds, and it is also reported whether the data applies to prototype, *P* or model *M*.

It can be clearly observed from table 1 that the predicted values of the dimensionless parameter, B_k/B, are very close to the measured data. In the same way, the comparison between measured and calculated values of the dimensionless parameter, B_1/L, shows that the present formulation matches well with the measured data.

It is remarked that although the dimensionless parameter, B_1/L, has previously received minor attention, it is of major importance since it defines the final shape of the shoreline and consequently, whether a tombolo or salient is formed.

TOMBOLOS		MEASURED PARAMETERS								Estimated from Fig. 14	
Location and Authors	M/P	T_s	h_0	L	B/L	Y/L	B_k/B	B_l/L	2B/Y	B_k/B	B_l/L
1 Kaike (Japan), Toyoshima (1974)	P	11	5.0	75	1.00	1.5	0.33	-	1.36	0.34	3.1
2 Haifa (Israel), Nir (1976)	P	10	3.0	53	2.70	3.8	0.46	-	1.40	0.44	5.8
3 Tel Baruch (Tel Avi), Nir (1976)	P	10	3.0	53	1.90	1.9	0.53	-	2.00	0.55	4.2
4 Venice Calif., Dally and Pope (1986)	P	18	2.0	80	1.25	2.6	0.15	-	0.95	0.14	3.8
5 Rosen and Vadja (1982)	M	1.0	0.03	0.53	1.89	1.9	0.49	3.8	2.00	0.53	3.7
6 Tarragona (Spain), González (1995)	P	8.5	0.8	20	3.25	4.5	0.40	6.5	1.44	0.43	6.7
7 Tarragona (Spain), González (1995)	P	8.5	0.8	20	3.50	7.5	0.20	7.8	0.93	0.17	7.7
8 Tarragona (Spain), González (1995)	P	8.5	1.4	25	3.20	4.0	0.50	6.4	1.60	0.48	6.4
9 Tarragona (Spain), González (1995)	P	8.5	0.8	20	3.25	3.0	0.62	6.0	2.17	0.62	6.1
10 Tarragona (Spain), González (1995)	P	10	0.6	24	1.70	3.3	0.13	4.4	1.00	0.15	4.6
11 Tarragona (Spain), González (1995)	P	10	0.8	28	2.70	4.6	0.24	6.0	1.15	0.26	6.0
12 Tarragona (Spain), González (1995)	P	10	1.5	38	2.60	3.9	0.35	5.7	1.33	0.38	5.8
13 Tarragona (Spain), González (1995)	P	10	1.5	38	2.60	3.2	0.45	5.3	1.67	0.46	5.5
14 Ming and Chiew (2000)	M	0.85	0.06	0.62	0.73	1.2	0.24	2.6	1.20	0.25	2.7
15 Ming and Chiew (2000)	M	0.85	0.06	0.62	0.97	1.3	0.38	2.8	1.40	0.40	3.0
16 Ming and Chiew (2000)	M	0.85	0.06	0.62	1.20	1.4	0.44	3.0	1.70	0.46	3.2
17 Ming and Chiew (2000)	M	0.85	0.08	0.70	0.86	1.63	0.17	2.6	1.10	0.18	3.1
18 Ming and Chiew (2000)	M	0.85	0.10	0.76	0.99	1.89	0.12	2.9	1.00	0.15	3.2

Table 1. Data regarding tombolo characteristics. The prototype (P) and model (M) measured parameters reported by several authors are presented and compared with predicted values obtained from fig. 14. (All the units are given in meters and seconds).

7.3.2 Salient

The proposed equilibrium shape model is able to adequately represent the equilibrium shoreline in cases where the beach is affected only by one diffracting point. These include the cases of tombolos and of salients formed by T-Groins, where each side of the salient is affected by only one tip of the offshore breakwater. Only in these cases, the salient apex, Y_0, given in figure 13, applies.

In general diffraction at the two breakwater tips affects both sides of a salient yielding an apex length, Y_S, shorter than Y_0, (see figure 15). Hsu and Silvester (1990) proposed an empirical formulation which defines the apex position, Y', $(Y' = Y - Y_S)$ as a function of the ratio of the distance, S, from the original shoreline to the breakwater and the breakwater length, $2B$. As stated previously, a constant value of the angle β ($\beta = 40^o$) was assumed in their work.

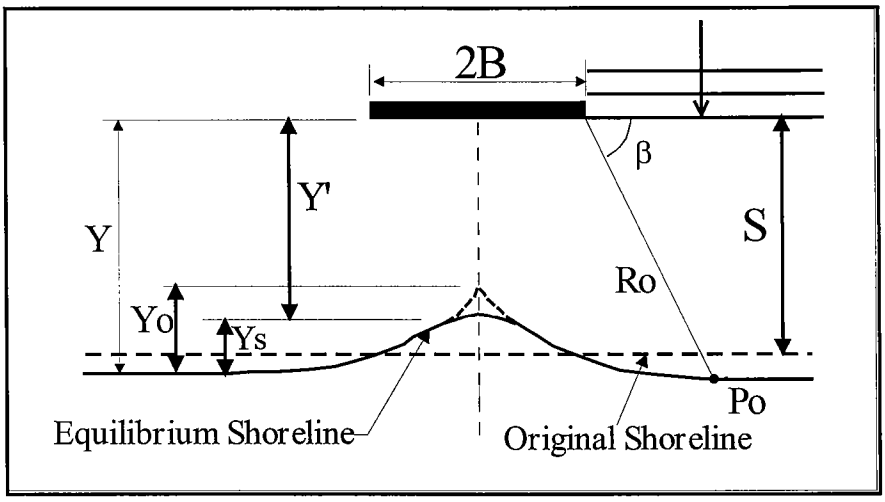

Figure 15. Definition sketch of a salient. In this figure both the theoretical (dashed line) and the actual salient shape (solid line) are graphed. Equilibrium shape formulations can only give information for the theoretical shape. In order to obtain the actual shape empirical data must be used. The differences between these shapes are usually expressed in terms of the ratio Y_0/Y_s or Y_0/Y'. Note that two distances from the breakwater to the shoreline are defined: Y and S. Laboratory data usually refers to S while analytical and field data are given using Y.

In the present work data from both field and laboratory measurements reported by Shinojara and Tsubaki (1966), Noble (1978), Rosen y Vajda (1982), Gonzalez (1995) and Ming and Chiew (2000) have been used to find a relationship between Y_S and Y_0. Data are presented in table 2.

Since the range of the available data for B/L and Y/L is too small for separating the influence of the wavelength in β, a single curve, valid for $0.3<B/L<1.5$ and $2.0<Y/L<4.0$ is proposed. The relationship obtained, eq. 20, is similar to the one

$$\frac{Y'}{2B} = 0.50\left(\frac{2B}{Y}\right)^{-\sqrt{2}} \tag{20}$$

proposed by Hsu and Silvester (1990) and is plotted in figure 16.

As in the tombolo case, the comparison of measured and calculated values of the dimensionless parameter, B_1/L, shows that the present formulation adequately represents the available data.

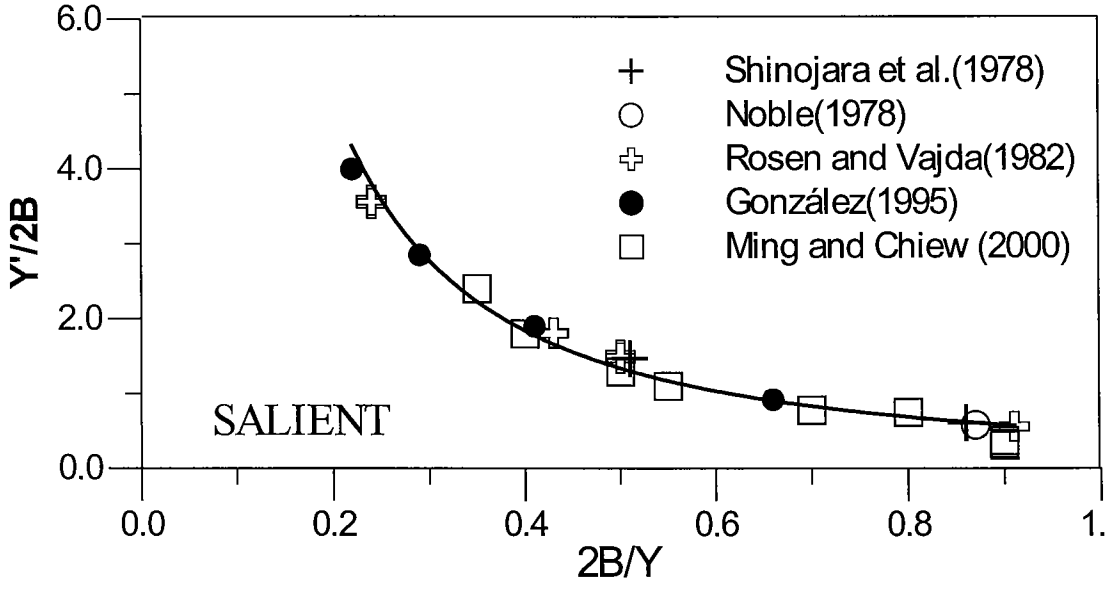

Figure 16. Relationship between the theoretical and the actual salient shape expressed in terms of Y and Y'(see figure 17). Dimensionless parameters, Y'/2B and 2B/Y are used to fit the field and laboratory data presented in table 2. Equation 20 is also graphed (solid line).

SALIENTS		Measured Parameters									Estimated from fig. 14	
Location and Authors	M/P	T_S	h_0	L	B/L	Y/L	Y_s/Y	B_1/L	$(2B)/Y$	$Y'/(2B)$	Y_0/Y	B_1/L
1 Shinohara & Tsubaki (1966)	M	0.92	0.10	0.84	0.89	2.08	0.47	-	0.86	0.61	0.65	3.30
2 Shinohara &Tsubaki (1966)	M	0.92	0.18	1.00	0.75	2.92	0.25	-	0.51	1.47	0.38	3.60
3 St. Monica, Noble (1978)	P	18.00	7.20	149.0	1.74	4.03	0.53	-	0.87	0.54	0.80	5.00
4 Rosen and Vajda (1982)	M	0.80	0.05	0.53	0.47	3.96	0.15	3.77	0.24	3.58	0.24	3.70
5 Rosen and Vajda (1982)	M	0.80	0.03	0.42	0.60	2.40	0.24	3.38	0.50	1.52	0.36	3.25
6 Rosen and Vajda (1982)	M	1.00	0.07	0.79	0.32	2.70	0.17	2.80	0.24	3.54	0.25	3.00
7 Rosen and Vajda (1982)	M	1.00	0.03	0.53	0.47	1.89	0.26	2.64	0.50	1.48	0.36	2.75
8 Rosen and Vajda (1982)	M	1.00	0.03	0.53	0.94	2.06	0.49	3.20	0.91	0.56	0.70	3.40
9 Rosen and Vajda (1982)	M	1.15	0.08	0.98	0.51	2.40	0.23	-	0.43	1.81	0.34	3.10
10 Cambril,González(1995)	P	10.00	1.30	35.00	0.71	3.43	0.21	-	0.41	1.90	0.32	3.70
11 Cambril,González(1995)	P	10.00	0.90	30.00	0.33	3.00	0.11	3.30	0.22	4.00	0.24	3.20
12 Cambril,González 1995)	P	10.00	1.00	31.00	0.32	2.26	0.18	2.70	0.29	2.85	0.29	2.80
13 Altafulla,González(1995)	P	9.00	3.50	51.00	1.18	3.52	0.39	4.50	0.66	0.92	0.50	4.25
14 Ming and Chiew (2000)	M	0.85	0.08	0.70	0.43	1.64	0.38	2.40	0.55	1.10	0.40	2.60
15 Ming and Chiew (2000)	M	0.85	0.08	0.70	0.64	1.49	0.72	2.60	0.90	0.31	0.80	2.80
16 Ming and Chiew (2000)	M	0.85	0.10	0.76	0.59	1.70	0.54	2.40	0.70	0.78	0.50	2.70
17 Ming and Chiew (2000)	M	0.85	0.10	0.76	0.79	1.71	0.71	2.80	0.90	0.33	0.74	3.00
18 Ming and Chiew (2000)	M	0.85	0.12	0.82	0.37	1.90	0.08	2.50	0.35	2.40	0.32	2.70
19 Ming and Chiew (2000)	M	0.85	0.12	0.82	0.55	2.06	0.27	-	0.50	1.29	0.40	3.00
20 Ming and Chiew (2000)	M	0.85	0.12	0.82	0.73	2.00	0.45	-	0.80	0.75	0.47	3.10
21 Ming and Chiew (2000)	M	0.85	0.12	0.82	0.91	2.12	0.66	-	0.90	0.37	0.68	3.30

Table 2. Data regarding salient characteristics. The prototype (P) and model (M) measured parameters reported by several authors are presented and compared with predicted values obtained from fig. 14. (All the units are given in meters and seconds).

7.3.3 Limiting Conditions of Tombolo-Salient

In the last few decades many authors have proposed empirical values for the geometry of a breakwater so that a tombolo is generated. From tables 3 and 4, it can be concluded that there is a large dispersion in the proposed values for determining the limiting conditions of tombolo-salient. One possible explanation of this dispersion could be the minor attention that the influence of the wave characteristics (e.g. Y/L) has received by previous investigators.

Condition	Comments	Reference
2B/S > 0.67 to 1.0	Tombolo	Gourlay (1981)
2B/S > 2.0	Tombolo	SPM (1984)
2B/S > 1.5 to 2.0	Tombolo	Dally & Pope (1986)
2B/S > 1.0	Tombolo	Suh & Dalrymple (1987)

Table 3. Limiting conditions for the formation of a tombolo proposed by several authors.

Condition	Comments	Reference
2B/S < 0.4 to 0.5	Salient	Gourlay (1981)
2B/S < 1.0	No tombolo	SPM (1984)
2B/S = 0.5 to 0.67	Salient	Dally & Pope (1986)
2B/S < 1.0	No tombolo	Such & Dalrymple (1987)
2B/S < 1.5	Well-developed salient	Ahrens & Cox (1990)
2B/S < 0.8 to 1.5	Subdued salient	Ahrens & Cox (1990)

Table 4. Limiting conditions for the formation of a salient proposed by several authors.

Using the proposed approach, it is possible to obtain the limiting condition for a tombolo or salient as a function of 2B/Y versus Y/L (see figure 17). It is noteworthy in figure 17, that for Y/L > 2.5, the curve slope is almost zero and, consequently, it is possible to define the limit for a tombolo formation as 2B/Y ≈0.86 to 0.88, in other words, the limit does not depend on the wave length. However, for Y/L < 2.5 the curve's slope increases sharply and it is not possible to determine the response of the shoreline just by means of 2B/Y, and the influence of Y/L must be taken into account. This could be the reason why, for the same 2B/S (≈ 0.7), Dally and Pope (1986) and Such and Dalrymple (1987) reported a salient while Gourlay (1981) reported a tombolo.

It is noted that caution must be taken when comparing the results of figure 17 with tables 3 and 4, since figure 17 uses the final equilibrium shoreline position, Y, while authors giving laboratory data, usually report the original shoreline position, S, (see figure 15). The relationship between Y and S is not unique since it depends on the lab set-up.

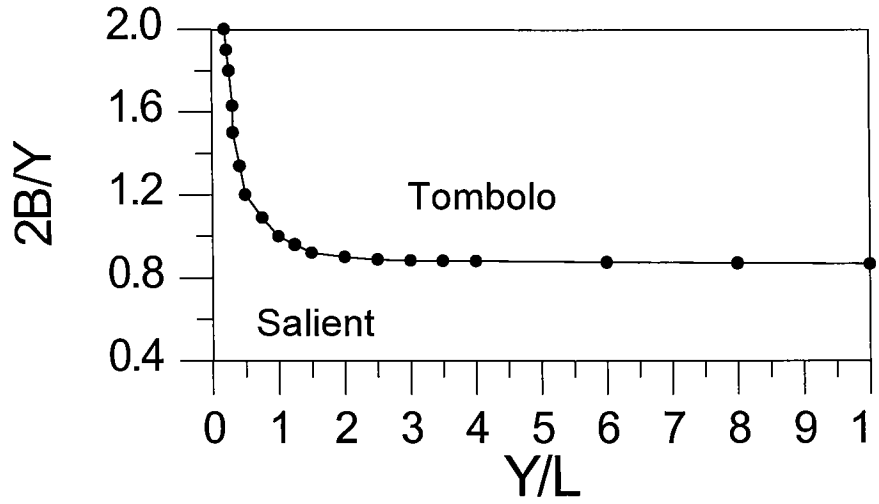

Figure 17. Proposed limiting condition for a tombolo or salient formation for a given length of the breakwater, *2B*, distance from the breakwater to the shoreline, *Y*, and wavelength, *L*. Note that for Y/L > 2.5, the curve slope is almost zero and, the limit for a tombolo formation is the only function of 2B/Y ≈0.86 to 0.88. However, for Y/L < 2.5 the influence of Y/L must be taken into account.

8. CONCLUSIONS

1. The procedure proposed by Hsu et al. (1989a, b) can be applicable in fully-developed beaches with good results, but by itself lacks theoretical support to define criterion for its application to testing the stability of existing undeveloped beaches or the prediction of new undeveloped beaches, including beaches affected simultaneously by different control points.

2. The new proposed model allows the determination of the angle αmin, which defines the downcoast limit from which the parabolic model is applicable in beaches with dominant refraction-diffraction effects. Also, it allows us to test the stability of undeveloped beaches or to predict new ones, by means of the definition of the front's orientation at the diffraction point in relation to the direction of the mean wave energy flux in the area.

3. A procedure is proposed to test stability or to design new static equilibrium crenulate beaches taking into account the equilibrium plan and profile. This methodology has been applied to various Spanish beaches on the Atlantic and

Mediterranean coasts with good results constituting a practical easy-to-use engineering tool in beach regeneration projects.

4. A semi-empirical analysis of the equilibrium shoreline behind an impermeable breakwater under normal wave attack has been presented. The analysis can be used to determine whether a tombolo salient or double salient is formed, as a function of the breakwater length, $2B$, the distance between the offshore breakwater and the coastline, Y, and the wavelength, L. The present formulation has been applied to several field and experimental data showing good agreement. It has been shown that if Y, B and L are known, it is possible to determine: (1) the kind of response (tombolo or salient), (2) the beach shape and (3) the affected area, $2B_1$, and therefore, the sand needed.

ACKNOWLEDGEMENTS

This study has been partly funded by the Commission of the European Communities in the framework of the Marine Science and Technology Programme (MAST), under the No. MAS3-CT97-0081 project "Surf and Swash Zone Mechanics" (SASME) and by the Comision Interministerial de Ciencia y Tecnologia under contract AMB99-0543. The authors are grateful for stimulating reviews by Professors John R. C. Hsu and Hans Hanson.

9. REFERENCES

Dally, W.R., and Pope, J. 1986. Detached breakwaters for shore protection. Tech. Report CERC-86-1, U.S. Army Engrs. Waterways Experiment Station, Vicksburg, Miss.,

Gonzalez, M., 1995. Morfologia de playas en equilibrio: planta y perfil, PhD Thesis, Departamento de Ciencias y Tecnicas del Agua y del Medio Ambiente, Universidad de Cantabria. Santander, Spain.

Gonzalez, M., R. Medina, 1997. Equilibrium beach profiles: effects of refraction. Proc. Coastal Dynamics'97, ASCE. pp. 933-942.

Gonzalez, M., R. Medina, 1999. Equilibrium shoreline response behind a single offshore breakwater. Proc. Coastal Sediment'99, ASCE, 1: pp. 933-942.

Ho, S.K., 1971. Crenulate shaped bays. Thesis n. 346, Assoc. Institute of Technology at Bangkok, Thailand.

Hsu, J.R.C., R. Silvester and Y.M. Xia, 1987. New characteristics of equilibrium shape bays. Proc. 8th Austral. Conf. on Coastal & Ocean Eng., pp. 140-144.

Hsu, J.R.C., and C. Evans, 1989. Parabolic bay shapes and applications. Proc., Institution of Civil Engineers, London, England, Vol. 87 (Part 2), 556 - 570.

Hsu, J.R.C., R. Silvester and Y.M. Xia, 1989a. Static equilibrium bays: New relationships. J. Waterway, Port, Coastal and Ocean Engineering, ASCE, 115(3), 285 - 298.

Hsu, J.R.C., R. Silvester and Y.M. Xia, 1989b. Generality on static equilibrium bays. Coastal Eng., 12, 353 - 369.

Hsu, J.R.C., R. Silvester and Y.M. Xia, 1989c. Applications of headland control. Journal of Waterway, Port, Coast and Oc. Eng. ASCE, 115 (3), pp. 299-310.

Hsu, J.R.C., and Silvester, R. 1990. Accretion behind single offshore breakwater. J. Wtrway., Port, Coast. and Oc. Engrg., ASCE, 116(3), 367 - 380.

Hsu, J.R.C., Uda, T. and Silvester, R. 1993. Beaches downcoast of harbours in bays. Coastal Eng. , 19:163-181.

Komar, P. and D.I. Inman, 1970. Longshore sand transport on beaches. Journal Geophys. Research, 75 (30), pp. 5914-5927.

Komar, P., 1975. Nearshore currents: generation by obliquely incident waves and longshore variations in breaker height. Proc. of the Symposium on Nearshore Sediment Dynamics, Ed. J. R. Hails and A. Carr, Wiley, London, pp. 17-45.

Longuet-Higgins, M.S., 1970. Longshore currents generated by obliquely incident seawaves. Jour. Geophys. Res. 75, pp. 6778-6801.

Medina R., Bernabeu A.M., Vidal C. and Gonzalez M., 2000. Relationship between beach morphodynamics and equilibrium profiles. Proc. 27th International Conf. Coastal Eng. ASCE. In press.

Ming, D.H. and Chiew, Y., 2000. Shoreline Changes behind Detached Breakwater. Journal of Waterway, Port, Coast and Oc. Eng. ASCE, 126 (2), pp. 63-70

Nir, Jacob 1976. Detached breakwaters, groynes and artificial structures on the Mediterranean shore and their influence on the structure of the Israeli SHORE. Rep. No. 3, 76/2, Jerusalem, March 1976 Ministry of Industry and Commerce, Geological Institute, Marine Geology Section (in Hebrew).

Noble, R.M. 1978. Coastal structures' effects on shorelines. Proc. 16th Conf. on Coastal Eng., Vol. III, ch. 125, pp. 2069 - 2085.

Ozasa, H. and Brampton, A.H.,1980. Mathematical modelling of beaches backed by seawalls. Coastal Eng., 4:47-63.

Penney, W.G. and A.T. Price, 1944. Diffraction of sea waves by breakwaters. Directorate of Miscellaneous Weapons Development, Technical History N1 26, Artificial Harbors, Sec. 3 - 4.

Rosen, D.S., and Vajda, M., 1982. Sedimentological influences of detached breakwaters. Proc. 18th Int. Conf. Coastal Engrg., ASCE, 3, 1930 - 1949.

Silvester, R., 1970a. Coastal defense. Proc. Inst. Civ. Eng., 45: 677 - 682.

Silvester, R., 1970b. Growth of crenulate shaped bays to equilibrium. J. Waterway and Harbor Div., ASCE, 96 (ww4): 275 - 287.

Silvester, R., Tsuchiya, Y. and Shibano, T., 1980. Zeta bays, pocket beaches and headland control. Proc. 17th Int. Conf. Coastal Eng., ASCE, 2:1306-1319.

Silvester, R., and Hsu, J.R.C., 1997. Coastal Stabilization. Advanced series on Ocean Engineering, Vol.14., Ed. World Scientific.

Shinohara, K., Tsubaki, T., 1966. Model Study on the Change of Shoreline of Sandy Beach by Offshore Breakwater. Proc. 10th Int. Conf. Coastal Eng., Tokyo, 1, pp 550-563.

Toyoshima, O., 1974. Design of a detached breakwater system. Proc., 14th Int. Conf. Coastal Eng., Copenhagen Denmark, pp. 1419 - 1431.

Vichetpan, N., 1969. Equilibrium shapes of coastline in plan. Thesis, No. 280, Asian Ins. of Technology, Bangkok, Thailand.

Yamashita, T. and Y. Tsuchiya, 1992. Numerical simulation of pocket beach formation. Proc. 23rd Int. Conf. Coastal Eng., pp. 2556 – 2566.

Yasso, W.E., 1965. Plan geometry of headland bay beaches. J. of Geology, 73, 702 – 714.

Publicado en los Proceedings de la International Conference on Coastal Engineering, ICCE 2000, Sydney

Relationship between beach morphodynamics and equilibrium profiles

R. Medina[1], A.M. Bernabeu[2], C. Vidal[1] and M. González[1]

Abstract

In this paper a new beach equilibrium formulation, that treats the shoaling portion of the profile independently from that of the breaking portion, is proposed. The two portions are matched at the breaking point. The formulation considers wave reflection from the beach and the tidal variation of the sea level. Both profiles are represented by a similar expression that depends on two parameters: A and C, which account for wave dissipation and B and D, which account for beach reflection. The parameters are then calibrated using over 50 profiles from 13 beaches along the Spanish Coast.

En este artículo se propone una nueva formulación de playa en equilibrio que trata de forma independiente la parte del perfil de asomeramiento y la parte en rotura. La formulación incorpora la reflexión producida en la playa y la variación del nivel del mar por efecto de la marea. Ambos perfiles se pueden representar con expresiones semejantes que dependen de dos parámetros: A y C, que tienen en cuenta la disipación y B y D que se ocupan de la reflexión. Los parámetros se calibran utilizando 50 perfiles de 13 playas del litoral español.

[1] Ocean & Coastal Research Group. Dept. de Ciencias y Técnicas del Agua y del Medio Ambiente. Universidad de Cantabria. 39005 Santander, Spain e-mail: medina@puer.unican.es.
[2] Dept. de Geociencias Marinas y Ordenación del Territorio. Universidad de Vigo. 36200, Vigo, Spain

Relationship between beach morphodynamics and equilibrium profiles

R. Medina[1], A.M. Bernabeu[2], C. Vidal[1] and M. González[1]

Abstract

In this paper a new beach equilibrium formulation, that treats the shoaling portion of the profile independently from that of the breaking portion, is proposed. The two portions are matched at the breaking point. The formulation considers wave reflection from the beach and the tidal variation of the sea level. Both profiles are represented by a similar expression that depends on two parameters: A and C, which account for wave dissipation and B and D, which account for beach reflection. The parameters are then calibrated using over 50 profiles from 13 beaches along the Spanish Coast.

Introduction

One of the most important approaches used for the determination of profile shape is that of the equilibrium beach profile (EBP). The hypothesis behind the EBP is that beaches respond to wave forcing by adjusting their form to an equilibrium or constant shape attributable to a given type of incident wave or sediment characteristic. Although several authors have questioned the validity of equilibrium concepts for describing all shorefaces profiles (e.g. Pilkey et al, 1993), the existence of a shoreface profile of equilibrium is generally accepted and has been a matter of great interest to numerous investigators. Various expressions have been proposed over the years (see Dean, 1991 as a general reference). The most widely used formulation, which is very simple and easy-to-apply, is the *2/3*-power profile shape proposed by Bruun (1954) and Dean (1977). Both authors concluded that the beach profile shape could be adequately represented by:

[1] Ocean & Coastal Research Group. Dept. de Ciencias y Técnicas del Agua y del Medio Ambiente. Universidad de Cantabria. 39005 Santander, Spain e-mail: medina@puer.unican.es.
[2] Dept. de Geociencias Marinas y Ordenación del Territorio. Universidad de Vigo. 36200, Vigo, Spain

$$h = Ax^{2/3} \tag{1}$$

where h is the total water depth, A is a dimensional shape parameter that depends on the grain size (Dean, 1991) and x is the horizontal distance from the shoreline. It is worth noting that Bruun (1954) obtained this expression by assuming that the bottom shear stress and the wave energy dissipation were constant at equilibrium. However, Dean (1977) motivated this power law by assuming that the wave energy dissipation per unit volume, due to wave breaking, is constant.

Despite the efforts carried out, none of the presently proposed EBP expressions are able to adequately represent some well-known features of beach profiles such as: a) the interaction between the surf and the shoaling part of the profile, b) the influence of the wave climate (summer-winter profiles) and the wave reflection from the beach on the profile shape or c) the influence of the tide on the equilibrium shape.

The aim of this paper is to present a general formulation of equilibrium for the entire active beach profile of reflective and dissipative beaches in tidal and non-tidal seas. The paper is organized as follows: First the proposed model for the breaking and non-breaking portions of the profile is presented. Assuming that reflection from the beach is negligible, a preliminary expression for both portions of the profile is obtained. Then a modified equilibrium profile model that takes reflection into account is formulated. In the next section the effect of the tide is included.

Theoretical model

Several approaches have been pursued in an attempt to characterize EBPs. One of the most popular is to consider the time-averaged wave energy flux equation for straight and parallel contours:

$$\frac{dF}{dx} = -\varepsilon \tag{3}$$

where F is the net shoreward energy flux per unit width and ε is the energy dissipation rate per unit area. Equation (3) allows taking into account wave reflection from the beach for those cases where this process is not negligible. In this case the net shoreward energy flux F must be computed considering the incident F_i and the reflected F_r energy fluxes.

$$\frac{dF_i}{dx} - \frac{dF_r}{dx} = -\varepsilon \tag{4}$$

Equation (3) involves three variables, namely: the wave height, H, the water depth, h, and the wave energy dissipation, ε. In the EBP problem one seeks the water

depth and, consequently, an appropriated wave energy dissipation model and wave height variation across the profile must be provided.

Thornton and Guza's (1983) dissipation model includes both breaking ε_b and frictional dissipation ε_f in the energy balance,

$$\varepsilon = \varepsilon_b + \varepsilon_f \tag{5}$$

In their model, the rate of energy dissipation due to shallow water wave breaking is modelled after a bore. The average rate of frictional energy dissipation is calculated by assuming the usual quadratic formulation for bottom shear stress,

$$\varepsilon_b \approx \varepsilon_{bore} = \frac{1}{4}\rho g \frac{(BH)^3}{h^2} Q \tag{6}$$

$$\varepsilon_f = U_b \tau_b = \rho c_f U_b^2 |U_b| \tag{7}$$

where Q is the volume discharge per unit area across the bore, B is a breaker coefficient of *0(1)* to be determined from the data, τ is the shear stress, U is wave orbital velocity, c_f is the bed friction coefficient and the $()_b$ subscript refers to bed.

In the shoaling portion of the profile bores are not presented and frictional dissipation is the most important energy loss process. Once waves start to break, friction becomes a minor dissipation mechanism and can be neglected compared with the dominant wave breaking dissipation (Thornton and Guza, 1983).

EBPs Under breaking and non-breaking waves

In order to solve equation (3) a relationship between water depth and wave height must be proposed. In general those variables are independent, however, the hypothesis behind equilibrium formulations is that there is only one combination that remains stable in time. In other words, they will interact with each other until equilibrium is reached. These equilibrium relationships must be proposed as hypothesis and validated by comparison with field or laboratory data. Different equilibrium relationships are considered for each profile portion according to the processes involved.

Breaking waves

The hypothesis for the surf zone is that wave energy saturates at equilibrium. That is, shoreward propagating wave energy exceeding a threshold value is assumed dissipated by wave breaking. Consequently, for a given water depth there is a limit in the wave height and in the wave energy dissipation. This hypothesis can be formulated as:

$$\varepsilon_b = D_b^* h \tag{8}$$

$$H = \gamma h \tag{9}$$

That is, the breaker-to-depth ratio, γ, and the wave energy dissipation per unit water depth, D_b^*, are constant. Introducing equation (8) and equation (9) into equation (3), and assuming the shallow water linear wave theory, equation (3) can be integrated to yield equation (1).

$$h = Ax^{2/3}, \qquad 0 \le x \le x_b \tag{10}$$

$$A = \left[\frac{24 D_b^*}{5\rho g^{3/2}\gamma^2}\right]$$

It is remarkable that equation (10) is only valid from the shoreline ($x=0$, $h=0$) up to the breaking point ($x=x_b$, $h=h_b$), see figure 1.

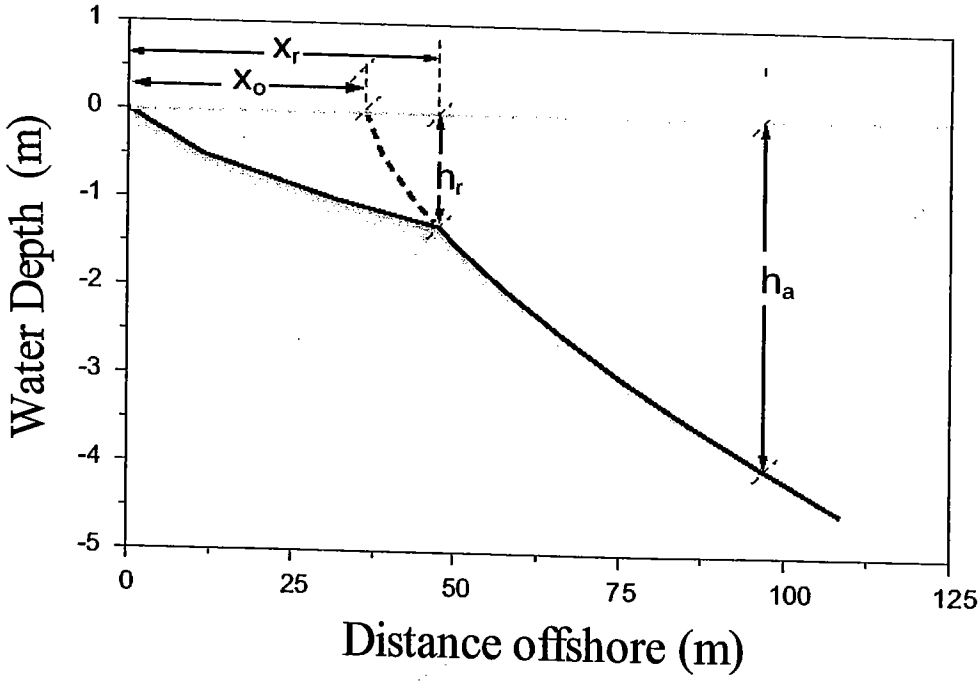

Figure 1: Definition sketch of surf and shoaling profiles. Surf profile extends from the shoreline to the breaking point. The offshore limit of the shoaling profile can be roughly estimated by, $h_a \approx 3.5\ Hs$ (Bernabeu, 1999)

Non-breaking Waves

The hypothesis for the shoaling zone is that the bottom shear stress is constant at equilibrium, Bruun (1954). Consequently, for a constant bed friction coefficient c_f, the frictional dissipation ε_f and the wave orbital velocity U_b are also constant.

$$\varepsilon_f = D_f^* \tag{11}$$

where D_f^* is the constant wave energy dissipation per unit area. Assuming shallow water linear wave theory for U_b it yields:

$$H = \beta\sqrt{h} \tag{12}$$

where β is a constant. Introducing equation (11) and equation (12) into equation (3), and assuming shallow water linear wave theory, equation (3) can be integrated from the breaking point ($x=x_b$, $h=h_b$) to an offshore location, x_a, to yield equation (13).

$$\left(h^{3/2} - h_b^{3/2}\right) = C^{3/2}(x - x_b), \qquad x_b \le x \le x_a$$

$$C^{3/2} = \frac{8D_f^*}{\rho g\sqrt{g}\,H_a^2 h_a} = 8c_f H_a\sqrt{h_a} \tag{13a}$$

where C is a dimensional shape parameter and the $()_a$ subscript refers to the offshore limit of the shoaling profile. It is noted that equation (13) is only valid for the shoaling portion of the profile ($x > x_b$, $h > h_b$), see figure 1.

Substituting h_b obtained from equation (10) into equation (13a) yields,

$$X = x - x_0 = \left(\frac{h}{C}\right)^{3/2}$$

$$x_0 = x_b\left(1 - \frac{A^{3/2}}{C^{3/2}}\right) \tag{13b}$$

Thus, the shoaling profile can be represented by a 2/3-power profile with a different reference system (X,h). Notice that if A is greater than C, x_0 is negative. For C values greater than A, x_0 will be a fraction of x_b. If A and C are equal, only one profile exists and x_0 is equal to zero, see figure 2.

Interaction between surf and shoaling profiles

The well-known and well-documented seasonal changes in beach profile in response to high waves in the winter and the lower waves in the summer can be analyzed by means of the surf and shoaling equilibrium profiles, equations (10) and (13). An increase in wave height will have two effects on the equilibrium shape. First, the shoaling profile will become steeper as the shape parameter C increases, equation (13). Second the offshore limit of the surf profile will also increase due to the greater

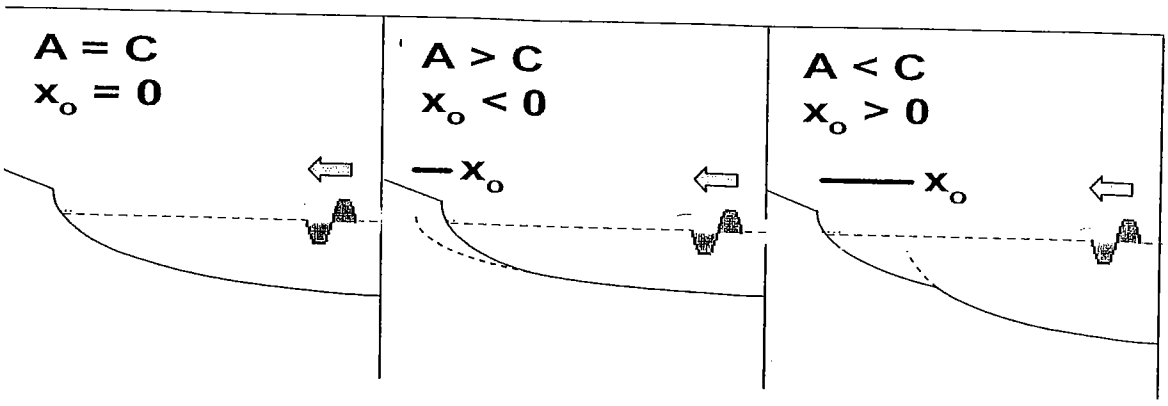

Figure 2. Definition sketch of profile offset, x_o, changes due to variation in A and C-parameters. If A is greater than C, x_0 is negative and the shoaling profile origin is located landward the breaking profile origin. For C values greater than A, the shoaling profile origin is located seaward the breaking profile origin.

breaking depth. Assuming that the sand volume remains constant, the changes in seasonal equilibrium will be manifested by self-similar displacements of the two portions of the profile (surf and shoaling) as a consequence of changes in surf zone width and in the shape parameters, see figure 3. This behavior has been previously suggested by Inman et al (1993) using a large field data set of beach profiles that cover a period of forty years. The sand volume involved in the seasonal changes of the profile as well as the corresponding shoreline recession, R, have been further analyzed by Bernabeu (1999).

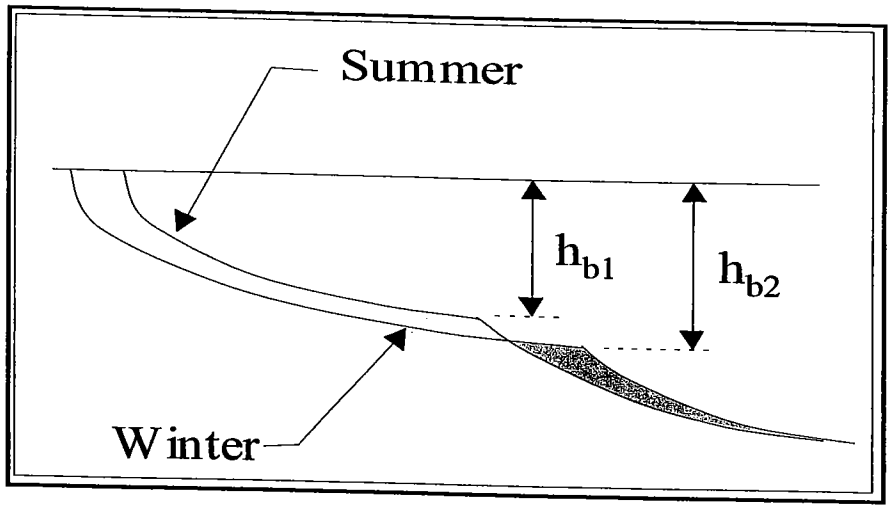

Figure 3. Definition sketch of seasonal beach changes due to variation in wave height. Changes in seasonal equilibrium are manifested by self-similar displacements of the two portions of the profile (surf and shoaling) as a consequence of changes in surf zone width and in the shape parameters

Wave reflection

As stated previously, a more general derivation of the energy flux balance can be derived if the total wave energy flux is considered. Thus, the equilibrium for the surf zone would yield,

$$\frac{1}{h}\frac{dF_t}{dx} = \frac{1}{h}\left[\frac{dF_i}{dx} - \frac{dF_R}{dx}\right] = -D_b^* \tag{16}$$

Baquerizo et al (1998) proposed the utilization of a function, $V_r(x)$, for the analysis of wave reflection from beaches. This function represents the local variation of the flux of energy per unit volume of beach profile and per unit flux of incident energy. Analyzing runs from the large-scale SUPERTANK data set, Bernabeu (1999) proposed the following expression for $V_r(x)$ for equilibrium beach profiles:

$$V_r(x) = \frac{-1}{h}\frac{1}{F_i}\frac{dF_R}{dx} = k\frac{1}{\sqrt{h}}\frac{dh}{dx} \tag{17}$$

where k is a constant that depends on the wave period.

Substituting equation (17) into equation (16) and assuming shallow water linear wave theory and constant breaker-to-depth ratio γ, equation (16) can be integrated to yield,

$$x = \left(\frac{h}{A}\right)^{3/2} + \frac{B}{A^{3/2}}h^3, \qquad 0 \le x \le x_b$$

$$A = \left[\frac{24D_b^*}{5\rho g^{3/2}\gamma^2}\right], \qquad B = \frac{k}{5} \tag{18}$$

It is remarked that, since surf EBP condition has been used to obtain equation (18), this expression is only valid from the shoreline ($x=0$, $h=0$) up to the breaking point ($x=x_b$, $h=h_b$). It is also noted that B-parameter comes from the reflected energy flux term and that Dean's (1977) EBP is recovered when B is equal to zero. In order to show the influence of A and B parameters on beach shape, several profiles with different values for A and B are plotted in figure 4. For convenience, A and B parameters are selected so that all the profiles coincide at $x=0$ and at $x=x_b$. Note that as both parameters increase, the shoreface slope increases and the submerged slope decreases.

In a similar way it is possible to obtain an expression for the shoaling profile that includes wave reflection. Substituting equation (17) into equation (4) and assuming shoaling equilibrium conditions for the wave height and the wave energy dissipation the following expression is obtained:

$$X = x - x_0 = \left(\frac{h}{C}\right)^{3/2} + \frac{D}{C^{3/2}} h^3 \qquad x_b \le x \le x_a$$

$$C^{3/2} = \frac{8D_f^*}{\rho g \sqrt{g} H_a^2 h_a} = 8 c_f H_a \sqrt{h_a} \quad D = \frac{k'}{5} \tag{19}$$

$$x_0 = x_b \left(1 - \frac{A^{3/2}}{C^{3/2}}\right) + \frac{B - D}{C^{3/2}} h_b^3$$

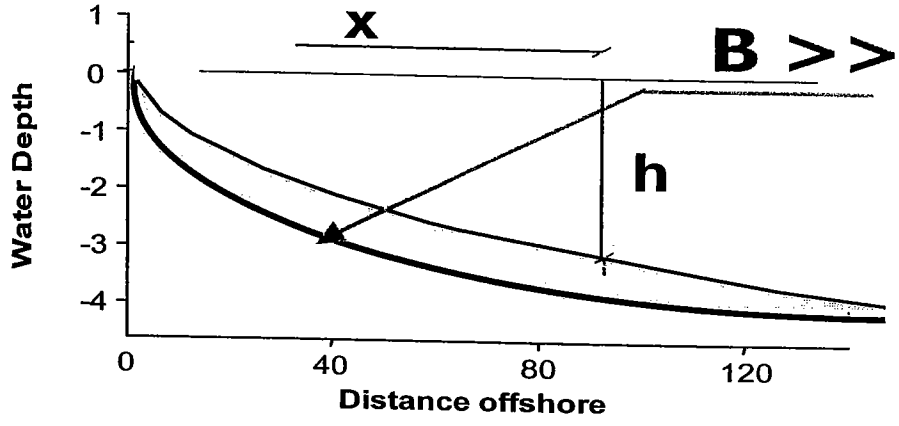

Figure 4. Influence of A and B parameters on the profile shape. Greater values of A and B increase shoreface slope and decrease submerged slope

Thus, the shoaling profile can be represented by an expression similar to that of the breaking portion of the profile with a different reference system (X,h).

It is interesting to note that, besides the previously stated interaction between the surf and the shoaling profiles due to variations in wave height, wave reflection adds a new link between both portions of the profile. A variation in the wave period will change the shape parameters B and D and consequently, the overall shape of the profile.

Tidal beaches

Investigators have long recognized that sea level variations induce modifications in the profile shape (e.g. Bruun 1962). It is also well-known that beach profiles show alterations that correspond to the tides (e.g. Komar 1997). However it is generally accepted that beach profiles in tidal seas exhibit an equilibrium shape. Furthermore, most of the field data used to validate EBP formulations are from tidal beaches.

Kriebel and Dean (1985) have considered profiles out of equilibrium by hypothesizing that the cross-shore transport, Q, is proportional to the difference between the actual, D, and equilibrium, D^*, wave energy dissipation,

$$Q = K(D - D^*) \tag{20}$$

where K is a coefficient. Equation (20) and a sand conservation relationship have been incorporated into several numerical models of sediment transport yielding good agreement with laboratory profiles and field results (Larson and Kraus, 1989). Sea level variations due to tides continuously modify the wave energy dissipation magnitude during the tidal cycle. Consequently, according to equation (20), every location of the profile will suffer sediment transport processes during the tidal cycle. Thus, the condition for the profile to be in equilibrium is that the tidal-averaged net sediment transport is zero.

$$\overline{Q} = \frac{1}{T}\int_{t}^{t+T} Q\,dt = 0 \tag{21}$$

Notice that within a tidal cycle a profile location can be located in the dry beach, in the surf zone, in the shoaling zone or even in the offshore portion of the profile. Bernabeu (1999) has considered the net sediment transport to be the addition of the sediment transport that occurs in the different episodes and has developed counterparts to equation (20) for each one, thus allowing the solution for the tidal EBP. The solution of the problem involves the calculation of the time that each process affects a particular location, yielding an implicit problem.

A simple approximation can be obtained taking into account the different order of magnitude of the sediment transport coefficients K. Assuming that the dry beach and the offshore portion of the profile are not active, coefficients K_d and K_o can be considered equal to zero ($K_d \cong K_o \cong 0$). Notice that this assumption is not adequate for beaches where swash transport is important. Following Larson and Kraus (1989), the sediment transport coefficient for the surf zone is much greater than the one for the shoaling portion of the profile ($K_b >>> K_s$). Furthermore, based on field data, Larson and Kraus (1989) suggested that no transport occurs if D becomes less than D_b^*,

$$\begin{aligned} K_b &\approx 0 \qquad D - D_b^* < 0 \\ K_b &= K_b \qquad D - D_b^* > 0 \end{aligned} \tag{22}$$

Consequently the equilibrium condition for any profile location that is affected by wave breaking during the tidal cycle can be approximated by,

$$\int_{t_2}^{t_3} K_b(D - D_b^*) \approx 0, \qquad D \geq D_b^* \tag{23}$$

In order to satisfy equation (23) it is necessary that $D \cong D_b^*$, that is, the breaking wave EBP condition must be fulfilled. Thus the solution of equation (23)

will be equation (10) if wave reflection from the beach is neglected or equation (18) if it is considered.

The physical interpretation of equation (23) is that the profile will be in equilibrium when the maximum erosion position is achieved. If any portion of the profile accretes during the tidal cycle, erosion due to wave breaking will reshape the profile. Since erosion transport is much faster, the final shape will be an erosion envelope.

Equation (23) holds from the high tide level to the low tide breaking point, see figure 5. Below that point no breaking occurs, $K_b=0$ and shoaling transport is then the most relevant process. Following arguments similar to those stated for the breaking zone, the equilibrium condition for the shoaling portion of a tidal profile yields $D \cong D_f^*$. Thus the shoaling EBP for a tidal beach will be equation (13) if wave reflection from the beach is neglected or equation (19) if it is considered, see figure 5.

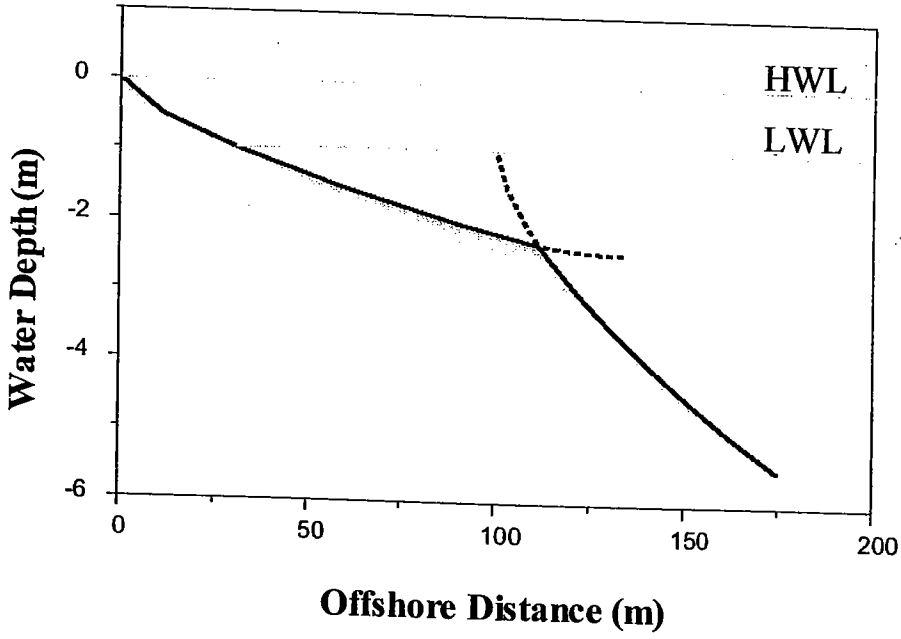

Figure 5. Definition sketch of EBP in a tidal sea. The main effect of the tide is that it acts as a stretching factor that increases the length of the breaking profile.

From figure 5 it can be concluded that the main effect of the tide is that it acts as a stretching factor that increases the length of the breaking profile. The higher the tidal range the longer the profile.

Shape parameters

Over 50 profiles from 13 beaches along the Spanish coast have been best-fitted using equations (18) and (19) in order to determine the relationship between the shape parameters (*A, B, C, D*) and the wave or the sediment characteristics of a beach

profile. The available data include profile and sediment measurements compiled by Gómez-Pina (1995) and wave and tidal data recorded by the Spanish wave-recording system (REMRO). Mean grain size values are obtained as the average value of the shoreface samples. Wave height and period represent the monthly average value of the significant wave height and peak period at the closure depth prior to the profile measurement date.

Different dimensionless variables have been tested for representing the shape parameters (*A, B, C, D*), see Bernabeu (1999). The best fit, using a single dimensionless variable, was obtained using the dimensionless fall velocity, Ω ($\Omega=H_b/\omega T$). For the range of dimensionless fall velocity $1.5<\Omega<5$, the following expressions were obtained:

$$A = (0.21 - 0.02\Omega) \tag{24}$$

$$B = 0.89\exp[-1.24\Omega] \tag{25}$$

$$C = (0.66 + 0.04\Omega) \tag{26}$$

$$D = 0.22\exp[-0.83\Omega] \tag{27}$$

$$h_r = 1.1H_{Sa} \tag{28}$$

Notice that, since both *A* and *B* parameters increase as Ω decreases, the beach profile for a reflective wave condition results in a steeper foreshore and a gentle submerged area. It is also noted that for $\Omega>3.0$, $B\approx O(10^{-2})$, thus the reflection term of equation (18) represents less than *10%* of the dissipation term for profile depths $h \leq 5$ meters. Consequently the effect of the wave reflection from the beach can be neglected. This range of Ω corresponds to the intermediate-dissipative beaches defined in Wright and Short's (1984) model.

Regarding the shoaling profile, it can be clearly observed that the *C* parameter increases as the beach becomes more dissipative, resulting in a submerged profile with a steeper slope. It is also noted that, assuming a constant sediment size across the profile, C parameter values are greater than the A parameter values if the beach is dissipative and smaller for reflective beaches. As in the case of the *B* parameter, the *D* parameter increases as Ω value decreases. It is again noted that for $\Omega>3.0$, $D\approx O(10^{-3})$ and the reflection term of equation (19) represents less than *10%* of the dissipation term for profile depths less than 20 meters. Consequently the effect of the wave reflection from the beach can be neglected.

Acknowledgements

This work is part of the Research Project AMB99-0543 funded by the Spanish Comisión Interministerial de Ciencia y Tecnología (CICYT). The support of the European Communities in the framework of the Marine Science and Technology

Programme (MAST), under the No MAS3-CT97-0081 project "Surf and Swash Zone Mechanics" (SASME) is also acknowledged. The field data have been kindly provided by the Dirección General de Costas (Ministerio de Medio Ambiente) and its support is hereby gratefully acknowledged.

References

Baquerizo, A., Losada, M. A., and Smith, J. M., 1998. Wave Reflection from Beaches: A Predictive Model. Journal of Coastal Research, Vol. 14, No 1, pp. 291-298.

Bernabeu, A. M., 1999. Desarrollo, validación y aplicaciones de un modelo general de perfil de equilibrio en playas. Tesis Doctoral. Universidad de Cantabria E.T.S.I.C.C.P. Dpto. de Ciencias y Técnicas del Agua y Medio Ambiente.

Bruun, P., 1954. Coast erosion and the development of beach profiles. Beach Erosion Board, Technical Memorandum, No 44.

Bruun, P. 1962. Sea Level Rise as a Cause of Beach Erosion. Journal of Waterway, Port, Coastal and Ocean Eng. A.S.C.E. Vol 88, pp. 117-130

Dean, R.G., 1977. Equilibrium beach profiles: U.S. Atlantic and Gulf coasts. Department of Civil Engineering, Ocean Engineering Report No. 12, University of Delaware, Newark, Delaware.

Dean, R.G., 1991. Equilibrium beach profiles: Characteristics and applications. Journal of Coastal Research. Vol 7, pp. 53-84.

Gómez-Pina, G., 1995. Análisis de perfiles de playa en las fachadas cantábrica y atlántica de la costa espa|ola y su aplicación a proyectos de regeneración. Universidad de Cantabria E.T.S.I.C.C.P. Dpto. de Ciencias y Técnicas del Agua y Medio Ambiente.

Inman, D. L., Hany, M., Elwany, S., and Jenkins, S. C., 1993. Shorerise and Bar-Berm Profiles on Ocean Beaches. Journal of Geophysical Research, Vol. 98, No C10. Pp18181-18199.

Komar, P. Beach processes and sedimentation. 2/e Prentice-Hall, New Jersey, pp. 295, 1997.

Kriebel, D. L. and Dean, R. G., 1985. Numerical Simulation of Time-Dependent Beach and Dune Erosion. Coastal Eng. Vol. 9(3), pp. 221-245.

Kriebel, D., Kraus, N. C., and Larson, M., 1991. Engineering methods for predicting beach profile response. Proc. Coastal Sediments91. ASCE, pp. 557 - 571.

Larson, M., and Kraus, N. C., 1989. SBEACH: Numerical model to simulate storm-induced beach change. Army Corps of Engr., Waterway Expt. Station, Tech. Rpt. CERC-89-9.

Pilkey, O., R. Young, S.R. Riggs, A.W. Smith, H. Wu and W.D. Pilkey, 1993. The concept of shoreface profile of equilibrium: A critical review. Journal of Coastal Research, Vol. 9, No. 1, pp. 255 - 278.

Thorton, E. B., and Guza, R. T., 1983. Transformation of wave height distribution. Journal of Geophysical Research. Vol. 18, pp. 5925-5938.

Wright, L.D., and Short, A. D., 1984. Morphodynamic Variability of Surf Zones and Beaches. Marine Geology, Vol 56, pp. 93-118.

Publicado en el Coastal Engineering, ELSEVIER

EQUILIBRIUM BEACH PROFILE MODEL FOR PERCHED BEACHES

by
M. González[1,2], R. Medina[1] and M. A. Losada[3]

[1] Ocean & Coastal Research Group. Departamento de Ciencias y Técnicas del Agua y del Medio Ambiente. Universidad de Cantabria. 39005 Santander, Spain.
[2] Departamento de Mecánica de Fluidos y Ciencias Térmicas. Universidad del Valle. A.A. 25360, Cali (Colombia)
[3] Universidad de Granada. Departamento de Ingeniería Civil. Campus de Cartuja. 18071 Granada, Spain.

ABSTRACT

A beach profile equilibrium model for perched beaches is presented. The model assumes that wave reflection at the seaward and leeward sides of the breakwater is the most important process that modifies Dean's (1977) equilibrium profile model for non-perched beaches. The influence of wave breaking over the submerged structure is also discussed.

Several laboratory data sets are used to analyze the merit of the proposed model for describing the equilibrium condition of a perched beach. A good comparison is obtained.

Results show that if the ratio between the water depth above the submerged structure, d, and the water depth at the toe of the structure, h_e, is large, $d/h_e>0.5$, only minor advance of the shoreline is achieved with the construction of a toe structure. A considerable advance is obtained for d/h_e less that 0.1. In these situations, however, resonant effects may result in an inefficient structure. The proposed model is used to provide an estimation for the required sand volume and the associated beach advance for the case of narrow breakwaters.

ELSEVIER

Coastal Engineering 36 (1999) 343–357

COASTAL ENGINEERING

www.elsevier.com/locate/coastaleng

Equilibrium beach profile model for perched beaches

M. González [a,b,*], R. Medina [a], M.A. Losada [c]

[a] *Ocean and Coastal Research Group, Departamento de Ciencias y Técnicas del Agua y del Medio Ambiente, Universidad de Cantabria, 39005 Santander, Spain*

[b] *Departamento de Mecánica de Fluidos y Ciencias Térmicas, Universidad del Valle, A.A. 25360, Cali, Colombia*

[c] *Universidad de Granada, Departamento de Ingeniería Civil, Campus de Cartuja, 18071 Granada, Spain*

Received 14 September 1998; received in revised form 4 February 1999; accepted 11 February 1999

Abstract

A beach profile equilibrium model for perched beaches is presented. The model assumes that wave reflection at the seaward and leeward sides of the breakwater is the most important process that modifies Dean's equilibrium profile model for non-perched beaches. The influence of wave breaking over the submerged structure is also discussed. Several laboratory data sets are used to analyze the merit of the proposed model for describing the equilibrium condition of a perched beach. A good comparison is obtained. Results show that if the ratio between the water depth above the submerged structure, d, and the water depth at the toe of the structure, h_e, is large, $d/h_e > 0.5$, only minor advance of the shoreline is achieved with the construction of a toe structure. A considerable advance is obtained for d/h_e less that 0.1. In these situations, however, resonant effects may result in an inefficient structure. The proposed model is used to provide an estimation for the required sand volume and the associated beach advance for the case of narrow breakwaters.

Keywords: Submerged breakwaters; Coastal structures; Equilibrium beach profile; Nourishment; Beach erosion

1. Introduction

Existing approaches for shoreline stabilization can be broadly classified as structural, non-structural and combined. Among the combined solutions perched beaches have received favorable attention during the last few decades for the purpose of expanding or creating recreational areas and providing more coastal areas for development. The basic concept of the perched beach is to reproduce the existing profile to some convenient seaward point and then intersect this profile with a submerged toe structure to retain the beach in a perched position (see Fig. 1). This kind of solution can be cost effective in places where there is not enough sand to advance the complete beach profile or if only much finer sand is available.

The design of a perched beach scheme requires the analysis of both the submerged structure and the perched beach stability. A reasonably large body of literature is available for the design of emerged or submerged detached breakwaters (Pope and Dean, 1986; Ahrens, 1987; Vidal et al., 1995). The hydrodynamics induced by this kind of breakwater have also received considerable attention (Longuet-Higgins, 1967; Dalrymple and Dean, 1971; Sawaragi, 1988).

It is generally accepted that submerged breakwaters influence the hydrodynamic field which in turn affects the sediment transport processes in the local vicinity of the structure. Several efforts have been made to determine the stability of beaches located behind submerged breakwaters. Sawaragi (1988) carried out an experimental study on the functionality of submerged breakwaters to control cross-shore sediment transport. Sorensen and Beil (1988) carried out wave tank experiments to investigate the response of perched beach profiles to storm wave attack. A more comprehensive laboratory study was conducted by Chatham (1972) in order to determine an estimate of the amount of sand which would be lost seaward over the submerged toe structure by normal and storm wave action as well as the optimum characteristics of the submerged structure (elevation and width).

Field monitoring studies have also been carried out to evaluate the effects of detached breakwaters and the performance of perched beaches (Silvard, 1971; Douglass and Weggel, 1987; Ferrante et al., 1992; Dean et al., 1997). It is somehow surprising that,

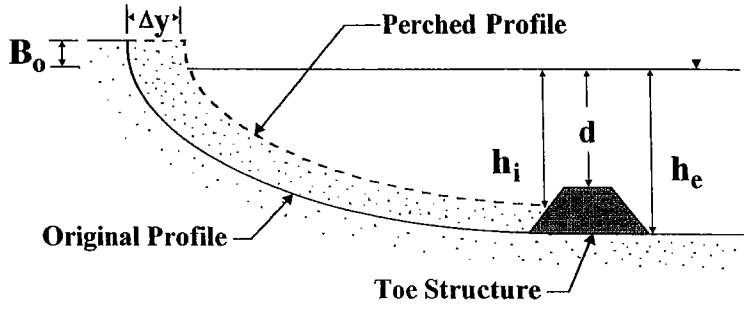

Fig. 1. Definition sketch of a perched beach. The main variables involved are the water depth over the breakwater, d, the water depth at the seaward and shoreward side of the toe structure, h_e and h_i, respectively, the advanced beach width, Δy, and the beach berm height, B_0.

although sediment transport processes, and particularly sand losses, have been a matter of interest to numerous investigators, the validation of the equilibrium beach profile form for a perched beach has received minor attention.

Equilibrium beach profile concepts have been widely used for beach nourishment project design (Houston, 1996). Dean (1991) illustrated by several examples the utility of equilibrium beach profile expressions for calculating the required sand volume in different nourishment projects. In particular, Dean (1991) analyzed the reduction in required sand volumes through the perching of a nourished beach by an offshore sill. In this analysis, Dean assumes that it is possible to reach an equilibrium beach profile for $h_i = d$ (see Fig. 1).

The hypothesis behind the equilibrium beach profile is that beaches respond to wave forcing by adjusting their form to an 'equilibrium' or constant shape attributable to a given type of incident wave and/or sediment characteristics. Dean (1977) proposed that the equilibrium beach profile shape depends only on the sediment size. Wave height has no influence on the shape but governs the position of the shoreline. If the actual wave energy flux at a particular point exceeds the equilibrium energy flux, the profile retreats (Kriebel and Dean, 1985). Consequently, the modification of the wave propagation due to a submerged breakwater should result in a modification of the shoreline location.

In this paper, the wave modification due to a submerged breakwater is used to determine the shoreline location of a perched beach. The profile shape of Dean (1977) is assumed to be valid. The paper is organized as follows: Firstly, the modification of the wave energy flux due to the submerged structure is analyzed. The analysis is focused on the relative importance of wave dissipation and wave reflection at the structure and, consequently, the transmitted wave energy flux that reaches the beach profile. According to this analysis, an equilibrium beach profile model, which takes into account the wave–structure–beach interaction, is proposed.

In Section 2, a comparison between the results obtained from the model and experimental data from Chatham (1972) and Sorensen and Beil (1988) is presented. Once the validation of the model is shown, several results are presented in order to analyze the influence of the different parameters involved in the required sand volume and the associated added beach width. Some important conclusions are given at the end of the paper.

2. Wave energy flux transformation on a submerged structure

The main hypothesis behind the heuristic equilibrium beach profile model presented by Dean (1977) is that the wave energy flux dissipated per unit volume in the surf zone is uniform. Assuming that this hypothesis is valid, the equilibrium beach profile for a perched beach depends on the amount of energy flux that is transmitted over the toe structure. Consequently, the design of perched beaches requires an understanding of how waves are reflected at the submerged structure and how they are dissipated as they travel across the structure-top.

A large body of literature is available on wave transformation on a reef breakwater (see Ahrens, 1987 as a general reference). An important conclusion of these studies, related with the stability of the perched beach, is that, although the submerged breakwater may induce wave breaking, it occurs well beyond the breakwater crown (Grilli et al., 1994).

An estimation of the structure width for the waves to break on the structure can be obtained from Gourlay (1994). In this work, Gourlay (1994) studied the wave transformation of waves approaching a fringing reef with a steep face and outer reef-top slope gently decreasing in the landward direction. A non-linear parameter, F_{c0}, was suggested for classifying wave transformation regimes on the reef:

$$F_{c0} = \frac{g^{1.25} H_e^{0.5} T^{2.5}}{d^{1.75}} \tag{1}$$

where, H_e is the wave height reaching the reef, T is the wave period and, d is the water depth over the reef.

In particular, when $F_{c0} > 150$, waves plunge on the reef edge and the amount of wave energy reaching the shore is small. However, for $150 > F_{c0} > 100$, the waves increase in height as they cross the reef edge and then break by spilling on the reef-top. The wave height on the reef-top can be as much as 1.2 times the incoming wave height and the wave energy reaching the shore is maximum.

The distance of the breaking point from the reef edge, l_p, for this kind of wave was found to be of the order of one reef-top wave length:

$$l_p \approx T\sqrt{gd}\,. \tag{2}$$

The surf zone width, l_s, for these kinds of waves was found to be within the range of two/three wave lengths, $l_s \approx 2\text{–}3T\sqrt{gd}$.

From Gourlay's results, it can be concluded that, at least at a distance of $l \approx T\sqrt{gd}$, the wave height can be greater than the incoming wave and the wave energy flux can exceed the stable value of wave energy flux given by the constant breaker-to-depth ratio $\gamma = 0.8$ for that particular depth, d. Furthermore, the breaking process will take a distance (one or two wave lengths) to reduce this wave energy flux to a stable value. This result agrees with the field data of Muñóz-Pérez et al. (1999) which show that for a natural reef-protected beach to exist, the reef width must exceed three wave lengths.

According to these studies, it is clear that in wide natural reefs, wave breaking over the reef limits the amount of energy reaching the beach profile and it is the most important factor affecting the beach profile shape (Muñóz-Pérez et al., 1999). In most cases of artificial structures, however, wave breaking over the structure can be neglected since the breakwater crest width is usually much smaller than the wavelength and breaking occurs at the perched beach. Furthermore, frictional damping over the breakwater can also be neglected and, consequently, wave reflection at the breakwater is the main process that determines the equilibrium beach profile behind the submerged breakwater.

3. Modified equilibrium beach profile

The most widely used formulation for equilibrium beach profile was proposed by Bruun (1954) and Dean (1977):

$$h = Ax^{2/3} \tag{3}$$

where h is the total water depth, A is a dimensional shape parameter, which depends only on the sediment size, and x is the horizontal distance from the shoreline. Although Eq. (3) was found by fitting beach profiles, Dean (1977) showed that Eq. (3) is consistent with uniform wave energy dissipation per unit volume, D^*, within the breaking zone, i.e.:

$$\frac{1}{h}\frac{\partial}{\partial x}(EC_g) = D^* \tag{4}$$

where E and C_g are the wave energy density and group velocity, respectively. It can be shown, assuming linear shallow water wave theory and constant breaker-to-depth ratio, that Eq. (4) can be integrated to yield Eq. (3) (Dean, 1991).

González (1995) showed that the correct application of Eq. (4) needs to take into account the variation of the available wave energy, E, along the profile due to processes such as shoaling, refraction, diffraction and reflection. Several modifications to Eq. (3) have been proposed in order to consider those processes. González et al. (1997) studied the influence of the convergence/divergence of wave-rays within the surf zone. Muñóz-Pérez et al. (1999) analyzed the effect of a strong decrease in the amount of available energy, E, due to wave breaking in reef-protected beaches (beaches in which the profile intersects a wide reef or hard shelf). Previously, Larson and Kraus (1989) used the dissipation model of Dally et al. (1985) to modify the constant breaker-to-depth ratio assumed by Dean (1977).

When a submerged structure is placed in a beach profile to retain the beach in a perched position, the structure modifies the wave energy propagation along the profile and, consequently, the profile shape. As stated previously, the most important modification is due to the wave reflection at the seaward and leeward side of the breakwater.

In order to solve Eq. (4) for a perched beach, the beach profile is divided into three regions as shown in Fig. 2.

Region 1 is the offshore part of the profile. In this area, the hypothesis of constant breaker-to-depth ratio and uniform wave energy dissipation per unit water volume of Dean (1977) is assumed. According to the work of Dean (1991), a beach profile located in front of a seawall can be adequately represented by a profile extending behind the seawall as if the seawall did not exist. In other words, the reflection of the seawall, F_{er}, does not modify the beach profile shape. Consequently, beach profile in region 1 is not affected by the submerged structure and can be determined using the virtual x-origin (see Fig. 1). This profile defines the water depth at the seaward side of the structure, h_e, and also the amount of energy flux reaching it, F_e (see Fig. 2).

Region 2 is the breakwater domain. This region is defined by the breakwater crest width, B, the water depth over the breakwater, d, and the water depth at the seaward

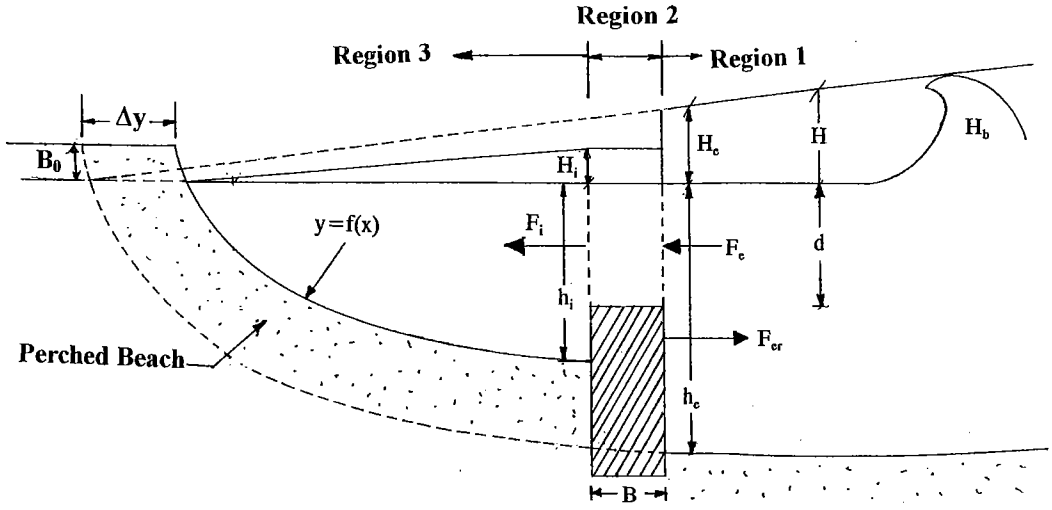

Fig. 2. Definition sketch of the three regions defined in order to solve the energy flux problem. Transmitted energy flux F_i and water depth at the shoreward side h_i are solved using an iterative process (Appendix A) and values of known data F_e, d, and h_e.

and shoreward side, h_e and h_i, respectively. The above mentioned parameters (B, d, h_e, h_i) determine the energy flux, F_i, which reaches the perched profile.

Region 3 is the shoreward part of the profile. In this domain, the hypothesis of Dean (1977), stated in region 1, is also assumed. Consequently, the perched beach profile shape in region 3 is defined by the parabolic Eq. (3).

Notice that the perched beach profile is completely defined if h_i is given, which, due to the constant breaker-to-depth ratio, can be determined if F_i is known. In order to calculate the value of F_i, the energy balance in region 2 must be solved:

$$F_i = F_e - F_{er} \tag{5}$$

where F_{er} is the wave energy flux reflected by the structure.

Assuming linear shallow water wave theory, constant breaker-to-depth ratio and that only the oscillatory (non-breaking) part of the wave contributes to the reflected flux of energy (Baquerizo, 1995), Eq. (5) can be written as:

$$h_i = h_e(1 - R^2)^{2/5} \tag{6}$$

where R is the reflection coefficient ($R = H_r/H_e$), H_e is the incoming wave and H_r is the reflected wave height.

The solution for the reflection coefficient, R, for the wave propagation over an impermeable step problem, can be found in several previous works (e.g., Losada et al., 1992) and is presented in Appendix A. The main characteristics of the solution are also shown in Fig. 3, where the reflection coefficient, R, is plotted as a function of the dimensionless breakwater crest width, B/L, for different values of the dimensionless water depth, d/h_e (where, L, is the wave length). In this figure, the well-known feature of wave resonance is clearly observed. Due to this phenomenon, the reflection coefficient goes to a value close to zero for some particular sets of parameters (d/h_e, B/L).

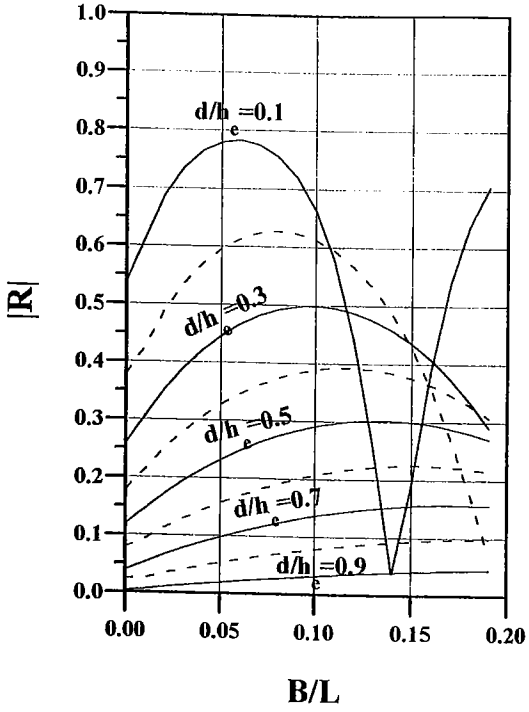

Fig. 3. Reflection coefficient R vs. relative width, B/L for different relative submergence of the breakwater, d/h_e. Notice that for any value of d/h_e, there is a value of B/L that yields no reflection so that all the energy flux is transmitted over the structure (resonant effect).

It is remarked that the reflection coefficient, R, depends on the actual value of h_i. Consequently, in order to solve R and h_i, an iterative process must be carried out. A first estimation of h_i is specified to solve the reflection coefficient following the procedure described in Appendix A. This reflection coefficient is then used to obtain a new value for h_i using Eq. (6). The iterative process continues until R and h_i converge.

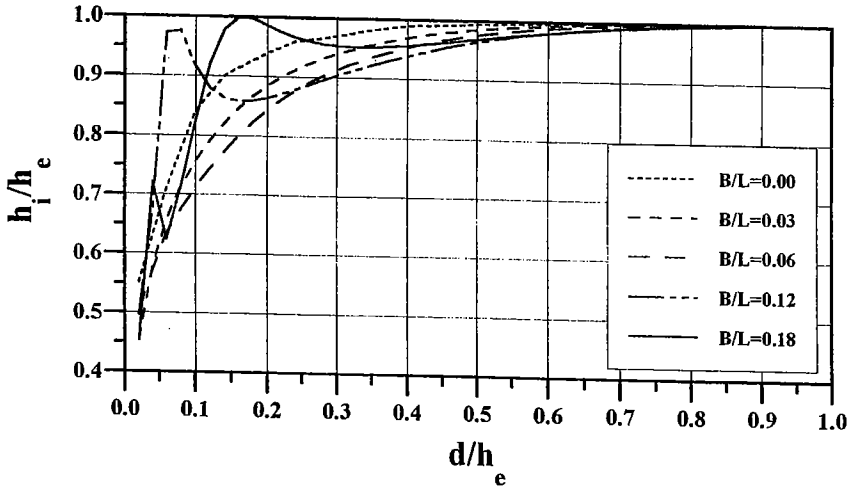

Fig. 4. Relative depths h_i/h_e vs. relative crest submergence, d/h_e for different relative width, B/L. Resonant effects are clearly observed for small d/h_e values and large values of B/L.

Table 1
Comparison between the laboratory data results of Chatham (1972) and present model

h_e (m)	d (m)	h_i (m)	T (s)	L (m)	B (m)	B/L	d/h_e	d/h_i (measured)	d/h_i (calculated)
5.72	3.43	5.55	7.0	50.2	2.3	0.046	0.600	0.610	0.606
8.23	5.72	8.19	7.0	55.8	2.3	0.041	0.695	0.698	0.697
7.10	4.60	7.00	7.9	60.9	2.3	0.038	0.648	0.657	0.651
6.28	3.43	6.20	10.0	75.2	2.3	0.031	0.546	0.553	0.551
7.43	6.63	7.35	10.0	81.1	2.3	0.028	0.892	0.902	0.892
6.29	3.43	6.10	16.0	123.6	2.3	0.019	0.545	0.562	0.548
7.43	7.20	7.35	16.0	133.9	2.3	0.017	0.969	0.980	0.969

Using the above mentioned procedure, in Fig. 4 the values of the water depth ratio h_i/h_e are plotted vs. the dimensionless water depth, d/h_e, for different breakwater crest widths, B/L. From Fig. 4, it can be concluded that for dimensionless water depths d/h_e greater than 0.5 minor benefits are achieved with the construction of a submerged breakwater ($h_i \sim h_e$). A considerable reduction in h_i/h_e is obtained for d/h_e less that $d/h_e < 0.1$. In this area, however, resonance effects may modify this picture resulting in an inefficient structure.

4. Laboratory data

Several laboratory data sets can be used in order to analyze the merit of Eq. (6) for describing the equilibrium condition of a perched beach. Chatham (1972) carried out two-dimensional studies to determine the amount of sand which would be lost seaward over the submerged toe structure by normal and storm wave action. The model beach was subjected to test waves until equilibrium was reached for a wide range of wave conditions. The values of parameters tested are listed in Table 1. Calculated values of the ratio d/h_i are also presented in Table 1.

Sorensen and Beil (1988) conducted two-dimensional experiments of perched beach profile response to storm waves. Five test cases were investigated. The first consisted of a nourished profile without a toe structure. The remaining four cases were perched beach conditions with a sill located at various depths. A complete list of the parameters studied are listed in Table 2. Calculated values of the ratio d/h_i are also presented in Table 2.

Table 2
Comparison between the laboratory data results of Sorensen and Beil (1988) and present model

h_e (m)	d (m)	h_i (m)	T (s)	L (m)	B (m)	B/L	d/h_e	d/h_i (measured)	d/h_i (calculated)
0.187	0.091	0.18	1.6	2.06	0.06	0.029	0.490	0.506	0.494
0.140	0.046	0.14	1.6	1.81	0.06	0.033	0.330	0.330	0.340
0.130	0.023	0.12	1.6	1.80	0.06	0.033	0.180	0.192	0.205
0.140	0.001	0.07	1.6	1.81	0.06	0.033	0.007	0.015	0.016

From Tables 1 and 2, it can be concluded that Eq. (6) gives an adequate estimation of the equilibrium water depth at the breakwater for a perched beach.

5. Model application

Dean (1991) illustrated the utility of Eq. (3) to engineering applications such as the design of a beach nourishment project. In particular, Eqs. (47) and (48) of Dean (1991) provide an estimation for the required sand volume, $\forall$, and the associated added beach width, Δy, for the case of a perched beach where the sand is just even with the top of the submerged breakwater ($h_i = d$).

From Eq. (6), it can be concluded that the situation depicted in the work of Dean (1991) is, in general, not feasible since the water depth at the landward part of the breakwater, h_i, is not a free parameter but a function of the reflection coefficient. In other words, h_i is a function of the breakwater geometry (B, d), the breakwater location, (h_e), and the incident wave length (L).

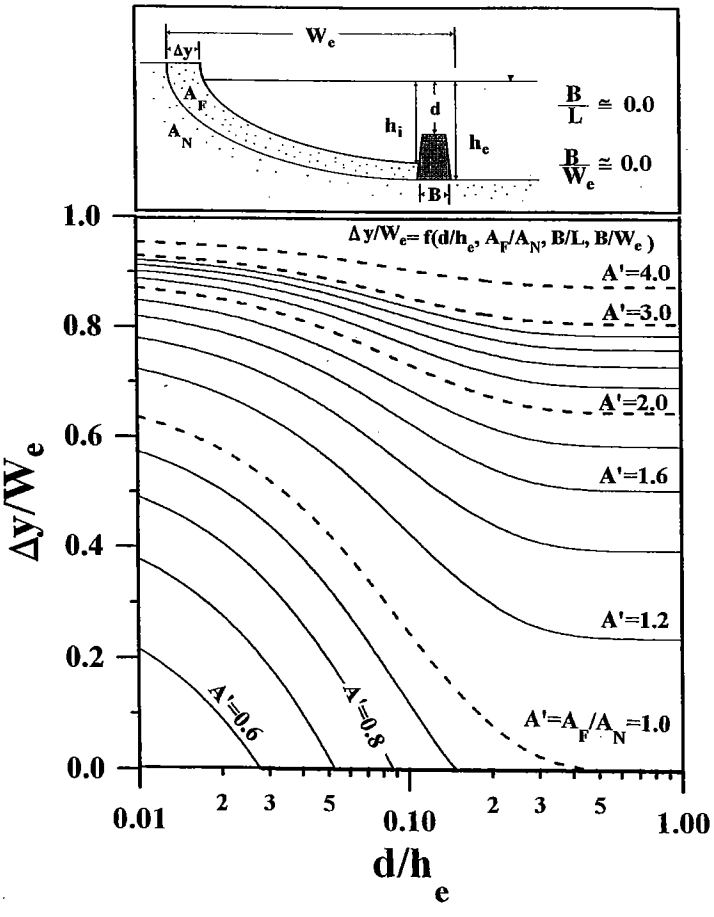

Fig. 5. Variation of non-dimensional shoreline advancement, $\Delta y / W_e$ with A' and d/h_e. Results for $B/L \cong 0.0$ and $B/W_e \cong 0.0$.

A simple estimation of the added beach width, Δy, using Eq. (6), can be obtained for some particular cases. For the case of a narrow breakwater crest ($B/L = 0$–0.06), the ratio h_i/h_e can be approximated as (see Fig. 4):

$$\frac{h_i}{h_e} = 1 - 0.55e^{-\alpha\frac{d}{h_e}} \tag{7}$$

where $\alpha = 11.5$ for $(B/L \sim 0)$, $\alpha = 7.7$ for $(B/L = 0.03)$ and $\alpha = 6.3$ for $(B/L = 0.06)$.

Consequently, the required volume of sand, $\forall$, is given by:

$$\forall = B_0 \Delta y + \frac{3}{5}\left[A_N\left(\frac{h_e}{A_N}\right)^{5/2} - A_F\left[\frac{h_e\left(1 - 0.55e^{-\alpha\frac{d}{h_e}}\right)}{A_F}\right]^{5/2}\right]$$

$$- A_N\left[\left(\frac{h_e}{A_N}\right)^{3/2} - \frac{B}{2}\right]^{2/3} B \tag{8}$$

where A_N and A_F are the native and fill sediment shape parameters, respectively, and B_0 is the beach berm height (see Fig. 1).

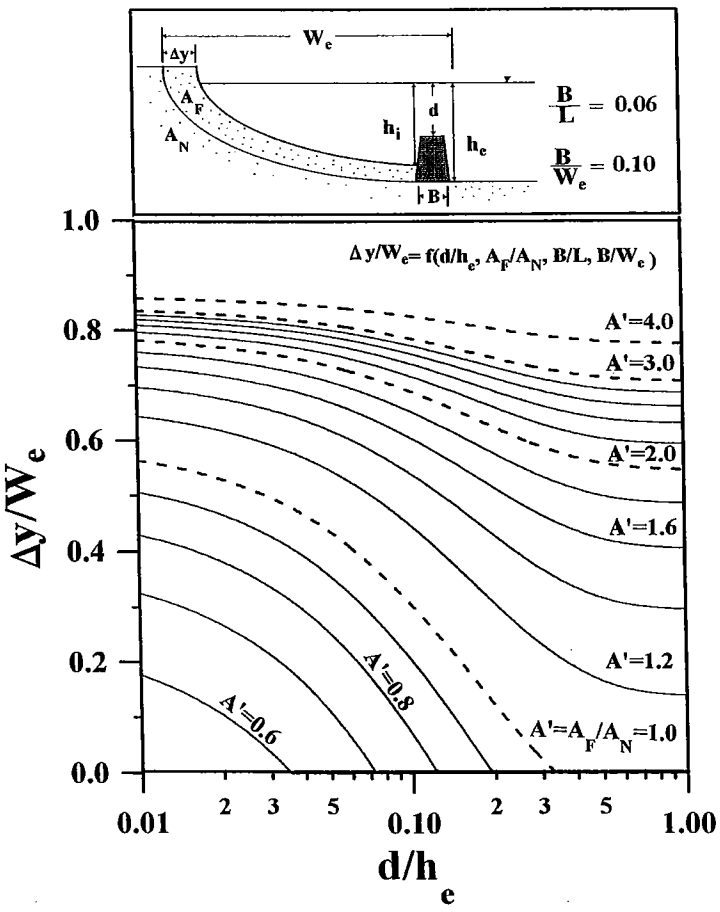

Fig. 6. Variation of non-dimensional shoreline advancement, $\Delta y / W_e$ with A' and d/h_e. Results for $B/L \cong 0.06$ and $B/W_e \cong 0.10$.

Table 3
Comparison between some beach nourishment project characteristics (from Ferrante et al., 1992; Dean et al., 1997) and present model

Project	h_e (m)	d (m)	d/h_e	B (m)	A'	W_e (m)	$\Delta y/W_e$ (measured)	$\Delta y/W_e$ (predicted)
Florida	3	1.2	0.4	~0	1	75	~0	~0
Italy	4	1.5	0.37	20	2.4	350	0.71	0.68

The corresponding added beach width, Δy, is:

$$\Delta y = \left(\frac{h_e}{A_N}\right)^{3/2} - \left\{\left[\frac{h_e\left(1-0.55e^{-\alpha\frac{d}{h_e}}\right)}{A_F}\right]^{3/2} + B\right\}. \tag{9}$$

In Figs. 5 and 6, the dimensionless added beach width, $\Delta y/W_e$ for different d/h_e values is shown for the case of $B/L=0$ and $B/L=0.06$, where W_e is defined as the offshore distance corresponding to the profile depth h_e (see Figs. 5 and 6). From this figures, it can be clearly seen that if a much coarser sand is used for the beach nourishment ($A'=A_F/A_N>3$), the influence of the breakwater configuration, d/h_e, on the added beach width, Δy, is minor. However, if the fill sediment shape parameter is in the range of $A_F/A_N \sim 1 \div 1.5$, which is usually the case, a dimensionless water depth, d/h_e, less than 0.1 is required for a significant advance of the shoreline, Δy. It is also noted that a seaward movement of the shoreline can be achieved by means of a finer fill sediment ($A_F<A_N$), if the breakwater dimensionless water depth, d/h_e, is small enough.

Results from Figs. 5 and 6 can also be compared with some beach nourishment projects. The main characteristics of the two projects considered, one in Florida and the other one in Italy and reported by Ferrante et al. (1992) and Dean et al. (1997), respectively, are presented in Table 3. The model estimation of non-dimensional added beach, $\Delta y/W_e$, is also included in Table 3.

The different behaviour of both projects, despite the similar d/h_e parameter ($d/h_e \sim 0.4$), can be clearly observed in Table 3. This different performance is due to the much coarser sand used for the nourishment in Italy ($D_{50N}=0.1$ mm, $D_{50F}\cong 0.6$ mm). The predicted values using the present model agree with the measured data. It is noted that the value of W_e in the Italian case has been determined using a parabolic profile with $D_{50}=0.1$ mm, since the initial profile was not complete.

6. Conclusions

This study has improved the equilibrium beach model for perched beaches. The model is based on the assumption that wave reflection at the breakwater is the most important modification of the wave energy flux reaching the protected beach due to the

submerged structure. Wave breaking over the structure has been neglected since the breakwater crest width is usually much smaller than the wavelength in most of the man-made submerged structures.

Two dimensionless parameters have been proposed to analyze the influence of the structure on the equilibrium beach profile: the dimensionless water depth, d/h_e, and the dimensionless breakwater crest width, B/L.

It is concluded that the maximum advance of the perched beach shoreline depends substantially on the dimensionless water depth. Minor advance is obtained for large d/h_e (> 0.5) while a considerable advance is achieved for d/h_e less than 0.1. In this area, however, resonance effects induced by the structure may modify the final picture resulting in an inefficient structure depending on the value of B/L.

The model has been applied to provide an estimation for the required sand volume and the associated added beach width, for the case of narrow breakwaters ($B/L \sim 0$, 0.06). It is also concluded that if a much coarser sand is used for the beach nourishment of a perched beach ($A_F/A_N > 3$), the influence of a submerged structure on the added beach width is minor.

Acknowledgements

This study has been partly funded by the Comisión Interministerial de Ciencia y Tecnología under contract MAR96-1833 and by the Commission of the European Communities in the framework of the Marine Science and Technology Programme (MAST), under No. MAS3-CT97-0081 project 'Surf and Swash Zone Mechanics' (SASME).

Appendix A. First-order solution of oblique incident waves on an impermeable step

The domain is divided into three regions, as shown in Fig. 7. The potential in each region is:

$$\phi_1 = I_{11}(z)e^{-iq_{11}x} + \sum_{n=1}^{\infty} R_n I_{1n}(z)e^{iq_{1n}x}$$

$$\phi_2 = \sum_{n=1}^{\infty} I_{2n}(z)\left[A_n e^{-iq_{2n}x} + B_n e^{iq_{2n}(x-B)}\right]$$

$$\phi_3 = \sum_{n=1}^{\infty} I_{3n}(z)T_n e^{-iq_{3n}(x-B)}$$

where:

$$q_{jn} = \sqrt{k_{jn}^2 - \lambda^2} \quad j = 1, 2 \text{ and } 3; \; n = 1, 2, \ldots$$

$$\lambda = k_{11}\sin\theta$$

$$I_{jn} = \frac{ig}{\sigma}\frac{\cosh k_{jn}(h_j + z)}{\cosh k_{jn}h_j}$$

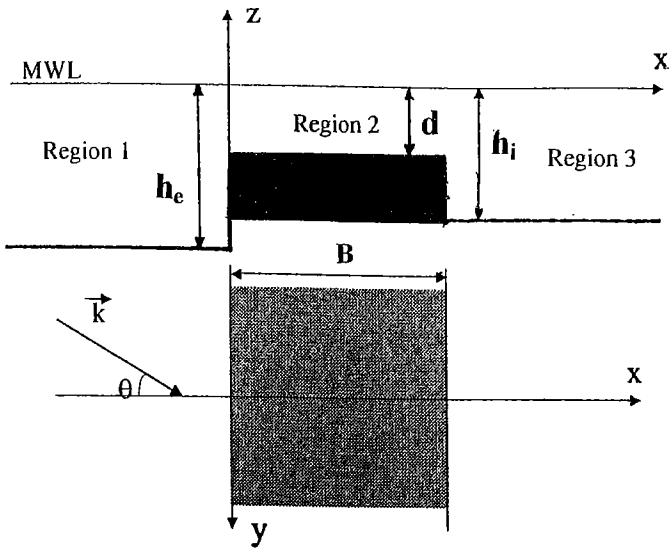

Fig. 7. Definition sketch of the rectangular impermeable step problem to be solved. One region is defined at each side of the step (regions 1 and 3) and another over the step (region 2). Incoming waves reach the step from region 1.

where:

$$\sigma = \frac{2\pi}{T} \quad T\,(\text{wave period})$$

$$k_{1n} = \frac{2\pi}{L} \quad L\,(\text{wave length})$$

and k_{jn} are the roots of the dispersion equation:

$$\frac{\sigma^2 h_j}{g} = k_{jn} h_j \tan h k_{jn} h_j \quad j = 1, 2 \text{ and } 3.$$

$R = R_1$ is the reflection coefficient, $T = T_1$ is the transmission coefficient. R_n $(n > 1)$ and T_n $(n > 1)$ are the coefficients of the evanescent modes. Expressions for the unknown coefficients, R_n, T_n, A_n and B_n are found by using the hypothesis that mass flux and pressure should match at the interfaces;
at $x = 0$:

$$\phi_1 = \phi_2 \qquad -h_1 + a < z < 0$$

$$\frac{\partial \phi_1}{\partial x} = \frac{\partial \phi_2}{\partial x} \qquad -h_1 + a < z < 0$$

at $x = B$:

$$\phi_2 = \phi_3 \qquad -h_1 + a < z < 0$$

$$\frac{\partial \phi_2}{\partial x} = \frac{\partial \phi_3}{\partial x} \qquad -h_1 < z < 0.$$

For N evanescent modes, a system of $4N$ equations with $4N$ unknowns is obtained after applying the orthogonality of the I_{jn} functions over the depth domain to simplify the algebra of the system.

References

Ahrens, J.P., 1987. Characteristics of reef breakwaters. US Army Corps of Engineers, Coastal Engineering Research Center, Tech. Rep. CERC-87-17.

Baquerizo, A., 1995. Reflexión del oleaje en Playas. Métodos de evaluación y de predicción. PhD Dissertation, Universidad de Cantabria, Santander, Spain, 180 pp.

Bruun, P., 1954. Coast erosion and the development of beach profiles. Beach Erosion Board, Technical Memorandum, No. 44, 79 pp.

Chatham, C.E., 1972. Movable-bed model studies of perched beach concept. Proc. 13th Int. Conf. on Coastal Eng. ASCE, pp. 1197–1216.

Dally, W., Dean, R., Dalrymple, R., 1985. Wave height variation across beaches of arbitrary profile. J. Geophys. Res. 90 (C6), 11917–11927.

Dalrymple, R.A., Dean, R.G., 1971. Piling-up behind low and submerged breakwaters. Discussion. J. Waterw. Harbors Coastal Eng. Div. ASCE 97 (WW2), 423–427.

Dean, R.G., 1977. Equilibrium beach profiles: U.S. Atlantic and Gulf coasts. Department of Civil Engineering, Ocean Engineering Report No. 12, University of Delaware, Newark, DE.

Dean, R.G., 1991. Equilibrium beach profiles: characteristics and applications. Journal of Coastal Research 7 (1), 53–84.

Dean, R.G., Chen, R., Browder, A.E., 1997. Full scale monitoring study of a submerged breakwater, Palm Beach, Florida, USA. Coastal Engineering, Vol. 29. Elsevier, pp. 291–315.

Douglass, S.L., Weggel, J.R., 1987. Performance of a perched beach slaughter beach, Delaware. Coastal Sediments '87. Vol. II, ASCE, New Orleans, pp. 1385–1398.

Ferrante, A., Franco, L., Boer, S., 1992. Modelling and monitoring of a perched beach at Lido Di Ostia (ROME). Proc. 23th Int. Conf. on Coastal Eng. ASCE, pp. 3305–3318.

González, M., 1995. Morfología de playas en equilibrio: planta y perfil. PhD Thesis. Universidad de Cantabria, pp. 270 (in Spanish).

González, M., Medina, R., Losada, M.A., 1997. Equilibrium beach profiles: effect of refraction. Proc. Coastal Dynamics 97 (in press).

Gourlay, M.R., 1994. Wave transformation on a coral reef. Coastal Engineering, Vol. 23. Elsevier, pp. 17–42.

Grilli, S.T., Losada, M.A., Martín, F.L., 1994. Characteristics of solitary wave breaking induced by breakwaters. J. Waterw. Port Coastal Ocean Eng. 120 (1), 74–92.

Houston, J.R., 1996. Beach fill design. In: Liu, P.L. (Ed.), Advances in Coastal and Ocean Engineering. World Scientific ISBN 981-02-2410-9, pp. 199–231.

Kriebel, D., Dean, R.G., 1985. Numerical simulation of time-dependent beach and dune erosion. Coastal Engineering 9.

Larson, M., Kraus, N.C., 1989. SBEACH: Numerical model to simulate storm-induced beach change. Army Corps of Eng., Waterway Expt. Station, Tech. Rep. CERC-89-9.

Longuet-Higgins, M.S., 1967. On the wave-induced difference in mean sea level between the two sides of a submerged breakwater. J. Mar. Res. 25 (2), 148–153.

Losada, I.J., Losada, M.A., Roldán, A.J., 1992. Oblique incident wave past vertical thin barriers. Applied Ocean Research 14 (3), 191–200.

Muñóz-Pérez, J.J., Tejedor, L., Medina, R., 1999. Equilibrium beach profile model for reef-protected beaches. Journal of Coastal Research (in press).

Pope, J., Dean, J.L., 1986. Development of design criteria for segmented breakwaters. Proc. 20th Int. Conf. on Coastal Eng., Taipei, ASCE, pp. 2149–2158.

Sawaragi, T., 1988. Current shore protection works in Japan. Journal of Coastal Research 4 (4), 531–541.

Silvard, F.L., 1971. Building a beach with an offshore sill, singer island, Florida. Shore and Beach 39 (1), 42–44.

Sorensen, R.M., Beil, N.J., 1988. Perched beach profile response to wave action. Proc. 21st Int. Conf. on Coastal Eng. ASCE, pp. 1482–1491.

Vidal, C., Losada, M.A., Mansard, E.P.D., 1995. Stability of low-crested rubblemound breakwater heads. J. Waterw. Port Coastal Ocean Eng. ASCE 121 (2), 114–130.

Publicado en los Proceedings de la Conferencia internacional Coastal Structures'99, Balkema

Influence of coastal structures on equilibrium beach

M. González, R. Medina
Ocean & Coastal Research Group. Departamento de Ciencias y Técnicas del Agua y del Medio Ambiente. Universidad de Cantabria. 39005 Santander, Spain.

J.J. Muñoz-Pérez
Departamento de Física Aplicada. Universidad de Cádiz. CASEM, Polígono Río S. Pedro, s/n. Puerto Real, Cádiz, Spain.

ABSTRACT

An equilibrium beach profile model for a beach affected by a coastal structure is presented. The model is based on the well-known energy flux approach proposed by Dean (1977). The effect of the structure is taken into account by considering the modification that the structure generates on the wave energy flux. The model is then applied to several cases that are usually found along the littoral, namely a perched beach and a reef-protected beach. Several field and laboratory data are used to analyze the merit of the proposed model for describing the equilibrium condition of a beach profile affected by a coastal structure. A good comparison is obtained.

En este trabajo se presenta un modelo de perfil de playa afectado por la presencia de una estructura. El modelo se basa en la conocida aproximación del flujo de masa de Dean (1977). El efecto de la estructura se incluye en el modelo considerando la modificación que la presencia de la estructura genera en el flujo de energía. El modelo se aplica a diferentes casos de los que se suelen encontrar en el litoral, más concretamente playas colgadas o playas protegidas por un arrecife. Para mostrar la bondad del modelo propuesto a la hora de describir la condición de equilibrio del perfil en presencia de una estructura se compara con datos de campo y laboratorio. Los resultados de la comparación son buenos.

Influence of coastal structures on equilibrium beach profile

M.González & R.Medina
Ocean and Coastal Research Group, Departamento de Ciencias y Técnicas del Agua y del Medio Ambiente, Universidad de Cantabria, Santander, Spain

J.J.Muñoz-Pérez
Departamento de Fisica Aplicada, Universidad de Cádiz & CASEM, Puerto Real, Cádiz, Spain

ABSTRACT: An equilibrium beach profile model for a beach affected by a coastal structure is presented. The model is based on the well-known energy flux approach proposed by Dean (1977). The effect of the structure is taken into account by considering the modification that the structure generates on the wave energy flux. The model is then applied to several cases that are usually found along the littoral, namely a perched beach and a reef-protected beach. Several field and laboratory data are used to analyze the merit of the proposed model for describing the equilibrium condition of a beach profile affected by a coastal structure. A good comparison is obtained.

1 INTRODUCTION

It is well known that coastal structures may modify both beach shoreline and beach profile. Actually many coastal structures are built in order to change the existing shoreline configuration and to generate a broader dry beach. Several authors have studied the shoreline response due to offshore breakwaters using a numerical approach (e.g. Hanson & Kraus 1989, Gravens et al., 1991) or an empirical approach (e.g. Hsu & Silvester 1990, Gonzalez & Medina 1999). However, the effect of coastal structures on the modification of the beach profile has received much less attention.

Investigators have long recognized that beach profiles can be complex and may exhibit series of bars and troughs. However, in overall form they tend to be concave upwards and have a progressively decreasing slope as the water depth increases in the offshore direction. This regularity has inspired several attempts to develop mathematical expressions to describe the profile shape.

One of the most important approaches used for the determination of profile shape is that of the equilibrium profile of beaches. In a broad sense, the equilibrium beach profile is the result of the constructive and destructive forces acting in a beach profile. The hypothesis behind the equilibrium beach profile is that beaches respond to wave forcing by adjusting their form to an equilibrium or constant shape attributable to a given type of incident wave or sediment characteristic.

Various expressions have been proposed over the years (see González et al. 1997 as a general reference). The most widely used formulation, very simple and easy to apply, is the 2/3-power profile shape proposed by Bruun (1954) and Dean (1977). Both authors concluded that the beach profile shape could be adequately represented by:

$$h = Ax^{2/3} \tag{1}$$

where h is the total water depth, A is a dimensional shape parameter that depends on the grain size (Moore, 1982) and x is the horizontal distance from the shoreline. However, none of the presently proposed equilibrium beach profile expressions are able to adequately represent the interaction between the beach profile and a coastal structure.

The aim of this paper is to develop a general formulation of equilibrium for a beach profile affected by a coastal structure. First the fundamentals of the model are presented. The starting point of the model is the well-known energy flux approach proposed by Dean (1977). The effect of the structure is taken into account in the energy flux balance. Different hypotheses are made in order to consider different kind of coastal structures. The modification of the energy flux balance yields a new expression for the beach profile configuration. The model is then applied to several cases that are usually found along the littoral, namely a perched beach and a reef-protected beach. All the fitting parameters needed in the developed expressions are calibrated using field and laboratory data.

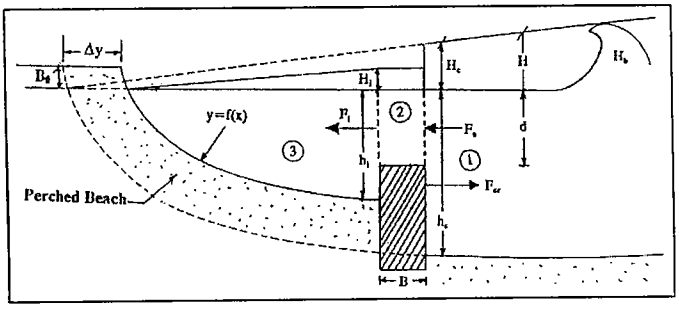

Figure 2. Definition sketch of parameters for the perched beach

to-depth ratio and uniform wave energy dissipation per unit water volume is assumed. According to Dean's (1991) work, a beach profile located in front of a seawall can be adequately represented by a profile extending behind the seawall as if the seawall did not exist. In other words, the reflection of the seawall, F_{er}, does not modify the beach profile shape. Consequently, beach profile in region 1 is not affected by the submerged structure and can be determined using the virtual x-origin (see Figure 1). This profile defines the water depth at the seaward side of the structure, h_e, and also the amount of energy flux reaching it, F_e (see Figure 2).

Region 2 is the breakwater domain. This region is defined by the breakwater crest width, B, the water depth over the breakwater, d, and the water depth at the seaward and leeward, h_e and h_i respectively. The above mentioned parameters (B, d, h_e, h_i) determine the energy flux, F_i, which reaches the perched profile.

Region 3 is the leeward part of the profile. In this domain Dean's (1977) hypothesis, stated in region 1, is also assumed. Consequently, the perched beach profile shape in region 3 is defined by the parabolic equation (1).

Notice that the perched beach profile is completely defined if h_i is given which, due to the constant breaker-to-depth ratio, can be determined if F_i is known. In order to calculate the value of F_i, the energy balance in region 2 must be solved:

$$F_i = F_e - F_{er} \tag{3}$$

where F_{er} is the wave energy flux reflected by the structure.

Assuming linear shallow wave theory, constant breaker-to-depth ratio and that only the oscillatory (non-breaking) part of the wave contributes to the reflected flux of energy (Baquerizo 1995); equation (3) can be written as:

$$h_i = h_e(1 - R^2)^{\frac{2}{5}} \tag{4}$$

where R is the reflection coefficient ($R = H_r / H_e$), H_e is the incoming wave and H_r is the reflected wave height.

The solution for the reflection coefficient, R, for the wave propagation over an impermeable step problem, can be found in several previous works (eg. Losada et al. 1992). The main characteristics of the solution are also showed in Figure 3, where the reflection coefficient, R, is plotted as a function of the dimensionless breakwater crest width, B/L, for different values of the dimensionless water depth, d/h_e. In this figure, the well-known feature of wave resonance is clearly observed. Due to this phenomenon, the reflection coefficient goes to a value close to zero for some particular sets of parameters (d/h_e, B/L).

In order to solve equation (4) an iterative process must be carried out, in which a first estimation of h_i is specified to solve the reflection coefficient. This reflection coefficient is then used to determine a new value for h_i.

Using the above mentioned procedure values of the water depth ratio h_i/h_e are plotted in Figure 4 versus the dimensionless water depth, d/h_e, for different breakwater crest widths, B/L. From Figure 4 it can be concluded that for dimensionless water depths d/h_e greater than 0.5 minor benefits are achieved with the construction of a submerged breakwater ($h_i \sim h_e$). A considerable reduction in h_i/h_e is obtained for d/h_e less that $d/h_e < 0.1$. In this area, however, resonance effects may modify this picture resulting in an inefficient structure.

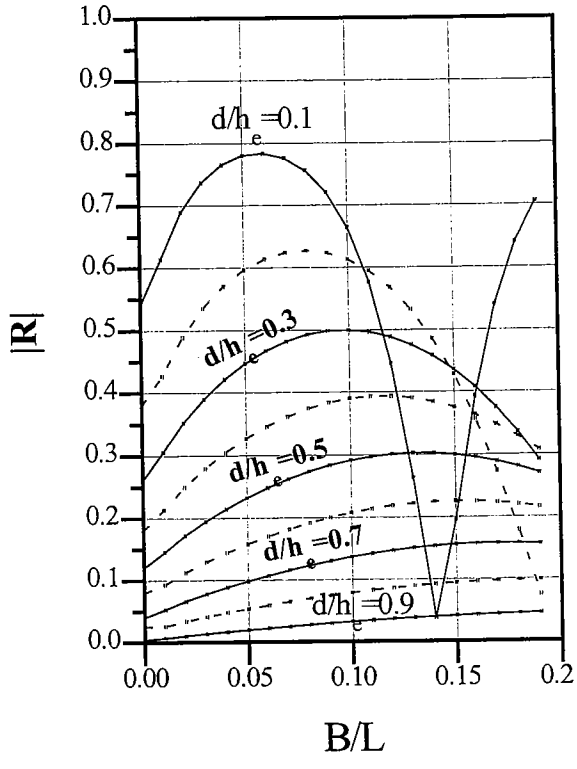

Figure 3. Reflection coefficient R versus width, B/L for different relative submergence of the breakwater, d/h_e

2 FUNDAMENTALS OF THE MODEL

Several approaches have been pursued in an attempt to characterize equilibrium beach profiles. One of the most popular is to consider the time-averaged wave energy flux equation for straight and parallel contours:

$$\frac{dF}{dx} = -\varepsilon \qquad (2)$$

where F is the net shoreward energy flux per unit width and ε is the energy dissipation rate per unit area. An extension of equation (2) for cases in which refraction or diffraction processes are important can be found in Gonzalez et al. (1997).

Equation (2) involves three variables, namely: the wave height, H, the water depth, h, and the energy dissipation, ε. Several authors have used equation (2) to develop a model for the wave energy dissipation by means of field or laboratory data of wave height and water depth (e.g. Battjes & Janssen 1978, Thornton & Guza 1983; Dally et al. 1985). Many numerical models take advantage of equation (2) to solve the wave height modifications during its propagation cross-shore, given the water depth and an energy dissipation model. In the equilibrium beach profile problem one seeks the water depth and, consequently, an appropriated energy dissipation model and wave height variation across the profile must be provided. The key point of the present work is that the equilibrium beach profile of a beach affected by a coastal structure can be obtained if the adequate energy dissipation model and wave height variation across the profile is used in the energy flux balance.

3 PERCHED BEACHES

3.1 *Introduction*

The basic concept of the perched beach is to reproduce the existing profile to some convenient seaward point and then intersect this profile with a submerged toe structure to retain the beach in a perched position, see Figure 1.

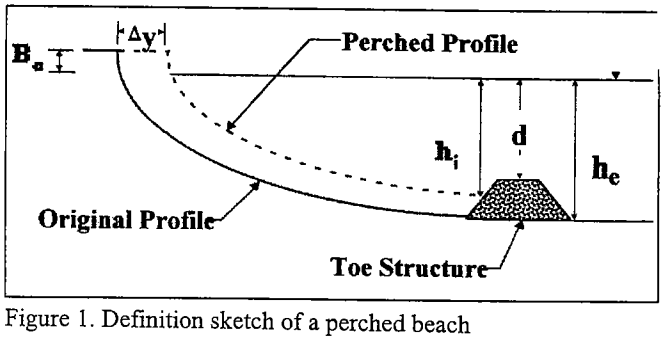

Figure 1. Definition sketch of a perched beach

Since the main hypothesis behind the equilibrium beach profile model is that the wave energy flux dissipated along the beach profile, the equilibrium beach profile for a perched beach will depend on the amount of energy flux that is transmitted over the toe structure. Consequently, the design of perched beaches requires an understanding of how waves are reflected at the submerged structure and how they are dissipated as they travel across the structure-top.

A large body of literature is available on wave transformation on a reef breakwater (see Ahrens 1987 as a general reference). An important conclusion of these studies, related with the stability of the perched beach, is that, although the submerged breakwater may induce wave breaking, it occurs well beyond the breakwater crown (Grilli et al. 1994).

An estimation of the structure width for the waves to break on the structure can be obtained from Gourlay (1994). In this work, Gourlay (1994) studied the wave transformation of waves approaching a fringing reef with a steep face and outer reef-top slope gently decreasing in the landward direction. From Gourlay's results it can be concluded that, at least, at a distance from the edge of the reef, l, of $l \approx T\sqrt{gd}$, the wave height can be greater than the incoming wave and the wave energy flux can exceed the stable value of wave energy flux given by the constant breaker-to-depth ratio $\gamma = 0.8$ for that particular depth, d. Furthermore, the breaking process will take a distance (one or two wave lengths) to reduce this wave energy flux to a stable value. This result agrees with Muñóz et al. (1998) field data which show that for a natural reef-protected beach to exist, the reef width must exceed three wave lengths.

According to these studies it is clear that in wide natural reefs, wave breaking over the reef limits the amount of energy reaching the beach profile and it is the most important factor affecting the beach profile shape (Muñóz-Pérez 1996). In most of the man-made structures, however, wave breaking over the structure can be neglected since the breakwater crest width is usually much smaller than the wave length and breaking occurs at the perched beach. Furthermore, frictional damping over the breakwater can also be neglected and, consequently, wave reflection at the breakwater is the main process that determines the beach profile shape in a perched beach.

3.2 *Energy Flux Balance*

In order to solve equation (2) for a perched beach, the beach profile is divided into three regions as shown in Figure 2.

Region 1 is the offshore part of the profile. In this area Dean's (1977) hypothesis of constant breaker-

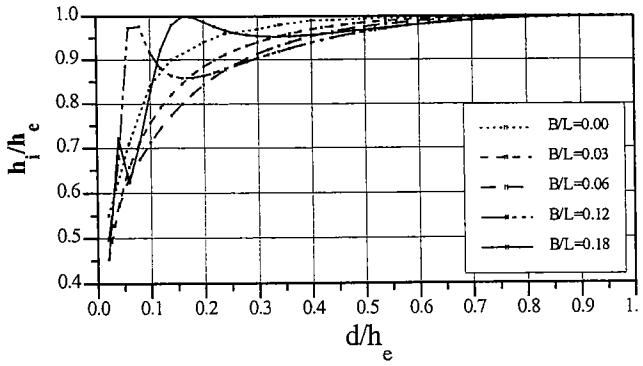

Figure 4. Relative depths h_i/h_e versus relative crest submergence, d/h_e for different relative width, B/L.

3.3 *Model Validation*

Several lab data sets can be used in order to analyze the merit of equation (4) for describing the equilibrium condition of a perched beach. Chatham (1972) carried out two-dimensional studies to determine the amount of sand which would be lost seaward over the submerged toe structure by normal and storm wave action. The model beach was subjected to test waves until equilibrium was reached for a wide range of wave conditions. The values of parameters tested are listed in Table 1. Calculated values of the ratio d/h_i are also presented in Table 1.

Sorensen & Beil (1988) conducted two-dimensional experiments of perched beach profile response to storm waves. Five test cases were investigated. The first consisted of a nourished profile without a toe structure. The remaining four cases were perched beach conditions with a sill located at various depths. A complete list of the parameters studied are listed in Table 2. Calculated values of the ratio d/h_i are also presented in Table 2. From Tables 1 and 2 and Figure 5, it can be concluded that equation (4) gives an adequate estimation of the equilibrium water depth at the breakwater for a perched beach.

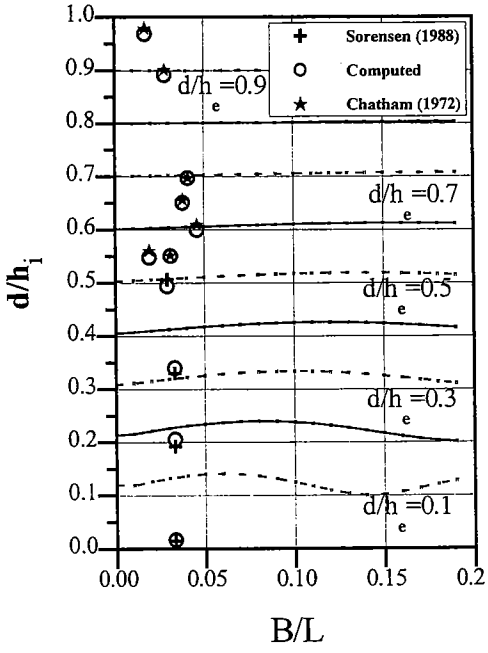

Figure 5. Numerical and experimental results of relative crest submergence, d/h_i versus relative width, B/L for different relative submergence, d/h_e

Table 1. Comparison between the laboratory data results of Chatman 1972 and present model

h_e(m)	d (m)	h_i (m)	T (s)	L(m)	B(m)	B/L	d/h_e	d/h_i (measured)	d/h_i (calculated)
5.72	3.43	5.55	7.0	50.2	2.3	0.046	0.600	0.610	0.606
8.23	5.72	8.19	7.0	55.8	2.3	0.041	0.695	0.698	0.697
7.10	4.60	7.00	7.9	60.9	2.3	0.038	0.648	0.657	0.651
6.28	3.43	6.20	10.0	75.2	2.3	0.031	0.546	0.553	0.551
7.43	6.63	7.35	10.0	81.1	2.3	0.028	0.892	0.902	0.892
6.29	3.43	6.10	16.0	123.6	2.3	0.019	0.545	0.562	0.548
7.43	7.20	7.35	16.0	133.9	2.3	0.017	0.969	0.980	0.969

Table 2. Comparison between the laboratory data results of Sorensen & Bei 1988 and present model

h_e(m)	d (m)	h_i (m)	T (s)	L(m)	B(m)	B/L	d/h_e	d/h_i (measured)	d/h_i (calculated)
0.187	0.091	0.18	1.6	2.06	0.06	0.029	0.490	0.506	0.494
0.140	0.046	0.14	1.6	1.81	0.06	0.033	0.330	0.330	0.340
0.130	0.023	0.12	1.6	1.80	0.06	0.033	0.180	0.192	0.205
0.140	0.001	0.07	1.6	1.81	0.06	0.033	0.007	0.015	0.016

Using the present model, some engineering applications such as the design of a beach nourishment project in a perched beach is presented by González et al. 1999. Dean (1991) analyzed the reduction in required sand volumes through the perching of a nourished beach by an offshore sill. In their analysis, Dean assumed a constant value, $h_i = d$ (see Figure 1).

4 REEF-PROTECTED BEACHES

4.1 *Introduction*

There are many locations in which the entire beach profile is not sand rich and areas of hard bottom or mud are encountered (e.g. coral reefs, perched barriers). Many characteristics and informative details about these kinds of beaches, which will be denoted as reef-protected beaches, have been previously studied (see Muñoz-Pérez 1996 as a general reference). In a special way, wave breaking and wave attenuation over submerged horizontal shelves have been considered (Horikawa & Kuo 1966; Gourlay 1994; Nelson 1994).

It is well known that the spilling-wave breaking assumption with a constant wave height to water depth ratio, γ, is not adequate for waves breaking on a shelf. Horikawa & Kuo (1966), computed theoretical curves that have a consistent agreement with experimental data in the case of wave transformation on a horizontal bottom. The ratio between the local wave height and the mean water depth decreases from 0.8, at the initial wave breaking point, to become almost constant, about 0.5, in the inner zone.

Several wave-decay expressions have been proposed (e.g. Dally et al. 1985; Andersen & Fredsoe 1983). Fredsoe & Deigaard (1992), for example, gave the following exponential decay:

$$\frac{H}{h_r} = 0.5 + 0.3\exp\left(-0.11\frac{1}{h_r}\right) \tag{5}$$

where h_r is the water depth over the reef, H is the wave height and l is inshore distance from the edge of the shelf (see Fig. 6). From equation (5) it can be concluded that the wave height that reaches the sandy beach toe, which is located at the depth h_r, is less than the wave height that would reach that particular depth in a beach without the hard shelf. Consequently, the total amount of energy that has to be dissipated by the sandy profile is minor.

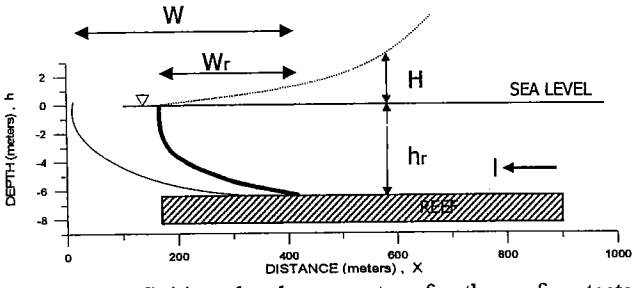

Figure 6. Definition sketch parameters for the reef-protected beach.

4.2 *Energy Flux Balance*

The beach profile form of a reef-protected beach can be determined by means of Larson & Kraus's (1989) derivation of the equilibrium profile, taking into account the available wave energy at the toe of the beach and assuming the dissipation model of Dally et al. (1985). The resulting beach profile form will be given by an expression similar to eq. (1). However, for the same grain size, the profile shape parameter for a reef-protected beach will not be the same as the A value used in the usual Dean equilibrium profile in equation (1) due to the shelf wave-decay dependence.

A simple relationship between the shape parameter for reef-protected beaches, hereafter denoted as A_{rp}, and non-reef-protected beaches can be obtained considering that the energy flux, Ec_g, at h_r must be dissipated along the beach profile in both cases.

$$(EC_g) = \int D * h\, dx \tag{6}$$

Assuming linear wave theory and that equation (1) is valid along the entire profile, it yields:

$$\left(\frac{H_{rp}}{H}\right)^2_{hr} = \left(\frac{W_{rp}}{W}\right) \tag{7}$$

where H is wave height, W is the total length of the profile and the subscript $(\ )_{rp}$ indicates the reef-protected beach (see Figure 6).

Since H_{rp} at h_r is less than H at the same depth, the total length of the profile for the reef-protected beach will also be less than the non-reef-protected beach and, consequently, the beach profile slope will be steeper.

Equation (7) can also be written in terms of the breaker-to depth ratio as:

$$W_{rp} = W\left(\frac{\Gamma}{\gamma}\right)^2 \tag{8}$$

where Γ is the breaker-to-depth ratio for a reef-protected beach (e.g. equation (5)) and γ is the

breaker-to-depth ratio in a non-reef-protected beach. For a wide shelf (l≈∞), typical values of Γ range between 0.55 to 0.35 (Nelson 1994). Values of γ depend on beach slope and wave steepness, and have a wider range of variability. Kaminsky and Kraus (1993) compiled a large database of wave breaking parameters and showed that for typical field beach slopes (1/30 to 1/80) most of γ values are encountered in the range 0.65 to 1.1 with an average value of 0.79.

Introducing equation (1) in equation (8), a relationship between the shape parameters can be found as:

$$\frac{A_{rp}}{A} = \left(\frac{\gamma}{\Gamma}\right)^{\frac{4}{3}} \tag{9}$$

where A_{rp} is the shape parameter for the reef-protected beach and A is the non-reef-protected beach shape parameter.

4.3 *Model Validation*

Using the set of field data compiled by Gomez-Pina (1995), beach profile data from reef-protected beaches along the Spanish coast have been collected to verify the proposed model. Over 50 profiles from seven beaches have been. The main characteristics of these beach profile data are shown in table 3. It is noted that the values of A_{rp} listed in Table 3 have been determined by best fitting and the values of A by means of Moore's (1982) relationship.

The predicted values of A_{rp} using equation (9) and the best-fitted values listed in Table 3 are compared in Figure 7. The predicted values are computed using Fredsoe & Deigard's (1992) model for Γ. It is seen in Figure 7 that equation (9) provides a good representation of the beach shape parameter A_{rp}. The asymptotic best fit for a wide shelf (l/h>60) is A_{rp}=1,48 A which corresponds to a value of W_{rp} = 0.56 W.

Table 3. Spanish Beach profile parameters

Beach	D_{50}(mm)	l (m)	h_r(m)	A ($m^{1/3}$)	A_{rp}($m^{1/3}$)
Ondarreta	0.33	200	4.50	0.12	0.18
Sta. María	0.42	500	8.50	0.14	0.21
Torregorda	0.25	330	3.50	0.11	0.16
Victoria	0.32	470	4.00	0.13	0.20
Arroyo Hondo	0.25	750	5.30	0.10	0.15
Regla	0.25	380	3.50	0.11	0.16
Fuentebravía	0.27	740	5.50	0.10	0.15

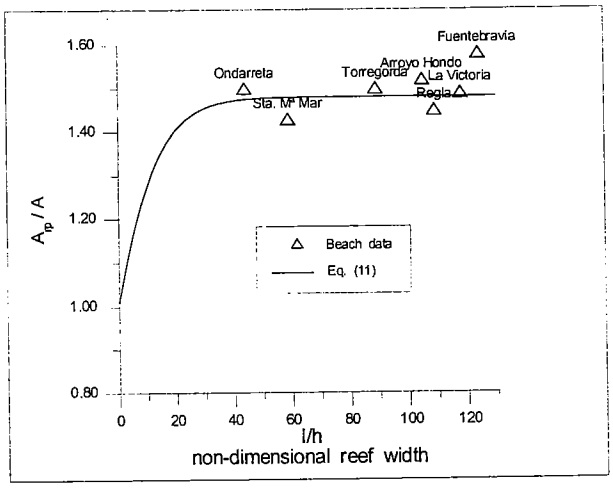

Figure 7. Non-dimensional shape parameter A_{rp}/A

5 CONCLUSIONS

This study has focused on the equilibrium shape of a beach profile affected by a coastal structure. The new shape has been obtained on the basis of the well-known energy flux approach proposed by Dean (1977). The main assumption of the present work is that the equilibrium beach profile of a beach affected by a coastal structure can be obtained if the adequate energy dissipation model and wave height variation across the profile is used in the energy flux balance. In this way the effect of the structure can easily be taken into account in the energy flux balance by considering the modification that the structure generates on the wave energy flux.

The model has been applied to a perched beach and a reef-protected beach. Several field and laboratory data have been used to analyze the merit of the proposed model for describing the equilibrium condition of a beach profile affected by a coastal structure. A good comparison has been obtained

For the case of the perched beach it is concluded that the maximum advance of the perched beach shoreline depends substantially on the dimensionless water depth. Minor advance is obtained for large d/h_e (>0.5) while a considerable advance is achieved for d/h_e less than 0.1. In this area, however, resonance effects induced by the structure may modify the final picture resulting in an inefficient structure depending on the value of B/L.

For the case of the reef-protected beach it is concluded that although the resulting beach profile form is similar to the one proposed by Dean (1977), the shape parameter is not the same as the A value used in the usual Dean (1977) equilibrium profile due to wave decay dependence. A simple expression has been proposed for the shape parameter A_{rp} for reef-protected beaches based on Andersen & Fredsoe's (1983) wave decay model.

ACKNOWLEDGEMENTS

This study has been partly funded by the European Communities in the framework of the Marine Science and Technology Programme (MAST), under the No MAS3-CT97-0081 project "Surf and Swash Zone Mechanics" (SASME). The field data have been kindly provided by the Dirección General de Costas (Ministerio de Medio Ambiente) and its support is hereby gratefully acknowledged.

REFERENCES

Ahrens, J.P. 1987. Characteristics of reef breakwaters. U.S. Army Corps of Engineers, *Coastal Engineering Research* Center, Tech. Rep. CERC-87-17.

Andersen, O.H. & J. Fredsoe 1983. Transport of suspended sediment along the coast. Progress Report No. *54 Inst. of Hydrodynamics and Hydraulic Eng.* ISVA. Tech. Univ. of Denmark. pp. 33 - 46.

Baquerizo, A. 1995. Reflexión del oleaje en Playas. Métodos de evaluación y de predicción. Ph. D. Dissertation, Universidad de Cantabria, Santander, Spain, 180 p.

Battjes, J. A., & J. P. F. M Janssen 1978. Energy loss and set-up due to breaking of random waves. *Proc. 16th Int. Conference on Coastal Eng.* ASCE. Vol. 1, pp. 569-587.

Bruun, P. 1954. Coast erosion and the development of beach profiles. Beach Erosion Board, Technical Memorandum, N° 44.

Chatham, C.E. 1972. Movable-bed model studies of perched beach concept. *Proc. 13th Int. Conf. Coastal Eng.* ASCE, pp. 1197-1216.

Dally, W., R. Dean & R. Dalrymple 1985. Wave height variation across beaches of arbitrary profile. *J. Geophys. Res.*, Vol. 90, No. C6.

Dean, R.G. 1977. Equilibrium beach profiles: U.S. Atlantic and Gulf coasts. Department of Civil Engineering, Ocean Engineering Report N°. 12, University of Delaware, Newark, Delaware.

Fredsoe J. & R. Deigaard 1992. Mechanics of coastal sediment transport. *Advanced Series on Ocean Eng.* Vol. 3. World Scientific, 369 pp.

Gómez-Pina, G. 1995. Análisis de perfiles de playa en las fachadas cantábrica y atlántica de la costa española y su aplicación a proyectos de regeneración. Universidad de Cantabria E.T.S.I.C.C.P. Dpto. de Ciencias y Técnicas del Agua y Medio Ambiente.

González, M., R. Medina & M.A. Losada 1997. Equilibrium beach profiles: effect of refraction. *Proc. Coastal Dynamics 97*, pp. 933-942.

Gonzalez, M & R. Medina 1999. Equilibrium Shoreline behind a Single Off-Shore Breakwater. *Proc. Coastal Sediments'99*. ASCE. pp844-859.

Gourlay, M.R. 1994. Wave transformation on a coral reef. *Coastal Eng.* Elsevier, 23: 17-42.

Gravens, M.B., N.C. Kraus, & H. Hanson 1991. GENESIS: Generalized model for simulating shoreline change, report 2, workbook and user's manual. *Technical Report CERC-89-19*, Report 2 of a series, U.S. Army Engr. Wtrways. Experiment Station, Vicksburg, Miss

Grilli S.T., M.A. Losada & F.L. Martín 1994. Characteristics of solitary wave breaking induced by breakwaters. *Journal of Waterway, Port, Coastal and Ocean Eng.* Vol. 120, N. 1, pp. 74 – 92.

Hanson, H., & N.C. Kraus 1989. GENESIS: Generalized model for simulating shoreline change. *Technical Report CERC-89-19*, U.S. Army Engr. Wtways. Experiment Station, *Coast. Engrg. Res.* Ctr., Vicksburg, Miss.

Hardy T. & I. Young 1996. Field study of wave attenuation of an offshore coral reef. *Journal of Geophysical Research.* Vol. 101, No.C6 pp. 14311 - 14326.

Horikawa, K. & C.T. Kuo 1966. A study on wave transformation inside surf zone. *Proc. 10th Coastal Eng. Conf.* Tokyo, pp. 217 - 233.

Hsu, J.R.C., & R. Silvester 1990. Accretion behind single offshore breakwater. *J. Wtrway., Port, Coast. and Oc. Engrg.*, ASCE, 116(3), 367 - 380.

Kaminsky, G.M. & N.C. Kraus 1993. Evaluation of depth-limited wave breaking criteria. *Porc. Ocean Wave Measurement and Anal., Waves 93.* ASCE, pp. 180-193.

Larson, M. & N.C. Kraus 1989. SBEACH: Numerical model to simulate storm-induced beach change. *Army Corps of Engr., Waterway Expt. Station., Tech. Rpt.* CERC-89-9.

Losada, I.J., M.A. Losada & A.J. Roldán 1992. Oblique incident wave past vertical thin barriers. *Applied Ocean Research,* Vol. 14, N° 3, pp. 191-200.

Moore, B. 1982. Beach profile evolution in response to changes in water level and wave height. *M.S. Thesis*, University of Delaware.

Muñóz-Pérez, J.J. 1996. Analisis de la morfologia y la variabilidad de playas apoyadas en lajas. *Phd Thesis* (in Spanish)

Nelson, R.C. 1994. Depth limited design wave heights in very flat regions. *Coastal Engineering*, Vol. 23, pp. 43-59.

Sorensen, R.M. & N.J. Beil 1988. Perched beach profile response to wave action. *Proc. 21st. International Conference on Coastal Eng.* ASCE, pp. 1482-1491.

Thorton, E. B., & R.T. Guza 1983. Transformation of wave height distribution. *Journal of Geophysical Research.* Vol. 18, pp. 5925-5938.

Publicado en el Journal of Geophysical Research, AGU

Standing edge waves in pocket beaches

Ozkan-Haller, H.T., Vidal, C., Losada, I.J., Medina, R. and Losada, M.A.

Abstract

Field measurements of edge waves obtained on a narrow pocket beach are described. The beach (named Usgo) is located on the north coast of Spain immediately to the west of the city of Santander and is exposed to the Atlantic ocean. Results from longshore array of current meters located in about 3 m of water depth are presented with the objective of analyzing the edge wave field on this beach. Frequency spectra of longshore velocities show that the edge wave field on this pocket beach displays several significant peaks. This is in contrast to observations on open coastal beaches [e.g. *Olman-Shay and Guza*, 1987] which show the existence of a broad banded edge wave field. We isolate four frequency peaks and analyze the longshore variation of the motions at these frequencies and find convincing evidence of a nodal structure. Utilizing the measured bathymetry, we compute theoretical wavelengths of edge waves at the dominant frequencies using a numerical solution method of the shallow water equations by *Howd et al.* [1992]. We find the edge waves at these frequencies satisfy the standing waves resonance condition, i.e. the width of the beach corresponds closely to an integer multiple of the computed half-wavelengths. In addition, assuming perfect sidewalls reflections, the theoretical nodal locations closely correspond to those inferred by the measurements. We conclude that discrete standing edge waves that are the results of resonances related to the longshore width of the beach are presente in Usgo.

En este trabajo se describen las medidas de campo de ondas de borde realizadas en una playa encajada. La playa (llamada Usgo) se encuentra en la costa norte española al Oeste de la ciudad de Santander y expuesta al océano Atlántico. Con el fin de analizar las ondas de borde presentes en dicha playa, se muestran los resultados obtenidos mediante un conjunto de correntímetros dispuestos longitudinalmente a 3 m de profundidad. Los espectros frecuenciales de las velocidades longitudinales muestran que las ondas de borde en esta playa encajada dan lugar a varios picos significativos. Este hecho está en contraposición de las observaciones realizadas en playas abiertas [e.g.

Olman-Shay and Guza, 1987] que se caracterizan por campos de ondas de borde de espectro de banda ancha. Aislando los cuatro picos y analizando la variación del movimiento longitudinal en esas frecuencias, se han encontrado fuertes evidencias de la presencia de una estructura nodal. Utilizando la batimetría medida, se han calculado las longitudes de onda teóricas de las ondas de borde en las frecuencias dominantes utilizando una solución numérica para las ecuaciones en profundidades reducidas de *Howd et al.* [1992]. Se ha encontrado que las ondas de borde en estas frecuencias satisfacen la condiciones de resonancia de ondas estacionarias, es decir, la anchura de la playa se corresponde con un múltiplo de la mitad de la longitud de onda calculada. Además, asumiendo reflexión perfecta en los contornos laterales, la localización de los nodos teóricos se corresponde casi perfectamente con los obtenidos experimentalmente. Se concluye que en la playa de Usgo existen ondas de borde estacionarias discretas resultado de la resonancia con la dimensión longitudinal de la playa.

Standing Edge Waves on a Pocket Beach

H. Tuba Özkan-Haller
Department of Naval Architecture and Marine Engineering, University of Michigan, Ann Arbor

César Vidal, Iñigo J. Losada, Raúl Medina
Ocean and Coastal Research Group, Departamento de Ciencias y Técnicas del Agua y del Medio Ambiente. E.T.S.I. de Caminos, Canales y Puertos, Universidad de Cantabria, Santander, Spain

Miguel A. Losada
Departamento de Ingenieria Civil, E.T.S.I. de Caminos, Canales y Puertos, Universidad de Granada, Spain

Short title: STANDING EDGE WAVES

Abstract.

Field measurements of edge waves obtained on a narrow pocket beach are described. The beach (named Usgo) is located on the north coast of Spain immediately to the west of the city of Santander and is exposed to the Atlantic ocean. Results from a longshore array of current meters located in about 3 m of water depth are presented with the objective of analyzing the edge wave field on this beach. Frequency spectra of longshore velocities show that the edge wave field on this pocket beach displays several significant peaks. This is in contrast to observations on open coastal beaches [e.g. *Oltman-Shay and Guza*, 1987] which show the existence of a broad banded edge wave field. We isolate four frequency peaks and analyze the longshore variation of the motions at these frequencies and find convincing evidence of a nodal structure. Utilizing the measured bathymetry, we compute the theoretical wavelengths of edge waves at the dominant frequencies using a numerical solution method of the shallow water equations by *Howd et al.* [1992]. We find that edge waves at these frequencies satisfy the standing wave resonance condition, i.e. the width of the beach corresponds closely to an integer multiple of the computed half-wavelengths. In addition, assuming perfect sidewall reflections, the theoretical nodal locations closely correspond to those inferred by the measurements. We conclude that discrete standing edge waves that are a result of resonances related to the longshore width of the beach are present on Usgo Beach.

1. Introduction

The low frequency range ($f < 0.05$ Hz) of the water wave spectrum in the nearshore region contains discrete edge wave modes, a continuum of leaky waves, as well as shear waves. Distinguishing individual modes within the low frequency band of field data is not an easy task. Since the 1960's, field investigators have employed increasingly sophisticated methods to aid in the completion of this task. Early studies [see e.g. *Huntley and Bowen*, 1973; *Huntley*, 1976] that concentrated on the identification of edge wave modes in the nearshore region, measured the cross-shore structure of the motions using cross-shore arrays of sensors in the surf zone. Observations confirmed that edge waves display a cross-shore standing structure with decaying amplitudes in the offshore direction. However, it quickly became apparent that many modes of edge waves and leaky waves coexist at a given frequency and that information about the cross-shore structure alone would not suffice in separating the modes unless the cross-shore array extends a large distance beyond the surf zone [*Guza*, 1974]. The early studies lacked information in the longshore direction that would aid in this process.

The next generation of field experiments involved analyzing the longshore structure of the low frequency motions in the surf zone. Field studies (such as the NSTS at Torrey Pines Beach and Leadbetter Beach as well as studies at Duck, NC) involved the deployment of large longshore arrays of current meters in the surf zone. These experiments were mostly carried out on coastal beaches that were not laterally confined in both longshore directions and that often displayed strong mean longshore currents. These experiments led to an improved understanding of infragravity waves [see e.g. *Huntley et al.*, 1981; *Oltman-Shay and Guza*, 1987; *Oltman-Shay et al.*, 1989]. Low mode edge waves were most easily identifiable in longshore velocity records. Cross-shore velocity records were often dominated by high mode edge wave or leaky wave signals. For this reason, the two velocity components, at times, showed low correlation with each other. Edge waves were in general found to be energetic and broad banded. Edge

waves on these beaches were primarily progressive, often with similar amounts of energy propagating in both direction.

The knowledge obtained from measurements on open, coastal beaches can be applied to the pocket beach environment, where the nearshore region is confined laterally by two headlands. Edge waves are believed to be primarily caused by wave grouping effects that provide forcing over a wide range of edge wave length and time scales [*Lippmann et al.*, 1997]. However, in an environment where headlands confine the lateral extent of the motions, the possible resonances are discrete, since the number of possible edge wave modes is expected to be restricted due to the finite longshore length of the beach. Only discrete standing edge waves that "fit" into the beach should be able to exist and will be resonantly forced (unless the edge wave extends far enough offshore to avoid being trapped between the headlands).

However, this notion is based on two assumptions. First, mean longshore current velocities must be small since the presence of a longshore current causes edge waves that propagate with the current to lengthen and those that propagate against the current to shorten [*Howd et al.*, 1992]. Such an effect will hinder the formation of a longshore standing pattern. A second consideration is the assumption that the environment is not highly dissipative. Dissipation will cause any resonances due to the finite beach width to detune. In this case, the frequency peaks associated with the resonances will not be sharp. If the effects of the dissipation are very pronounced, the energy may be spread over a fairly broad range of frequencies, making it impossible to identify any resonances. In this case, resonant standing edge wave modes may not be detectable.

Our objective here is to apply the methods that were developed during comprehensive field studies on open, coastal beaches [e.g. *Oltman-Shay and Guza*, 1987; *Oltman-Shay et al.*, 1989] to the study of the infragravity field on a drastically different beach planform. The planform of a pocket beach is of interest especially since it usually represents an equilibrium with the wave climate resulting in small mean longshore

velocities [*Komar*, 1998]. A narrow pocket beach with a relatively longshore uniform bathymetry and steep side walls also presents an environment where sidewall reflections may be effective, causing little dissipation. Hence, a pocket beach is an environment where resonances associated with discrete standing edge wave motions, that have the potential of modifying the nearshore bathymetry, are likely to exist.

The number of comprehensive experiments that involved measurements of edge waves in the nearshore region have, in general, been limited [*Bowen*, 1997]. However, such studies on pocket beaches have been especially scant. *Katoh* [1981] analyzed digitized runup images on a beach with only one lateral reflector and found evidence of standing edge waves that possessed an antinode at the location of the reflector. The absence of a second reflector prevented *Katoh* [1981] from observing resonances dictated by the longshore extent of the beach. *Culley* [1986] analyzed runup measurements in time and longshore direction that were obtained utilizing digitized images of the swash region. In this study preliminary evidence of the presence of standing edge wave resonances was presented. *Culley* [1986] found that the resonances were not sharp, but that they were, nonetheless, detectable in the runup measurements. The results by *Culley* [1986] motivate a detailed study of the edge wave resonance on pocket beaches and provide evidence that such resonances should be detectable. Since the literature concerning standing edge waves is extremely limited, it is expected that the data set described herein will be a very useful addition to the study of these motions.

We briefly review the relevant properties of edge waves in Section 2. A description of the field site studied in this paper is given in Section 3. We show results of the data analysis in Section 4 and compare the observations with edge wave theory in Section 5. The results are summarized and conclusions are stated in Section 6.

2. Theory

In this study we are primarily interested in observing low mode edge waves in the nearshore zone. Although edge waves can extend into deep water, *Oltman-Shay and Guza* [1987] and *Oltman-Shay and Howd* [1993] showed that the kinematics of edge waves can be closely approximated by shallow water wave theory. On a plane beach with slope m, linear shallow water theory predicts a dispersion relation given by

$$\sigma^2 = gmk(2n+1) \tag{1}$$

where n is the (integer) cross-shore mode number and σ is the angular frequency related to the period T with $\sigma = 2\pi/T$. The longshore wavenumber $k = 2\pi/L$, where L is the longshore wavelength. The water surface elevation due to edge waves, $\hat{\eta}$, is given by

$$\hat{\eta} = a_n L_n(2kx)e^{-kx}\cos(kx - \sigma t), \tag{2}$$

where a_n is the shoreline amplitude of the mode n edge wave and L_n is the Laguerre polynomial of order n.

The above formulations are valid for a planar beach. However, Usgo Beach is not planar, and a numerical solution is necessary to solve for the dispersion relationship and cross-shore profile on arbitrary depth. Following the derivation of *Holman and Bowen* [1979] we consider the linearized inviscid shallow water equations for the conservation of momentum and mass given by

$$\begin{aligned} \hat{u}_t &= -g\hat{\eta}_x, \\ \hat{v}_t &= -g\hat{\eta}_y, \\ \hat{\eta}_t + [h\hat{u}]_x + [h\hat{v}]_y &= 0, \end{aligned} \tag{3}$$

where $\hat{u}$ and $\hat{v}$ are the cross-shore and longshore velocities, respectively, h is the still water depth and the subscripts indicate differentiation. The x axis points offshore and the y axis points alongshore. We consider a longshore uniform beach where h is a

function of x alone and introduce the form $\hat{f}(x,y,t) = \Re e\{f(x)e^{i(ky-\sigma t)}\}$ for $\hat{u}$, $\hat{v}$ and $\hat{\eta}$ in the governing equations. Here, $\Re e$ indicates the real part. Further manipulation the resulting equations leads to a second-order differential equation in η [*Holman and Bowen*, 1979].

$$\left(\frac{gh\eta_x}{\sigma^2}\right)_x + \left(1 - \frac{k^2gh}{\sigma^2}\right)\eta = 0. \tag{4}$$

We utilize a solution method developed by *Howd et al.* [1992], who considered the linearized shallow water equations in the presence of arbitrary depth as well as longshore current profiles. Their equations collapse to (4) for no mean longshore current. *Howd et al.* [1992] utilized a Runge-Kutta integration method and identified solutions by locating (σ, k) pairs for which the velocities and water surface elevation decay to zero offshore. The solution method results in (σ, k) pairs and the corresponding cross-shore profiles $\eta(x)$ for an arbitrary depth profile $h(x)$.

In an environment where the beach is confined laterally in both directions by headlands, only edge waves with given longshore length scales can exist. Assuming that the headlands are perfect reflectors, the longest edge wave that can exist on a pocket beach with longshore width of L_b would have a wavelength equal to twice the width of the beach and is referred to as an edge wave with longshore mode number p of 1. In the general case the edge waves that will fit into this beach are characterized by

$$L = \frac{2L_b}{p} \tag{5}$$

where L is the edge wave wavelength and p is the longshore mode number defined to be a positive integer.

3. Field Experiments

3.1. Field Site and Measurements

Our field site is a pocket beach on the North Coast of Spain and is named Usgo Beach. It is located immediately to the west of the city of Santander. The beach faces

north and has a planform shape that is somewhat concave seaward. It is open to waves from the Atlantic ocean. The dominant wave climate consists of swell waves from the northwest. Usgo Beach is approximately 356 m wide and is laterally confined in both directions by large headlands. The headlands protrude offshore approximately 350 m (see Figure 1). In the planform the beach usually displays cusp features that are about 60 to 80 m in width (see Figure 2). However, these features are only present in the swash zone, and the beach is fairly uniform in the longshore direction at locations offshore of the mean water level. Two typical profiles that are depicted in Figure 3 illustrate this fact. The two profiles correspond to longshore locations at the horn and the middle of a cusp feature, respectively, and only display significant differences shoreward of the mean water level. The profiles show a steep foreshore with a slope of approximately 0.1, a terrace about 200 m offshore in 5 m water depth and a mild slope of 0.03 farther offshore.

Our approach is to obtain measurements of the infragravity field using longshore and cross-shore arrays of current meters and pressure sensors in the surf zone. The following sensors were available to us: 3 co-located Marsh-McBirney dual axis electro-magnetic current meters and pressure sensors, 2 Marsh-McBirney dual axis electro-magnetic current meters, 3 pressure sensors, 1 bottom mounted p-u-v gage. These instruments were used to construct a longshore array of current meters with a partially co-located longshore array of pressure sensors along with a cross-shore array of pressure sensors. The locations of the sensors are shown in Figure 2. The current meters were positioned in the form of a lagged array with a minimum sensor separation of 5 m and a total array length of 65 m. The current meters are referred to as sensors 1 through 5, where the sensor closest to the east headland is referred to as sensor 1. The separations between adjacent sensors (from east to west) were 35 m, 5 m, 15 m, and 10 m. The bottom mounted p-u-v gage was utilized to measure the incident wave climate by placing it in approximately 7 m water depth.

In this paper, results from the longshore current meter array from a data set obtained on October 2, 1997 are reported. On this day the incident swell with a period of about 11 s was approaching from the northwest at approximately 12° from north. The offshore significant wave height was approximately 0.75 m. The longshore array was located approximately 35 m from the high water line in approximately 3 m water depth. Our experimental procedure consisted of surveying the beach and deploying the instruments on the dry beach during low tide and taking 4 hours of continuous measurements at 2 Hz centered around high tide.

3.2. Kinematics of Edge Waves at Usgo Beach

Usgo Beach is located in a macro-tidal environment and the change in tidal elevation during the 4 hours of data acquisition on October 2 was 0.85 m, resulting in a horizontal translation of the mean water level of about 8.5 m. This translation is expected to cause a translation and possible modification of the edge wave field over the time span of the measurements. Therefore, we compute the kinematic properties of edge waves at Usgo Beach for several tidal elevations. Since the depth profiles at Usgo Beach display only minor variation in the longshore direction we use a profile resulting from an average of the two profiles depicted in Figure 3. The resulting dispersion lines for the high tide condition as well as for the lowest tidal elevation experienced during the 4 hours of data acquisition are shown in Figure 4 for edge waves with cross-shore mode number n of 0 and 1. Figure 4 depicts the frequency $f(= 1/T)$ versus the cyclic wavenumber $K(= 1/L)$ and also shows the possible resonant edge waves that can exist on a pocket beach with a width of 356 m. Resonances for p in a range from 1 to 21 are considered and the resonant wavenumbers $K = p \times (1/2L_b)$ are marked by vertical grid lines. Since the wavenumbers at which edge waves can exist are fixed due to the finite longshore scale of the beach, the frequencies at which these waves occur increase with the rising tide. The effect is least pronounced at low wavenumbers and most pronounced

for higher mode edge waves at higher wavenumbers. We will consider this variation in frequency when comparing the theoretical results to measurements in Section 5.

Oltman-Shay and Guza [1987] show that low mode edge waves are most easily detectable in measurements of longshore velocities. Cross-shore velocities are shown to be dominated by high mode edge waves and leaky waves. Since we are primarily interested in low mode edge waves, we will heavily utilize measurements of longshore velocities. *Oltman-Shay and Guza* [1987] also state that the analysis of longshore velocity data indicates that there is a transition to higher modes with increased frequency. This transition is associated with the fact the the longshore array is located at a fixed cross-shore location. The offshore extent of low mode edge waves decreases with increased frequency so that low mode edge waves at frequencies higher than a threshold can not be observed at the cross-shore location of the array. Instead edge waves with consecutively higher cross-shore mode numbers will be dominantly observed. The threshold frequency at which the transition from mode zero to mode one edge waves occurs can be estimated by assuming that all modes exist with a shoreline amplitude of unity. We once again utilize the solution method by *Howd et al.* [1992] to estimate the amplitude of several edge wave modes at the cross-shore location of the measurement array. Figure 5 shows computed amplitudes of longshore velocities at 35 m as a function of frequency. We find that the transition from mode zero edge waves to mode one edge waves is expected to occur at about 0.04 Hz.

Measured longshore velocity spectra often display a valley at or around the mode transition frequency [*Oltman-Shay and Guza*, 1987]. In contrast, cross-shore velocity spectra may display valleys at frequency nodes associated with leaky waves. This is due to the fact that cross-shore velocity signals are dominated by higher mode edge waves. The frequencies at which the measurement array will be located at a cross-shore node can once again be constructed by assuming uniform shoreline amplitudes. We find that these nodes occur at about 0.055 Hz for the cross-shore velocities and at about 0.035

and 0.08 Hz for the water surface elevation, which is also likely to be dominated by high mode edge waves.

In order for standing edge waves to exist on Usgo Beach, a large portion of the energy associated with the resonant modes has to be trapped between the headlands. Therefore, we investigate the offshore extent of edge waves at the resonant frequencies next. On monotonically increasing depth edge waves with higher wavenumbers decay faster in the offshore direction. Hence, among the resonant edge waves with cross-shore mode number n of 0, the edge wave with the lowest wavenumber, and hence lowest longshore mode number p, will extend farthest offshore. The computed cross-shore profile of the surface elevation for this wave with $(n, p) = (0, 1)$ is depicted in Figure 6a. As stated above, edge waves with cross-shore mode n of 1 will be observed in the longshore velocity records for frequencies higher than about 0.04 Hz. An edge wave with longshore mode number p of 5 is located at about 0.046 Hz at high tide. Since resonances with higher p-values will have higher wavenumbers associated with them, the edge wave with $(n, p) = (1, 5)$ will decay slowest when compared to other possible edge waves with $n = 1$ that can be observed in our longshore velocity records. The cross-shore profile for this wave is depicted in Figure 6b. To assess if these waves are trapped between the two headlands, we construct a plot of the cumulative energy as a function of offshore location. The percent cumulative energy at a cross-shore location is defined as the percentage of the total energy that is contained shoreward of this location. Such a plot is shown in Figure 7 for $(n, p) = (0, 1)$ and $(n, p) = (1, 5)$. We note that 95% of the energy of the edge wave with $n = 0$ is contained within 223 m of the shoreline, 99% of the energy is contained within 320 m. For the cross-shore mode 1 edge wave, 95% of the energy is contained within 165 m of the shoreline, 99% of the energy is contained within 197 m. Since the longshore velocity records are expected to be dominated by edge waves with cross-shore mode number n of 0 or 1 with p-values of 1 or higher, these considerations indicate that the energy associated with these waves

should be confined between the two headlands, which protrude approximately 350 m offshore, making standing edge wave resonances at Usgo Beach possible.

Assuming that resonances due to the finite longshore width of Usgo Beach will be observed, we can estimate the locations of the nodal lines in the longshore velocity. In Figure 8 we show the nodes that would occur for several longshore mode numbers (p-values) as nodes in a sinusoidal pattern. The origin is placed at the location of the east headland and corresponds to a nodal location assuming the headland is a perfect reflector. Also shown are the locations of the five sensors in relation to the east headland. Note that the locations of these nodes are not altered by changes in tidal elevation since they are dictated only by the longshore width of the beach. However, the frequencies at which these waves will exist will increase with increasing tidal elevation.

4. Analysis of Observations

The data analysis methods used herein are based on Fourier analysis. Spatially lagged phase and coherence estimates are also used to obtain information about the progressive or standing nature of the motions. Correlation analysis of this type does not assume a spatially homogeneous wave field and can, therefore, give information about longshore length scales even in situations where a nodal structure is expected to occur.

4.1. Time Series and Frequency Spectra

Sample time series of one hour length centered around high tide are shown in Figure 9. The time series shown correspond to the co-located current meter and pressure sensor located in the middle of the five sensor longshore array. The signal from the pressure sensor has been converted to surface elevation assuming shallow water conditions. Time series of longshore velocities show that there is no mean longshore current. Also, oscillations at time scales longer than the incident wave period are especially evident in the longshore velocity signal.

Frequency spectra are constructed utilizing 239 minutes (3.98 hours) of measurements and using 512 s ensembles of data resulting in 56 degrees of freedom and a frequency bandwidth of 1.95 $\times 10^{-3}$ Hz. The resulting spectra along with the 95% confidence intervals are shown for sensor 3 (located in the middle of the five sensor longshore array) in Figure 10. The incident wave energy is visible in all the spectra around 0.09 Hz. Especially the longshore velocity spectra show several peaks at infragravity frequencies. Although the peaks are significant the energy is spread over several frequency bins indicating a possibly detuned resonance. This detuning may be due to dissipation mechanisms such as bottom friction and imperfect sidewall reflections. In fact the sidewalls at Usgo Beach are not expected to be perfect reflectors since they are not perfectly perpendicular to the shoreline and also do not possess a smooth, planar surface. Experiments carried out on a pocket beach of similar size by *Culley* [1986] also showed that the frequency peaks were not narrow banded. Also marked in Figure 10 are the expected leaky wave zero-crossing frequencies for u and η as well as the mode transition frequency from cross-shore mode 0 to cross-shore mode 1 for v. The valleys in the cross-shore velocity spectra agree well with the zero-crossing frequencies for leaky waves whereas the valleys in the longshore velocity spectra agree with mode transition frequencies, indicating that the cross-shore and longshore velocities are dominated by leaky and low mode waves, respectively.

This analysis was also carried out with time series as short as 2.3 hours. In shorter time series the non-stationary effects due to the presence of the tide are reduced significantly but the resulting spectra have low degrees of freedom, hence a high amount of uncertainty. However, we find that the locations of the frequency peaks visible in Figure 10 are not altered significantly by the length of the time series used in the analysis.

Figure 11 shows the frequency spectra for the longshore velocity signals at each of the five sensors. The spectral densities seen at the sensors have been multiplied

by multiples of two orders of magnitude so that they are easily distinguishable. The vertical lines mark five significant peaks located at 0.0098 Hz, 0.0156 Hz, 0.0254 Hz, 0.0723 Hz, and 0.0879 Hz. The two peaks at the low frequency end of the spectrum are apparent for all five sensors and are fairly narrow banded whereas the third and fourth peaks are broader. The third peak at 0.0254 Hz is not observed at this frequency for all sensors. Sensors 3 and 4 display a broad peak at a somewhat higher frequency. Hence, the location of this peak is fluctuating between 0.0254 Hz and 0.0293 Hz. The latter frequency is marked using a dashed line. The frequency peaks at 0.0723 Hz and 0.0879 Hz are represented in all sensors. The highest frequency peak (0.0879 Hz) is at the incident wave frequency. We will analyze motions at the remaining four infragravity frequency peaks in more detail utilizing cross-spectral analysis next.

4.2. Alongshore Spatial Cross-Spectra

The analysis of co-linear (co) and quadrature (quad) components of the spatially lagged cross-spectra between sensors can lead to information related to the progressive or standing character of the motions [see *Bendat and Piersol*, 1986]. If the observed motions are progressive, the normalized co-spectra between two sensors 1 and 2 at a given frequency will trace a cosine function whereas the normalized quad-spectra will trace a sine function so that

$$\begin{aligned} \mathrm{Co}_{12}(f) &= \cos\{2\pi k\,(y_1 - y_2)\} \\ \mathrm{Quad}_{12}(f) &= \sin\{2\pi k\,(y_1 - y_2)\}\,, \end{aligned} \tag{6}$$

where y_1 and y_2 are the longshore locations of the sensors. The phase as a function of spatial separation can be obtained using the quotient of quad- and co-spectra at the chosen frequency and will be characterized by advancing phase with sensor separation. The normalized quad-spectrum also gives an indication about the direction of propagation. It will trace a positive sine function if the propagation is in the

$+k$-direction, but a negative sine function if the propagation direction is in the $-k$-direction. For an application of the co- and quad-spectra to the identification of progressive motions in the surf zone, the reader is referred to *Huntley et al.* [1981] and *Oltman-Shay et al.* [1989].

The absence of a smooth variation over a wavelength in the co- and quad-spectra indicates that progressive motions at that frequency do not exist. Instead, the motions at the chosen frequency could be standing waves. In that case the normalized co-spectra will display a jump discontinuity from $+1$ to -1 at the node of the standing wave. In this case the normalized quad-spectra is expected to be near zero and the phase function will mimic the behavior of the co-spectrum and display jump discontinuities. If two sensors under consideration are located between two nodes, the normalized co-spectrum is expected to be unity and the phase will show a 0° phase shift. However, if the two sensors are positioned such that a node is located between them, the time series will be 180° out of phase, the normalized co-spectrum will equal -1, and the phase function will show a phase shift of 180°. Therefore,

$$\begin{aligned} \mathrm{Co}_{12}(f) &= \begin{cases} 1 & \text{if } n_{\text{nodes}} = 0, 2, 4, \ldots \\ -1 & \text{if } n_{\text{nodes}} = 1, 3, 5, \ldots \end{cases} \\ \mathrm{Quad}_{12}(f) &= 0, \end{aligned} \tag{7}$$

where n_{nodes} is the number of nodes located between the sensor pair. *Huntley et al.* [1981] utilized these ideas while trying to identify the progressive or standing nature of edge waves at Torrey Pines Beach.

Cross-spectra were computed utilizing 239 minutes (3.98 hours) of measurements and using 512 s ensembles of data, once again resulting in 56 degrees of freedom. Results from the cross-spectral analysis for several frequencies at which energy peaks were observed are shown in Figures 12 through 17. Each figure depicts the co-spectrum, quad-spectrum, phase and coherence as a function of sensor separation. Error bars indicating the 95% confidence intervals are indicated for the phase estimates. These

intervals are at times very small and may not be distinguishable from the bullets representing the values of the phase function. The horizontal line in the coherence plots is the 90% confidence interval for zero coherence. Therefore, coherence values below the horizontal line can be interpreted as zero coherence. In that case, values for the co-, quad-spectra and phase are indicated with open circles since these values are derived from a pair of time series that are not correlated to each other to a sufficient degree. Values indicated with open circles should, therefore, be interpreted with care. The sensor pairs and the corresponding spatial separations are noted in Table 1. Note that the minimum lag of 5 m corresponds to the minimum sensor separation and the maximum lag of 65 m corresponds to the total array length.

Results for the lowest two frequency peaks (f=0.0098 and 0.0156 Hz) are shown in Figures 12 and 13. We find that the motions at all the sensors are correlated remarkably well. The co-spectrum is close to unity throughout the array whereas the quad-spectrum and the phase are nearly zero. This could result from the presence of a very long progressive wave. Alternatively, this could be indicative of standing motion at this frequency if the wavelength of the motions are such that no node is located within the sensor array.

Figure 14 shows results for the third frequency peak at f=0.0254 Hz. The signals at all sensors are again very well correlated. The quad-spectrum is near zero. All sensors with sensor separations less than 35 m are in phase and the co-spectra show a value of unity. However, all sensors at separations equal to or larger than 35 m show motions that are 180° out of phase. Since all sensor lags larger than 30 m involve sensor 1 these results suggest that a node is located between sensors 1 and 2. As mentioned in the previous section, the peak at 0.0254 Hz is broad and energy is located in a band bounded by 0.0254 Hz and 0.0293 Hz. We have carried out cross-spectral analysis for the frequencies 0.0273 Hz and 0.0293 Hz and the results are shown in Figures 15 and 16. The situation at these frequencies is similar to Figure 14 for 0.0254 Hz, indicating a node

in the longshore velocities between sensors 1 and 2. It is noted that the quad-spectra for 0.0293 Hz deviates somewhat from zero and that the magnitude of the co-spectra at these locations is less than unity. However, the results for these three frequencies strongly indicate a nodal pattern.

The phase and coherence values for the peak at f=0.0723 Hz are shown in Figure 17. In this case, the quad-spectrum does not remain near zero and the co-spectrum is difficult to interpret. Analyzing the phase plot we can see that the values are close to 0° for lags less than 20 m. Between 20 m and 40 m the phase values are close to ±180° whereas at lags larger than 55 m the phase differences are once again fairly close to 0°. The coherences drop around the locations where the phase jumps occur. Note that all low coherences involve sensor 4, this is consistent with the presence of a node located close to this sensor. However, the coherences are high in all the other regions. These results suggest that a node of longshore velocity is located between sensors 1 and 2 and a second node is located between sensors 3 and 4, possibly close to sensor 4.

The interpretation of Figure 17 is somewhat difficult. In order to clarify the situation at $f = 0.0723$ Hz we also plot the co-spectrum at this frequency as a function of the absolute longshore location of the sensors. This method has been employed by *Huntley* [1988] and proved useful in identifying phase coupling between edge wave modes in field data. In Figure 18 co-spectra computed using time series from sensor pairs are plotted as a function of the absolute location of each sensor involved. The origin is placed at the location of the east headland. Co-spectra that involve sensor pairs with low coherences are represented by open circles and should once again be interpreted with care. Co-spectra involving a given sensor are connected using solid lines. We note that, for instance, sensor 1 is out of phase with sensors 2 and 3 but in phase with sensors 4 and 5. We note that all co-spectra change their sign between the locations of sensors 1 and 2. This is strong indication that a node exists between these two sensors. Such a switch also occurs between sensors 3 and 5. However the co-spectral

values around the location of sensor 4 are inconclusive at best, since they involve low coherences. Therefore, Figures 17 and 18 suggest that a node of longshore velocity is located between sensors 1 and 2 and a second node is located between sensors 3 and 5, but the location of this second node in relation to sensor 4 is difficult to discern. However, the low coherences associated with sensor 4 suggest that a node may be located in close proximity to this sensor.

In summary, our results suggest that at least some of the energy peaks seen in the energy spectra of longshore velocities may be due to standing edge waves. A question that remains unanswered is: Will standing edge waves at these frequencies "fit" into the beach? This question will be addressed in the next section using comparisons between observations and model predictions.

5. Comparison of Observations and Model Predictions

Figure 19 illustrates the agreement between the measured and predicted resonances. Shown are the theoretically possible standing edge waves at mid-tide level assuming perfectly reflecting side wall boundaries. We have included bars around the frequencies at which the theoretical resonances occur. The upper bounds indicate the frequencies at which resonances will occur for high tide conditions, whereas the lower bounds indicate the location of the resonant frequencies at the lowest observed tide level. Note that the resonant frequencies at mid-tide are not located exactly in the middle of the possible range. This is due to the fact that the foreshore slope changes significantly at low tide especially affecting the dispersion relation at high wavenumbers.

Also noted in Figure 19 are the frequencies at which energy peaks are observed. Utilizing the theoretical dispersion lines depicted in Figure 19, we estimate the wavelength of edge waves that would occur at the observed peak frequencies. We also compute the value of the longshore mode number p using the relationship in (5). These values are given for high, mid and low tide levels in Table 2. Utilizing both Figure 19

and Table 2, we find that the lowest two frequency peaks closely correspond to standing edge waves with cross-shore mode number n of 0 and longshore mode number p of 1 and 2. The observed third peak is located between 0.0254 Hz and 0.0293 Hz and we found strong evidence that standing motions existed at 0.0254 Hz, 0.0273 Hz and 0.0293 Hz. At low tide, the motions at 0.0254 Hz and 0.0293 Hz closely correspond to standing edge waves with p of 4 and 5, whereas at high tide the energy at 0.0273 corresponds to an edge wave with longshore mode number p of 4. Finally, the peak at 0.0723 Hz is the only peak located at a frequency higher than the theoretical mode transition frequency above which no edge waves with cross-shore mode number 0 should be observed. It is noted that this peak closely corresponds to a standing edge wave with a cross-shore mode number n of 1 and a longshore mode number p of 9 at high tide, but is more closely located to a resonant edge wave with $p = 10$ at the lowest observed tide.

Utilizing Figure 19 we suggest that motions at f =0.0098 Hz and 0.0156 Hz correspond to edge waves with $(n, p) = (0, 1)$ and (0,2). Further utilizing Figures 12 and 13, we conclude that no nodes were observed within the measurement array for these frequencies. This is consistent with the fact that standing edge waves with p-values of 1 and 2 should not display any nodes within the measurement array (see Figure 8. It is noted that the array encompasses somewhat less than a quarter of the wavelength of the edge wave with $p = 2$ (observed at 0.0156 Hz). This is usually long enough to observe sinusoidal variations in the co- and quad-spectra [*Oltman-Shay et al.*, 1989]. The complete absence of such variations in the observations further supports the presence of standing edge waves at these frequencies.

The frequencies within the range of 0.0254 Hz $< f <$ 0.02983 Hz appear to be affected by edge waves with $(n, p) = (0, 4)$ and (0,5). Returning to Figure 8 we find that for both $p = 4$ and 5, a node should be located between sensors 1 and 2. Note that we found convincing evidence of standing waves at these frequencies and the observed node was located consistently between sensors 1 and 2.

Finally, for f=0.0723 Hz, there is indication that the analyzed time series contains effects of a $p = 9$ as well as a $p = 10$ resonance. The cross-spectral analysis for this peak was inconclusive, but evidence suggesting the existence of a node between sensors 1 and 2 was convincing. The possibility of a node between sensors 3 and 4 also existed (see Figures 17 and 18). Figure 8 suggests that for both $p = 9$ and 10 a node should be observed between sensors 1 and 2. This is consistent with observations. However, a second node should theoretically occur between sensors 3 and 4 for $p = 10$, but between sensors 4 and 5 for $p = 9$. In the latter case, the node is predicted to be located very close to sensor 4. Coherences between sensor pairs involving sensor 4 were low, again suggesting that a node might be present near this sensor. Therefore, our findings are consistent with the idea that a node between sensors 1 and 2 existed throughout the time series, whereas the second node close to sensor 4 migrated significantly during data collection as the tidal level increased and subsequently decreased, yielding inconclusive results about the location of a second node near sensor 4.

6. Summary and Conclusions

Generation mechanisms for edge waves center around the idea that wave grouping effects in the incoming incident wave field supply the forcing at edge wave length and time scales through either nonlinear difference interactions or the presence of a temporally and spatially varying breaker location [see *Lippmann et al.* 1997]. Wave grouping of the incident waves can often be broad-banded. However, the possible resonances in a laterally confined domain are discrete. Although these resonances should, in theory, be sharp, and hence be dominant features of the data, the presence of any form of dissipation or the existence of tidal variations of the mean water level will detune the resonances. The presence of realistic friction may cause severe detuning and may preclude the existence of standing edge waves even in the presence of reflective sidewalls.

We have carried out a field experiment on a pocket beach and have sought to find out if detectable resonances exist. We have analyzed data obtained using a longshore array of velocity sensors. In contrast to the broad banded edge wave field observed on open coastal beaches, the edge wave field on this pocket beach displayed several significant peaks. Further analysis of the spatial character of the motions at four frequency peaks was performed by analyzing cross-spectra between sensor pairs located in the longshore array. The analysis revealed convincing evidence of a nodal structure in the longshore direction at the analyzed peaks. The evidence was most convincing for the peaks at lower frequencies. These peaks were also more energetic and prominent.

We have analyzed the effect of variations in the mean water level due to tides and have found that especially higher frequency waves were affected. The presence of a strong tidal signature contributes to the fact that the observed resonances are not sharp and precludes our ability to draw quantitative information about the magnitude of the dissipation by analyzing the width of the frequency peaks.

Using shallow water theory we estimated the wavelengths of edge waves at the four frequency peaks that were identified. These wavelengths were shown to correspond closely to edge waves that would "fit" into Usgo Beach. In other words, the width of the pocket beach was a near integer multiple of the the associated half-wavelengths. Assuming perfect side wall reflections, a node of the longshore velocity was assumed to be located at the eastern headland and the locations of subsequent nodes were inferred. In three of the four frequency peaks the theoretical nodal location coincided with the approximate node location obtained from observations.

Therefore, the results of this study indicate that, although the pocket beach system produces broad and detuned resonances in the form of longshore standing edge waves, these resonances are nonetheless possible and detectable.

Acknowledgments. Many thanks to Joan Oltman-Shay and Peter Howd for generously

providing the software used in the calculation of edge wave kinematics. We would also like to thank Tom Lippmann and Rob Holman for many enlightening discussions. Thanks also to two anonymous reviewers whose comments helped enhance the manuscript. Thanks also go to Fernando Méndez, Pedro Lomanóco, Francisco Martin, Eduardo Alonso, Agustín Vidal and Javier Rubio who helped carry all the "plomos". This project has been funded by the Direccion General de Costas (Ministerio de Medio Ambiente), Spain, and also partially by the Comission of the European Communities as part of the project "Surf and Swash Zone Mechanics" in the framework of the Marine Science and Technology Programme (MAST) under contract no. MAS3-CT95-0081. Support for the preparation of the final draft and publication of this paper came from the Office of Naval Research under contract

References

Bendat, J.S. and A.G. Piersol (1986). *Random Data Analysis and Measurement Procedures*, Second Edition, John Wiley and Sons, New York, pp. 118-129.

Bowen, A.J. (1997). "Patterns in the water: Patterns in the sand." in *Coastal Dynamics '97: Proceedings of the Third Coastal Dynamics Conference*, edited by E.B. Thornton, pp. 1–10, Am. Soc. of Civ. Eng., Reston, Virginia.

Culley, S.K. (1986). "Standing edge waves on a pocket beach." *Master's thesis*, Oregon State University.

Guza, R.T. (1974). "Comment on 'Standing waves on beaches' by J.N. Suhayda." *J. Geophys. Res.*, **79**, 5671–5672.

Holman, R.A. and A.J. Bowen (1979). "Edge waves on complex beach profiles." *J. Geophys. Res.*, **84**, 6339–6346.

Howd, P.A., A.J. Bowen and R.A. Holman (1992). "Edge waves in the presence of strong longshore currents." *J. Geophys. Res.*, **97**, 11,357–11,371.

Huntley, D.A. (1976). "Long-period waves on a natural beach." *J. Geophys. Res.*, **81**, 6441–6449.

Huntley, D.A. (1988). "Evidence of phase coupling between edge wave modes." *J. Geophys. Res.*, **93**, 12,393–12,408.

Huntley, D.A. and A.J. Bowen (1973). "Field observations of edge waves." *Nature*, **243**, 160–162.

Huntley, D.A., R.T. Guza and E.B. Thornton (1981). "Field observations of surf beat 1. Progressive edge waves." *J. Geophys. Res.*, **86**, 6451–6466.

Katoh, K. (1981). "Analysis of edge waves by means of empirical eigenfunctions." *Report of the Port and Harbour Research Institute, Japan*, **20**, pp. 51.

Komar, P.D. (1998). *Beach Processes and Sedimentation*, Prentice Hall, New Jersey.

Lippmann, T.C. R.A. Holman and A.J. Bowen (1997). "Generation of edge waves in shallow water." *J. Geophys. Res.*, **102**, 8663–8679.

Oltman-Shay J. and R.T. Guza (1987). "Infragravity edge wave observations on two California beaches." *J. Phys. Oceanography*, **17**, 644–663.

Oltman-Shay, J., P.A. Howd and W.A. Birkemeier (1989). "Shear instabilities of the mean longshore current. 2. Field observations." *J. Geophys. Res.*, **94**, 18031–18042.

Oltman-Shay J. and P.A. Howd (1993). "Edge waves on nonplanar bathymetry and alongshore currents: A model and data comparison." *J. Geophys. Res.*, **98**, 2495–2507.

M. Losada, Departamento de Ingenieria Civil, E.T.S.I. de Caminos, Canales y Puertos, Universidad de Granada, Spain

I. J. Losada, R. Medina, C. Vidal, Ocean and Coastal Research Group, Departamento de Ciencias y Técnicas del Agua y del Medio Ambiente. E.T.S.I. de Caminos, Canales y Puertos, Universidad de Cantabria, Santander, Spain

H. T. Özkan-Haller, Department of Naval Architecture and Marine Engineering, University of Michigan, 2600 Draper Road, Ann Arbor, MI 48109-2145 (e-mail: ozkan@engin.umich.edu)

Received _____

Table 1. Spatial Lag Values and Associated Sensor Pairs

Spatial separation (Lag)	Sensor Pair
5 m	2 & 3
10 m	4 & 5
15 m	3 & 4
20 m	2 & 4
25 m	3 & 5
30 m	2 & 5
35 m	1 & 2
40 m	1 & 3
55 m	1 & 4
65 m	1 & 5

Table 2. Observed Frequency, Cross-shore Mode Number n, Theoretical Wavelength L_p and Longshore Mode number p for the Observed Peaks at Low, Mid, and High Tide.

		Low Tide		Mid Tide		High Tide	
Frequency	n	L_p	p	L	p	L	p
Hz		m		m		m	
0.0098	0	606	1.17	653	1.09	695	1.02
0.0156	0	328	2.17	353	2.01	376	1.89
0.0254	0	172	4.14	186	3.83	197	3.61
0.0273	0	155	4.58	168	4.24	178	4.00
0.0293	0	140	5.08	151	4.70	160	4.45
0.0723	1	70	10.13	76	9.41	80	8.91

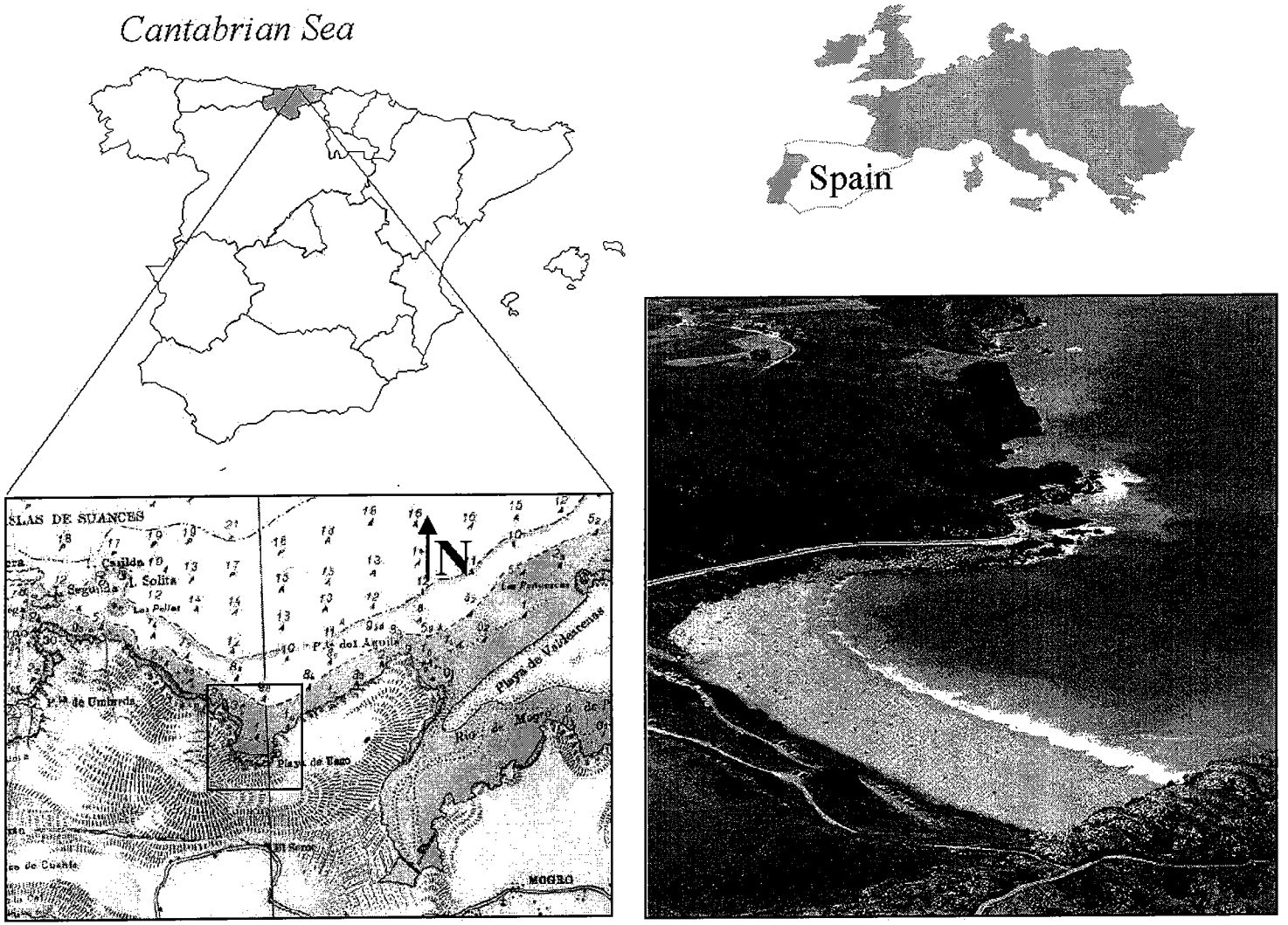

Figure 1. General map of Usgo Beach

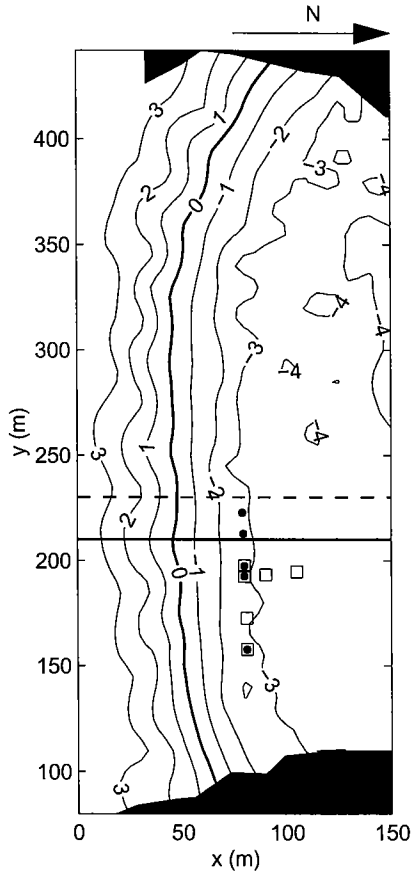

Figure 2. Measured bathymetry and instrument setup at Usgo beach. The available instruments were pressure sensors (squares), and bi-directional current meters (bullets). Also shown is the high tide shoreline (thick solid line).

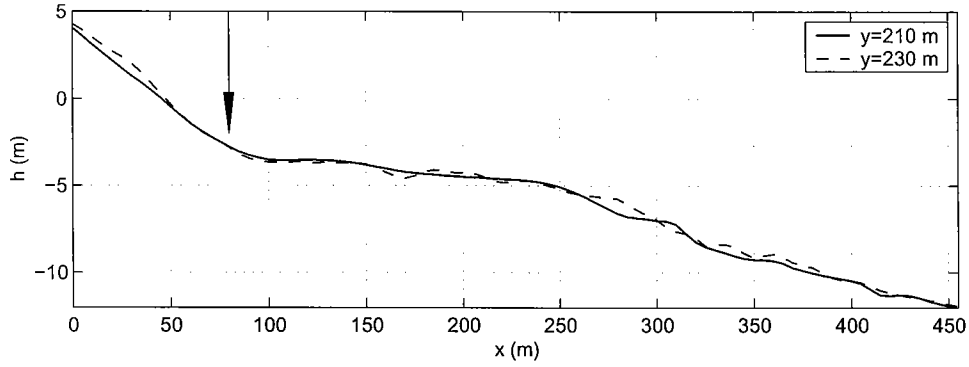

Figure 3. Cross-shore depth transects at longshore locations indicated by lines of corresponding type in Figure 2. The location of the longshore measurement array is marked with an arrow.

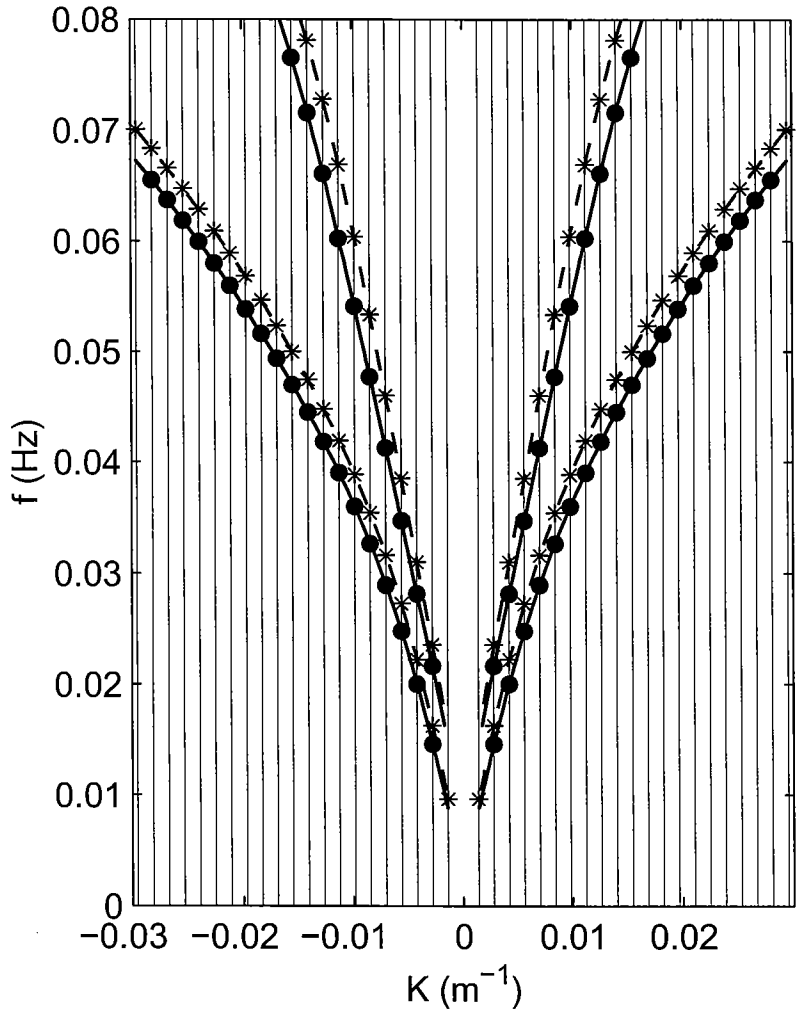

Figure 4. Dispersion lines for edge waves with cross-shore mode numbers n =0 and 1 for Usgo Beach at high tide (dashed line) and lowest tide (solid line) experienced during the four hours of data acquisition. Also noted are the theoretical edge wave resonances for a lateral beach width of 356 m for longshore mode numbers p 1 through 21 for high tide (stars) and low tide (bullets). Note that the frequency $f = 1/T$, and the cyclic wavenumber $K = 1/L$.

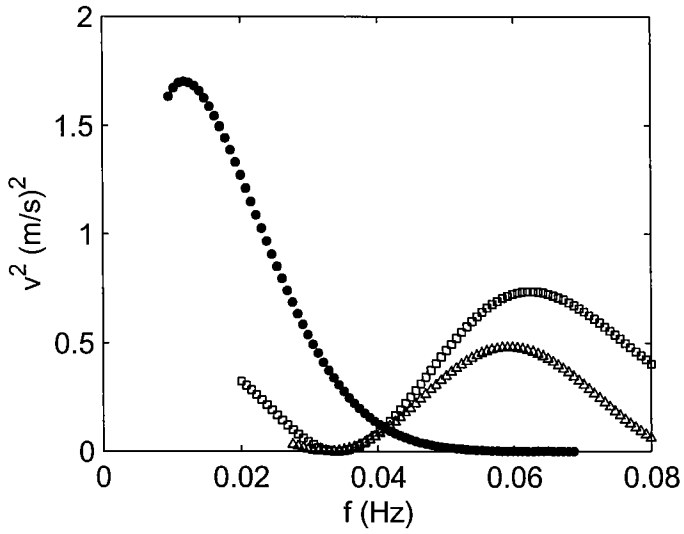

Figure 5. Simulated longshore velocity variance at the longshore array (located 35 m from the shoreline) as a function of frequency for edge waves with cross-shore mode number 0 (bullets), 1 (squares) and 2 (triangles).

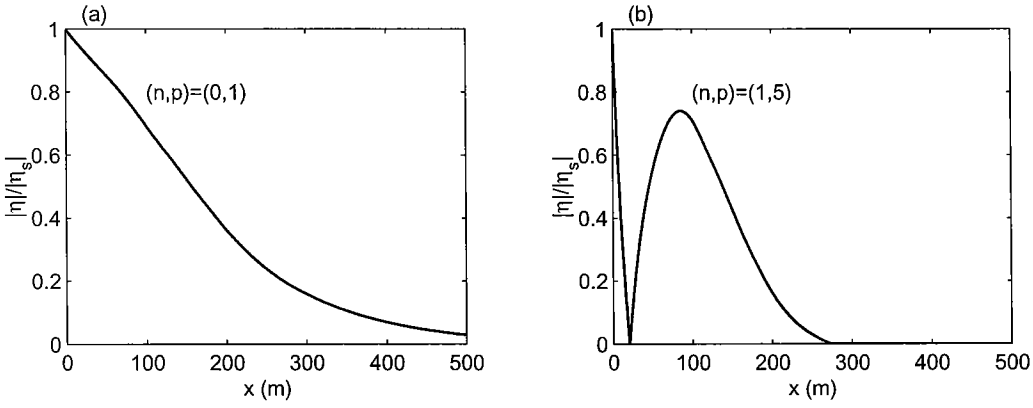

Figure 6. Simulated cross-shore profiles of the surface elevation due to edge waves for (a) $(n, p) = (0, 1)$ and (b) $(n, p) = (1, 5)$.

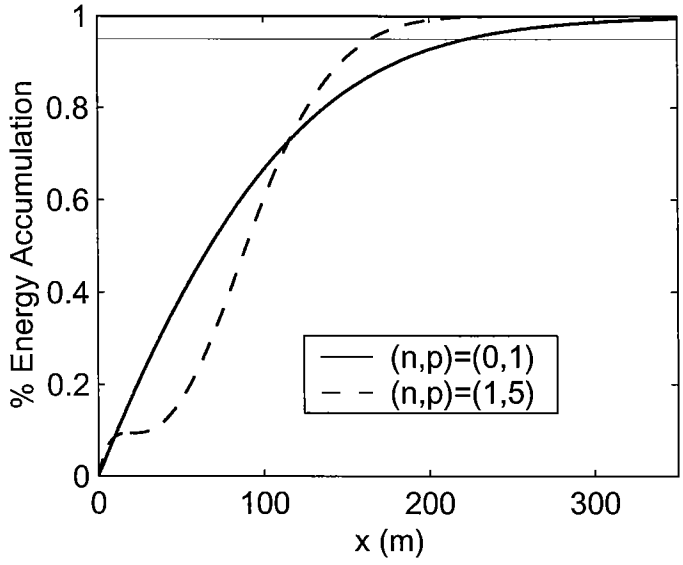

Figure 7. Energy accumulation of edge waves with $(n,p) = (0,1)$ and $(n,p) = (1,5)$. 95% accumulation is also shown.

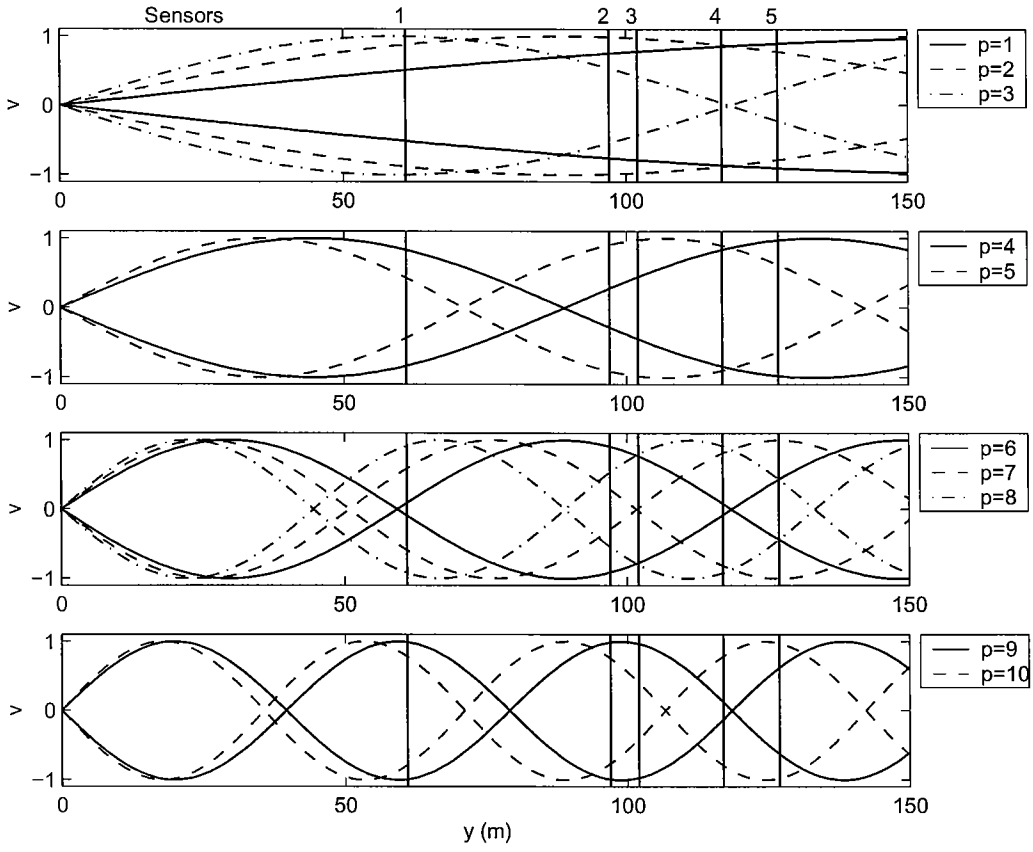

Figure 8. Theoretical nodal locations of the longshore velocity for several resonant edge wave modes. The vertical lines note the locations of the sensors.

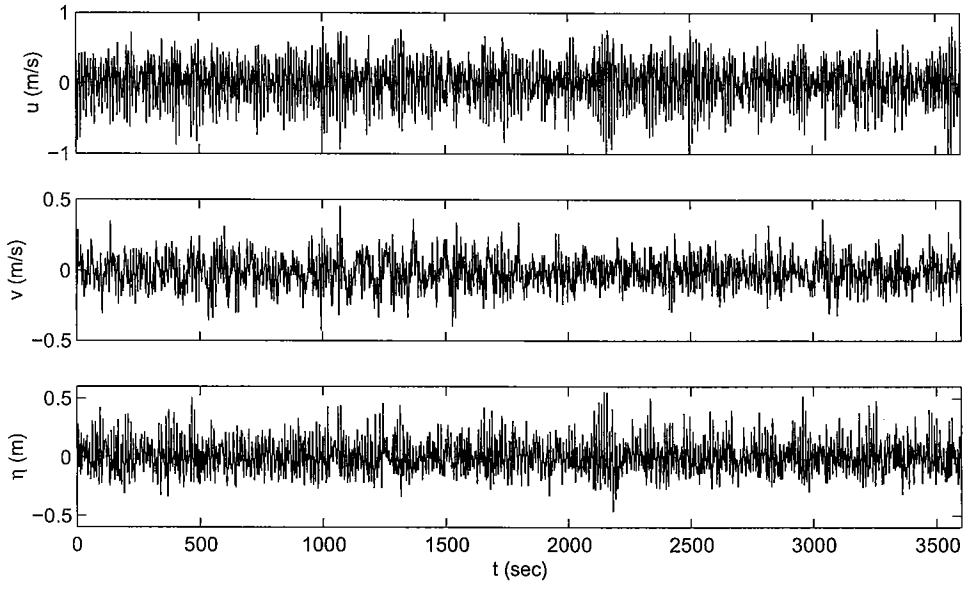

Figure 9. One-hour time series of cross-shore velocity u, longshore velocity v and pressure p for sensor 3.

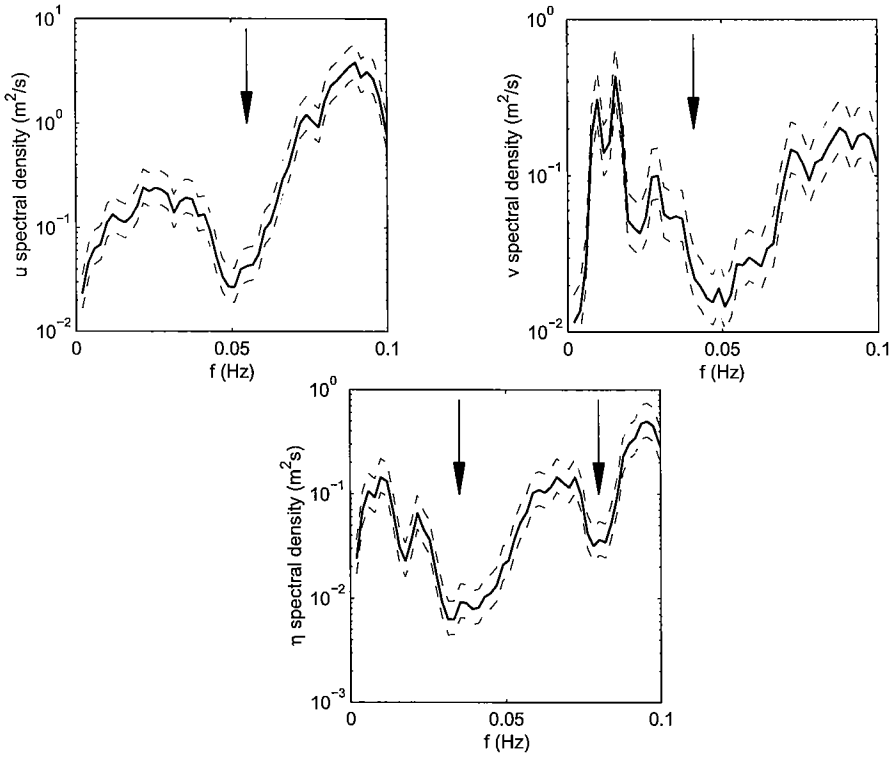

Figure 10. Frequency spectra of cross-shore velocity u , longshore velocity v and pressure p for sensor 3 (solid lines). The spectra involve 56 degrees of freedom and a frequency bandwidth of 1.95 $\times 10^{-3}$ Hz. The arrows indicate the locations of leaky wave zero-crossings for u and p and locations of mode transitions for v. The 95% confidence intervals are also shown (dashed lines).

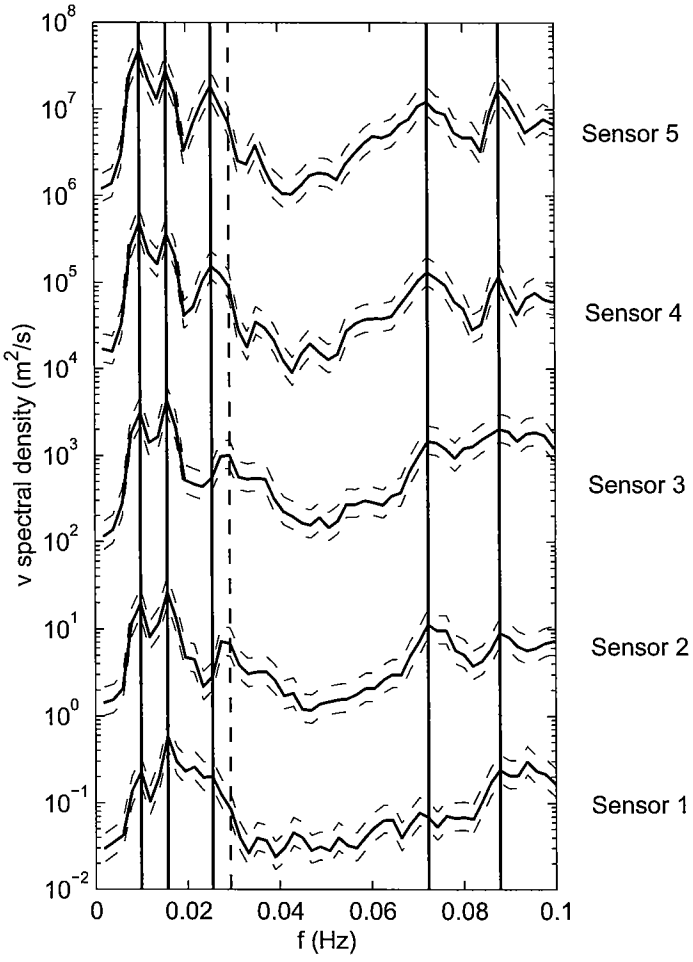

Figure 11. Frequency spectra of longshore velocities for sensors 1–5. Spectra have been multiplied by multiples of two orders of magnitude. The spectra involve 56 degrees of freedom and a frequency bandwidth of 1.95 $\times 10^{-3}$ Hz.

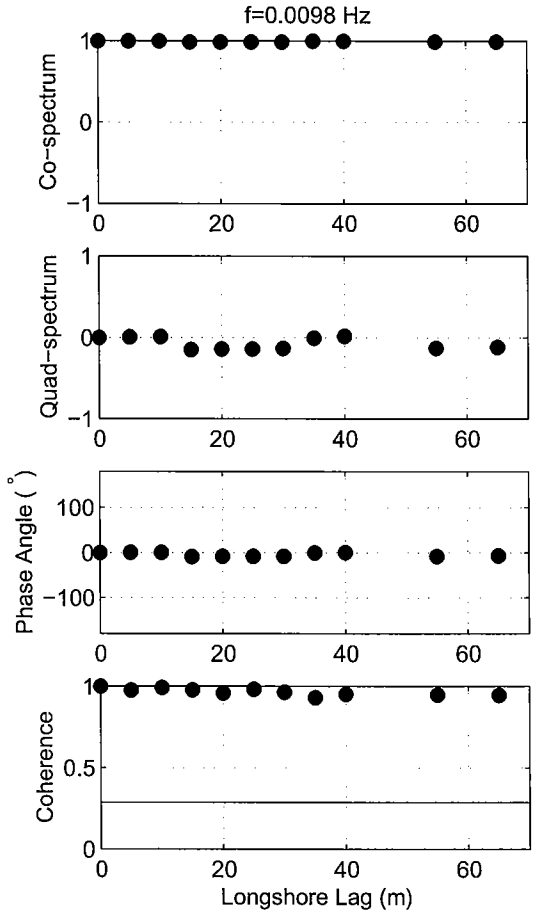

Figure 12. Co-spectrum, quad-spectrum, phase and coherence versus sensor separation for f=0.0098 Hz. The spectra involve 56 degrees of freedom and a frequency bandwidth of 1.95 $\times 10^{-3}$ Hz.

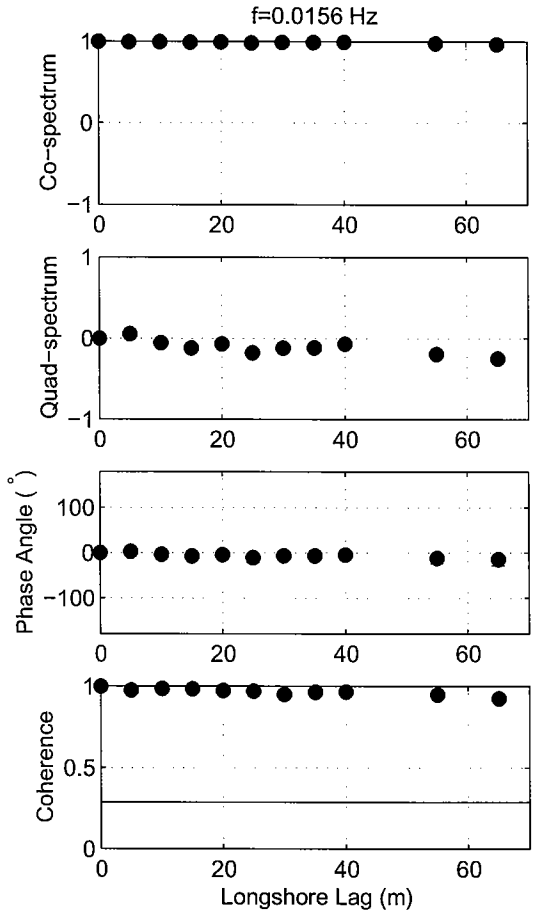

Figure 13. Co-spectrum, quad-spectrum, phase and coherence versus sensor separation for f=0.0156 Hz. The spectra involve 56 degrees of freedom and a frequency bandwidth of 1.95 $\times 10^{-3}$ Hz.

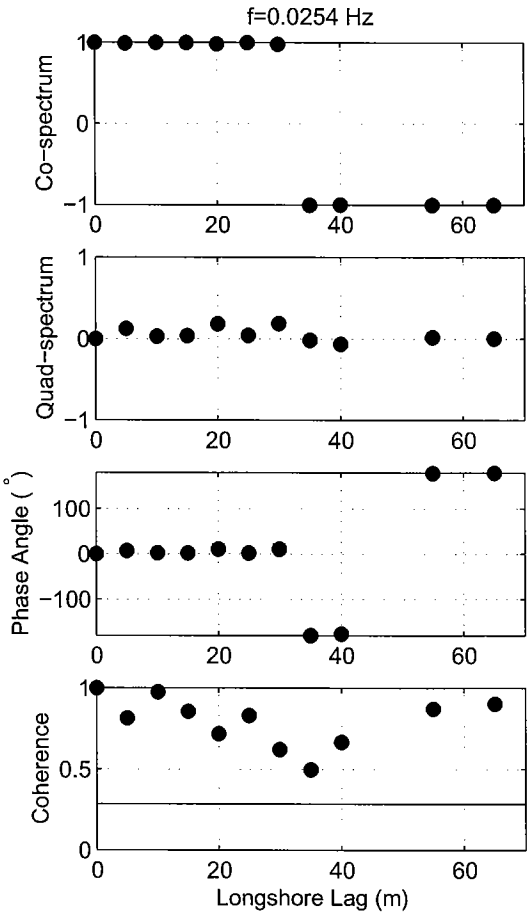

Figure 14. Co-spectrum, quad-spectrum, phase and coherence versus sensor separation for f=0.0254 Hz. The spectra involve 56 degrees of freedom and a frequency bandwidth of 1.95 $\times 10^{-3}$ Hz.

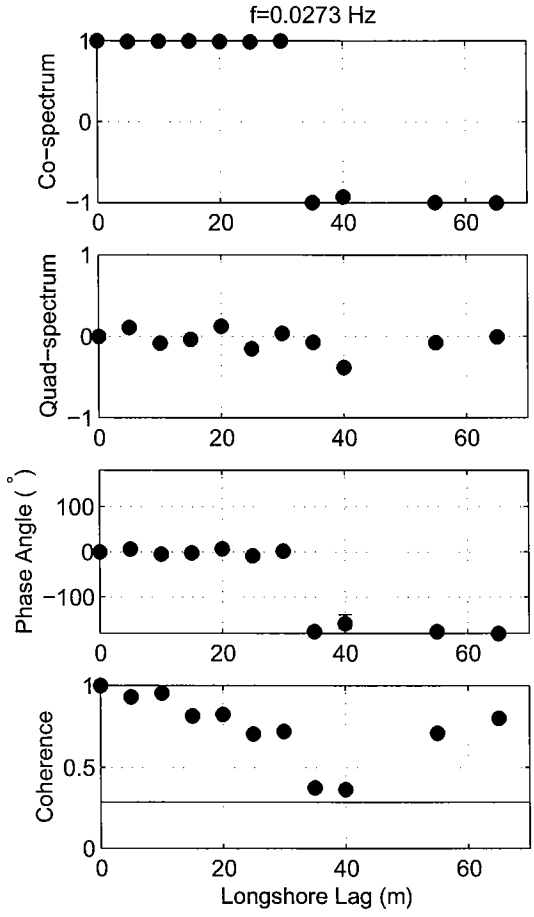

Figure 15. Co-spectrum, quad-spectrum, phase and coherence versus sensor separation for f=0.0273 Hz. The spectra involve 56 degrees of freedom and a frequency bandwidth of 1.95 $\times 10^{-3}$ Hz.

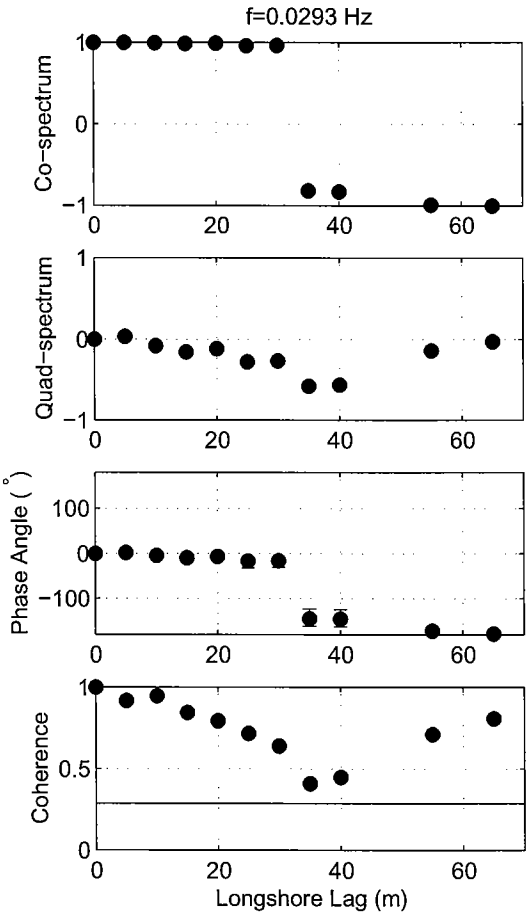

Figure 16. Co-spectrum, quad-spectrum, phase and coherence versus sensor separation for f=0.0293 Hz. The spectra involve 56 degrees of freedom and a frequency bandwidth of 1.95 $\times 10^{-3}$ Hz.

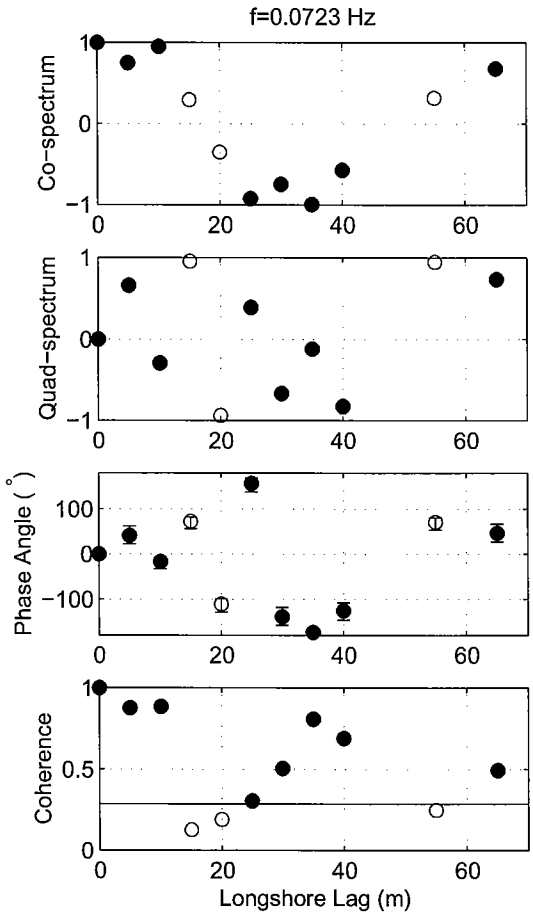

Figure 17. Co-spectrum, quad-spectrum, phase and coherence versus sensor separation for f=0.0723 Hz. The spectra involve 56 degrees of freedom and a frequency bandwidth of 1.95 $\times 10^{-3}$ Hz.

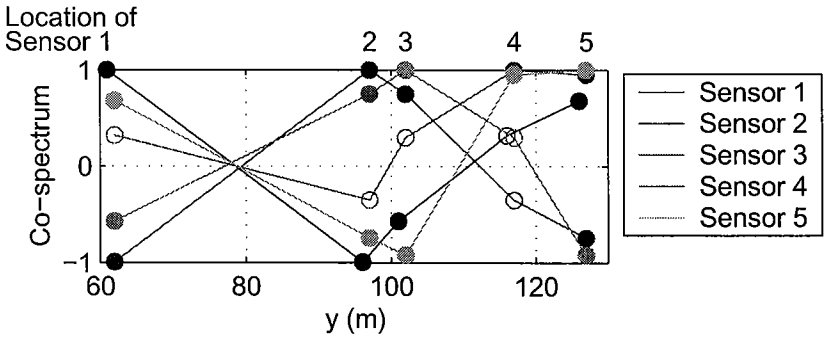

Figure 18. Co-spectrum, quad-spectrum, phase and coherence versus absolute sensor location for f=0.0723 Hz. The spectra involve 56 degrees of freedom and a frequency bandwidth of 1.95 $\times 10^{-3}$ Hz.

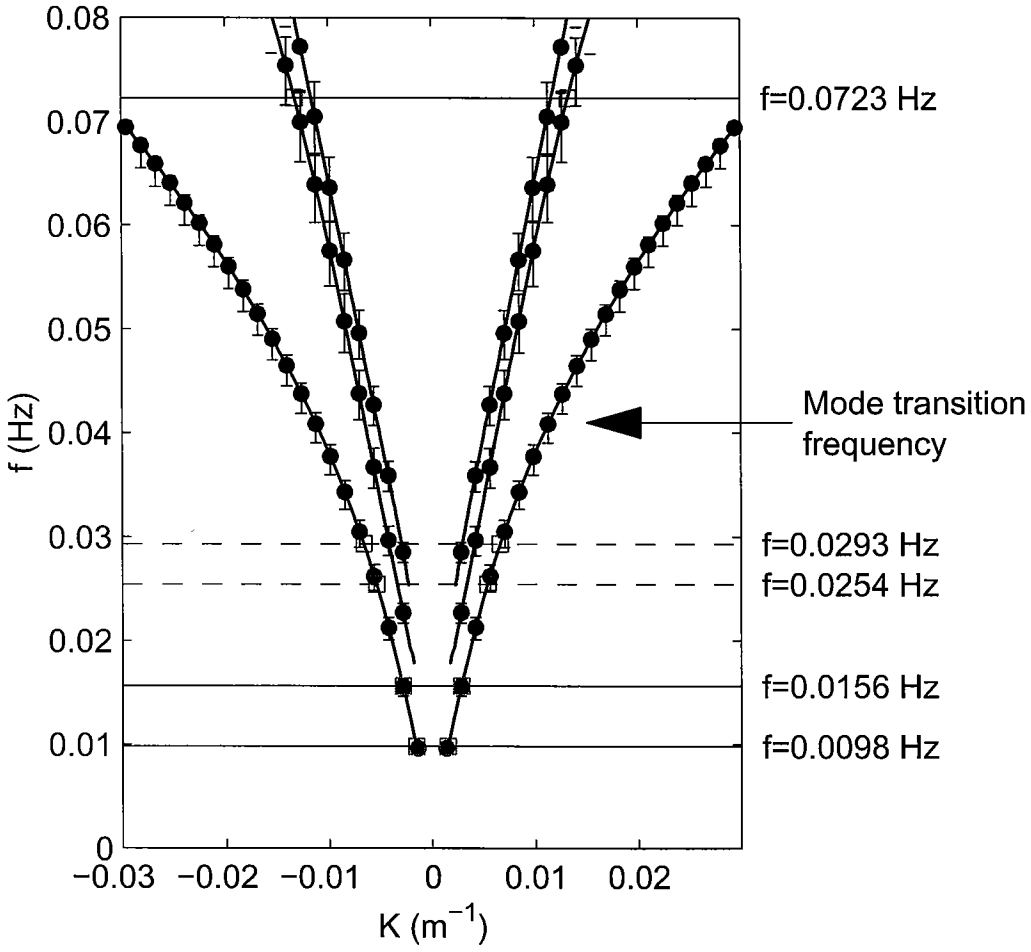

Figure 19. Theoretical edge wave resonances (bullets) and observed edge waves (squares). The mode transition frequency from cross-shore mode 0 to cross-shore mode 1 is also noted.